NASA TECHNICAL NOTE

NASA TN D-2181
C.1

NASA TN D-2181

ANALYTICAL STUDY OF AIRCRAFT-DEVELOPED SPINS AND DETERMINATION OF MOMENTS REQUIRED FOR SATISFACTORY SPIN RECOVERY

by Ernie L. Anglin and Stanley H. Scher

Langley Research Center
Langley Station, Hampton, Va.

NATIONAL AERONAUTICS AND SPACE ADMINISTRATION • WASHINGTON, D. C. • FEBRUARY 1964

ANALYTICAL STUDY OF AIRCRAFT-DEVELOPED SPINS AND DETERMINATION OF MOMENTS REQUIRED FOR SATISFACTORY SPIN RECOVERY

By Ernie L. Anglin and Stanley H. Scher

Langley Research Center
Langley Station, Hampton, Va.

NATIONAL AERONAUTICS AND SPACE ADMINISTRATION

For sale by the Office of Technical Services, Department of Commerce,
Washington, D.C. 20230 -- Price $2.25

ANALYTICAL STUDY OF AIRCRAFT-DEVELOPED SPINS AND DETERMINATION OF MOMENTS REQUIRED FOR SATISFACTORY SPIN RECOVERY

By Ernie L. Anglin and Stanley H. Scher

SUMMARY

An analytical study has been made of fairly steady developed spins and recoveries of a sweptback-wing aircraft configuration by using rotation-balance aerodynamic wind-tunnel data and a digital computer. Changes in aerodynamic, inertia, and relative-density factors resulted in varied spins from which recoveries were attempted by applying an external antispin yawing or rolling moment.

In order to indicate the relative difficulty of spin recovery, a nondimensional spin-energy factor based on the kinetic energy of spin rotation was devised. The antispin yawing-moment coefficient required to provide a satisfactory recovery is shown to be related to this factor. The antispin rolling-moment coefficient required to provide a satisfactory recovery was found to depend on both this spin-energy factor and upon the moment of inertia about the longitudinal axis.

A method is also presented for estimating the approximate nature of steady developed spin characteristics by using certain aerodynamic and inertia factors.

INTRODUCTION

Modern aircraft still inadvertently enter spins which sometimes result in loss of life and property. Spin entries and developed spins are large-angle motions which are affected by nonlinear aerodynamics and cross-coupled inertia factors, and it is likely that these dangerous motions will also occur during flights of winged atmospheric reentry vehicles.

For a number of years, the developed spin and recovery characteristics of aircraft have been determined by experimental investigations using small dynamically ballasted models in a vertical free-spinning tunnel. Properly interpreted, the results so obtained have usually been adequate for use in predicting confidently the developed spin and recovery characteristics of the craft represented by the dynamic models. However, modern trends in design have caused Reynolds number and spin-entry technique differences between the vehicles and the models to become important factors which may in some instances make proper interpretation

of model results very difficult. (See ref. 1.) Analytical spin research is currently being conducted in order to enable better prediction of spin entries and of developed spin and recovery characteristics, and to aid in understanding how various factors may affect these motions.

Spin experience has shown that recoveries are difficult to obtain in general, from relatively steady, rapidly rotating spins with angles of attack remaining approximately at some value between 70° and 90°. As was indicated in reference 2, there is a need for more information on moments required for obtaining satisfactory recoveries from these spins. The present paper describes an analytical study of steady developed spins and recoveries therefrom made by using low Reynolds number rotation-balance aerodynamic wind-tunnel data representing a sweptback-wing aircraft design. (See fig. 1.) Six-degree-of-freedom equations of motion were arranged in a form suitable for using this type of aerodynamic input, and a digital computer was used to solve these equations and some auxiliary formulas and thereby to calculate spin and recovery motions.

Variations were made in aerodynamic, inertia, and relative-density factors in order to obtain a number of different developed spins. Various amounts of yawing moments or rolling moments were then applied to determine their effects on the number of turns required for recovery from the various developed spins obtained. A nondimensional spin-energy factor was devised based on the kinetic energy of spin rotation, and the antispin yawing or rolling moment necessary to provide a satisfactory recovery from the spin is shown to be a function of this factor. Also included is the presentation of a method for estimating the approximate nature of steady developed spin characteristics by using certain aerodynamic and inertia factors.

SYMBOLS

The body system of axes is used. This system of axes, related angles, and positive directions of corresponding forces and moments are illustrated in figure 2.

b wing span, 39.67 ft

C_D drag coefficient, $\dfrac{F_D}{\frac{1}{2}\rho V_R^2 S}$

C_l rolling-moment coefficient, $\dfrac{M_X}{\frac{1}{2}\rho V_R^2 Sb}$

C_m pitching-moment coefficient, $\dfrac{M_Y}{\frac{1}{2}\rho V_R^2 Sb}$

C_n yawing-moment coefficient, $\frac{M_Z}{\frac{1}{2}\rho V_R^2 Sb}$

C_X longitudinal-force coefficient, $\frac{F_X}{\frac{1}{2}\rho V_R^2 S}$

C_Y side-force coefficient, $\frac{F_Y}{\frac{1}{2}\rho V_R^2 S}$

C_Z vertical-force coefficient, $\frac{F_Z}{\frac{1}{2}\rho V_R^2 S}$

ΔC_l incremental rolling-moment coefficient

ΔC_n incremental yawing-moment coefficient

$$C_{l_p} = \frac{\partial C_l}{\partial\left(\frac{pb}{2V_R}\right)}$$

$$C_{l_r} = \frac{\partial C_l}{\partial\left(\frac{rb}{2V_R}\right)}$$

$$C_{m_q} = \frac{\partial C_m}{\partial\left(\frac{qb}{2V_R}\right)}$$

$$C_{n_p} = \frac{\partial C_n}{\partial\left(\frac{pb}{2V_R}\right)}$$

$$C_{n_r} = \frac{\partial C_n}{\partial\left(\frac{rb}{2V_R}\right)}$$

E_s nondimensional kinetic energy of spin rotation, $\frac{\frac{1}{2} I_V \Omega^2}{\frac{1}{2}\rho V_R^2 Sb}$

F_D drag force, lb

F_X force acting along X body axis, lb

F_Y force acting along Y body axis, lb

F_Z force acting along Z body axis, lb

g acceleration due to gravity, taken as 32.17 ft/sec^2

h altitude, ft

I_V moment of inertia about vertical axis, slug-ft^2

I_X, I_Y, I_Z moments of inertia about X, Y, and Z body axes, respectively, slug-ft^2

$K = \frac{I_Z - I_X}{\rho S b}$, sq ft

M_X rolling moment acting about X body axis, ft-lb

M_Y pitching moment acting about Y body axis, ft-lb

M_Z yawing moment acting about Z body axis, ft-lb

m mass, $\frac{\text{Weight}}{g}$, slugs

p, q, r components of Ω about X, Y, and Z body axes, respectively, radians/sec

S wing area, 350 sq ft

t time, sec

u, v, w components of V_R along X, Y, and Z body axes, respectively, ft/sec

V vertical component of velocity of airplane center of gravity (rate of descent), ft/sec

V_R resultant linear velocity, ft/sec

W weight, lb

X, Y, Z body axes

X_R longitudinal rocket force, lb

X_V, Y_V, Z_V three mutually perpendicular space axes, with $X_V Y_V$ space axes in horizontal plane measured from center of gravity, positive in direction of projections of positive Z body axis on vertical, positive X body axis on horizontal plane, and positive Y body axis on horizontal plane

x, y, z linear distances along X, Y, and Z body axes, respectively, measured from center of gravity, positive in sense indicated in figure 2, ft

x_V, y_V, z_V linear distances along X_V, Y_V, Z_V axes, ft

Z_R vertical rocket force, lb

α angle of attack, angle between relative wind V_R projected into the XZ plane of symmetry and the X body axis, positive when relative wind comes from below XY body plane, deg

β angle of sideslip, angle between relative wind V_R and projection of relative wind on XZ-plane, positive when relative wind comes from the right of plane of symmetry, deg

θ_e angle between X body axis and horizontal plane measured in vertical plane, positive when airplane nose is above horizontal plane, radians or deg

μ relative-density coefficient, $\frac{m}{\rho S b}$

ρ air density, slugs/cu ft

ϕ angle between Y body axis and horizontal measured in vertical plane, positive for erect spins when right wing is downward and for inverted spins when left wing is downward, radians or deg

ϕ_e total angular movement of Y body axis from horizontal plane measured in YZ body plane, positive when viewed clockwise from rear of airplane (if X body axis is vertical, ϕ_e is measured from a position in horizontal plane), radians or deg

ψ_e horizontal component of total angular deflection of X body axis from reference position in horizontal plane, positive when viewed clockwise vertically from above the airplane, radians or deg

Ω resultant angular velocity, radians/sec

Subscripts:

0 value at $t = 0$

o component due to oscillations superimposed on steady rotation

r component due to steady rotation

rb aerodynamic data measured by rotation-balance force-test method

s aerodynamic data measured by static-force test method

A dot over a symbol represents a derivative with respect to time; for example, $\dot{u} = \frac{du}{dt}$.

METHODS

For the digital computer calculations, the equations of motion were arranged in a form suitable for using rotation-balance aerodynamic data and these equations are presented in appendix A, along with some spin-geometry formulas that were also used. The steady-state rotation-balance aerodynamic data were used as a function of three variables: α, β, and $\Omega b/2V_R$. A description of the rotation-balance equipment and of the methods used to obtain rotation-balance aerodynamic data is presented in reference 2. Oscillation-balance-type damping derivatives were used in combination with the steady-state rotation-balance aerodynamic data in the manner shown in appendix A.

The basic aerodynamic data inputs used in the digital computer calculations are presented in figures 3 to 9. The data presented in figures 3 to 8 were obtained from rotation-balance measurements made in the Langley 20-foot free-spinning tunnel. Some of the damping derivatives used are shown in figure 9 and were estimated on the basis of experience with measured values for other configurations; the other two damping derivatives, C_{l_r} and C_{n_p}, were arbitrarily used as zero, as is noted in appendix A. Calculations were made to determine the nature of the developed spins that would be obtained for various combinations of the aerodynamic, inertia, and relative-density factors. The relative-density factors and their corresponding effective altitudes are:

Relative density, μ	Effective altitude
25.6	15,000
43.1	30,000
83.5	45,000
171.1	60,000

The aerodynamic variations used are:

Yawing moment	Rolling moment	Pitching moment
Basic (see fig. 5)	Basic (see fig. 3)	Basic (See fig. 4)
$C_n + 0.028$	$(C_l$ and $C_{l_p})(1.5)$	$(C_m$ and $C_{m_q})(1.5)$
$C_n + 0.0375$	$(C_l$ and $C_{l_p})(0.1)$	
$C_n + 0.05$		

The loadings used represent three typical mass arrangements and are:

Loading	Weight, W, lb	I_X, slug-ft^2	I_Y, slug-ft^2	I_Z, slug-ft^2	$\frac{I_X - I_Y}{mb^2}$
I	16,801	7,374	59,764	64,302	-637×10^{-4}
II	16,801	17,374	49,764	64,302	-394
III	16,801	37,374	29,764	64,302	93

From the spins obtained (right spins) recoveries were attempted by application of yawing or rolling moments, which were assumed to be due to rockets mounted at the wing tips. These moments were nondimensionalized to coefficient form by dividing the moment by the value of $\frac{1}{2}\rho V_R^2 Sb$ present during the developed spin. Although constant moments were used, the values of the coefficients will decrease as the velocity of descent increases during the recovery motion. Initial values of yawing-moment coefficients used ranged from 0 to -0.25, and initial values of rolling-moment coefficients used ranged from 0 to 0.20.

A two and one-quarter turn recovery is arbitrarily taken as the criterion for a satisfactory recovery based on previous analyses (ref. 1) which indicate that when model recovery in the free-spinning tunnel required more than this number of turns, the controls were not sufficiently effective and the corresponding airplane probably would have unsatisfactory recovery characteristics. Such a model result in some instances is an indication that the airplane controls are so ineffective as not to produce a recovery at all.

RESULTS AND DISCUSSION

Spin Estimation

A method was devised to estimate approximate values of spin angle of attack, rate of rotation, and descent velocity for steady-state developed spins by using certain aerodynamic and inertia factors. The spin estimation results were used in this investigation to choose initial attitude and velocity conditions for the digital computer to minimize the amount of transient spin-motion computations needed to achieve the developed spin and thereby to save as much digital computer time as possible. This estimation method was devised by assuming that a steady-state developed spin would occur whenever the resultant pitching and yawing moments were both zero simultaneously. However, since rolling moments did not enter into the estimations, some spins predicted by this method will not exist because the rolling moments are not balanced. The complete analysis upon which the spin-estimation method was based, and a description of the method is presented in appendix B.

The results obtained by using the spin-estimation method for the various aerodynamic, inertia, and relative-density combinations are presented as part

of the information in table I. Some of these estimated results are also plotted as flagged symbols in figures 10 to 19, where they may be compared with the digital computer results.

The spin-estimation method was especially helpful for certain cases investigated in which it was found that two types of spin existed. For instance, calculations 68 and 69 on table I show that two different developed spins are possible with all aerodynamic and inertia inputs remaining the same. For cases such as these, digital computer calculations made without benefit of the spin-estimation method would normally have resulted in failure to realize the existence of more than one of these spins. In following normal techniques one developed spin will be obtained by using a single set of initial attitude and velocity conditions; to attempt to determine whether another developed spin exists, an exhaustive number of variations of these initial attitude and velocity conditions would be required and, even then, there would still be no assurance that no other developed spin exists.

It must be remembered, however, that this spin-estimation method was designed to point out the possible existence of approximately steady-state developed spins. Even if no spins of this type are indicated, it is still possible for a vehicle to have a rather oscillatory type of developed spin. (See ref. 3.) Therefore, this estimation method cannot be used as the final answer on developed spin characteristics but should be used only as an aid in more detailed investigations.

Spin-Energy Factor

Spin research is principally concerned with the ability of a craft to terminate satisfactorily the spin rotation for any developed spin of which that craft is capable. Experience has shown that higher rates of rotation in the developed spin and higher moments of inertia make it more difficult to insure satisfactory recovery through the use of available controls on the aircraft. (See ref. 1.) Since the kinetic energy of spin rotation $\frac{1}{2} I_V \Omega^2$ includes both of these variables, and since the effectiveness of any applied antispin moment depends on its ability to do work either directly or indirectly against this energy of spin rotation, it appeared that some factor incorporating the kinetic energy of spin rotation could serve as an indicator of the relative difficulty of spin recovery. In other words, the higher the value of this spin-energy factor, the more antispin moment would be required to obtain a satisfactory spin recovery. The factor used was $E_S = \frac{\frac{1}{2} I_V \Omega^2}{\frac{1}{2} \rho V_R^2 S b}$, the kinetic energy of rotation in a nondimensional form.

In calculating the spin-energy factor, the moment of inertia about a vertical spin axis I_V together with the rotation rate about that axis Ω must be known for each spin. As shown in appendixes A and B, Ω is obtained directly from the computer results or by the spin-estimation method. The formula used to calculate I_V is derived and discussed in appendix C. This formula is based on

the premise that I_V is a function of I_X, I_Z, and θ_e and that the effects of small angles of wing tilt are not significant. As shown in appendix C, an alternate formula for I_V was also derived which included the effects of wing tilt angle, and calculations indicated no appreciable effect on I_V for wing tilt angles of the magnitude encountered in this investigation. Figure 20 presents the variation of I_V with θ_e for the loadings of the present study.

In general, when a specific value of Ω or V_R is not necessarily desired, the spin-energy factor may be estimated by $E_s = \dfrac{-I_V C_m}{(I_Z - I_X)\sin 2\alpha}$. This relation is obtained by substituting $\Omega^2 = -\dfrac{\frac{1}{2}\rho V_R^2 S b C_m}{\frac{1}{2}(I_Z - I_X)\sin 2\alpha}$ into the relation

$$E_s = \frac{\frac{1}{2} I_V \Omega^2}{\frac{1}{2}\rho V_R^2 S b}.$$

Calculated Spins

As mentioned earlier, the results obtained by digital computer calculations for the various aerodynamic, inertia, and relative-density combinations are included in table II. Some of these results are also plotted in figures 10 to 16 showing variations of α, Ω, and E_s with ΔC_n, and, in addition, Ω is plotted against α in figure 17. The results obtained for changes of aerodynamic rolling- and pitching-moment coefficients are shown in figures 18 and 19, respectively, where α, Ω, and E_s are plotted against μ.

For the mass-loading conditions investigated, several trends were noted regarding the effects on spin characteristics of the aerodynamic variations made. Adding positive C_n increments led to more rapidly rotating, higher angle of attack spins, that have a higher spin energy factor, as expected. (See fig. 17.) Within the range of aerodynamic rolling moments used, multiplying the basic measured values by a factor of either 0.1 or 1.5 generally caused only very small variation in developed spin conditions, as shown in figure 18.

An appreciable numerical increase in the values of the negative aerodynamic pitching moment (arbitrarily, a factor of 1.5 times the basic measured values was used) generally led to increases in the rate of rotation, and hence increases in spin-energy factor, as would be expected from spin research experience. Also, the spins thus obtained generally had slightly lower angles of attack. (Compare calculations 19, 24, 30, and 35 with calculations 64, 65, 66, and 67, respectively, or see fig. 19.) In one case presented, it was shown that two spinning conditions were obtained from a single original spin, each of which had higher rates of rotation than did the original; one of the new spins had a lower angle of attack and the other had a higher angle of attack than did the original spin.

(Compare calculation 9 with calculations 68 and 69 in table I.) As mentioned previously, this effect was predicted by the use of the spin-estimation method.

For a given mass loading, increasing values of relative density generally resulted in increasing values of angle of attack, rate of rotation, and spin-energy factor. (See figs. 14 to 16.) In a few cases, however, oscillations were induced in the spin which continued to build up until the craft oscillated out of the spin condition. (See calculations 11, 15, and 62 on table I.) These cases occurred at high relative densities and probably result from an instability in roll brought about by the relative decrease of roll damping effectiveness with increasing relative density. (See ref. 4.) This tendency to oscillate out of the spin was greater, that is, it occurred at lower relative densities for the loading used in which mass was distributed most heavily along the fuselage $\left(\frac{I_X - I_Y}{mb^2} \times 10^4 = -637\right)$. This result is in agreement with trends obtained in free dynamic model tests of the present configuration, as described in reference 5.

A comparison of the calculated spin characteristics with experimental dynamic model results (from ref. 5) is shown in the following table:

Source	α, deg	ϕ, deg	$\frac{\Omega b}{2V_R}$
Calculated spin (calculation 19)	37	≈ 0	0.148
Dynamic model result	36	≈ 0	.145

Since the aerodynamic data used for this investigation were for a particular control setting (elevator up, ailerons neutral and rudder with the spin), it is possible to compare only one of the calculated and experimental results. As can be seen, the calculated results are in very good agreement with the dynamic model results.

Calculated Recoveries

The results of calculations simulating the applying of constant external yawing or rolling moments for attempted spin recovery are presented in tables II and III, respectively. As would be expected, increases in the negative (antispin) applied yawing moments led to faster recoveries for all loadings. For negative loadings (loadings I and II on table I) increases in positive applied rolling moments led to faster recoveries. Although no rolling-moment recoveries were attempted from spins with the positive loading (loading III on table I), increasing positive applied rolling moments would have given no recovery. (A negative rolling moment would be necessary for recovery.) A discussion of the reasons for and the significance of this effect, stressing the importance of the algebraic sign of $(I_X - I_Y)$, is contained in reference 1.

Several trends were evidenced of the effects on the moment required for recovery due to variations in the aerodynamic and relative-density factors investigated. Adding positive C_n increments, increasing magnitudes of negative C_m,

or increasing relative densities indicated a need for increased magnitudes of recovery moments (rolling or yawing) because of the higher spin energy factor of the spins from which recoveries were attempted. Changing the magnitude of aerodynamic rolling moments acting from 1.0 to 0.1 times the basic measured values led to decreased yawing moments required for recovery, and changing the magnitude of aerodynamic rolling moments acting from 1.0 to 1.5 times the basic measured values led to increased yawing moments required for recovery, even though E_s did not vary with these changes in aerodynamic rolling moment.

Some of the recovery results are also presented in figures 21 and 22 where the yawing- or rolling-moment coefficient required to achieve a satisfactory recovery is plotted against E_s, different symbols being used for each loading. As shown in figure 21, the yawing-moment coefficient required for a satisfactory recovery is shown to be related to the spin-energy factor E_s for all mass loadings investigated. The rolling-moment coefficient required for a satisfactory recovery plotted in figure 22 indicates a similar trend, although the magnitude varied with the loading. Different rolling-moment coefficients are required to overcome different values of moment of inertia about the X-axis since an applied rolling moment achieves a recovery by causing an immediate large roll angle (right wing down in an erect spin turning to the pilot's right) and thereby brings into play a cross-coupled antispin inertia yawing moment.

Inasmuch as experience has shown that recoveries from oscillatory-type spins invariably require less moment than do recoveries from fairly steady spins, indications are that figures 21 and 22 can be used to determine an amount of constant yawing or rolling moment which, when applied, will normally cause a satisfactory spin recovery, regardless of whether the spin is obtained during dynamic model results, airplane tests, application of the spin-estimation method, or computer calculations. If a rudder and/or ailerons are to be used for recovery, their position, size, and deflection should be chosen so that ΔC_n and/or ΔC_l obtained from the recovery controls are at least as large at the spin angle of attack as the minimum required constant yawing and/or rolling moment shown in figures 21 and 22. Since, for conventional design, ΔC_n and ΔC_l due to the rudder and ailerons, respectively, get larger as the angle of attack decreases, as it does during a recovery, a satisfactory spin recovery must ensue. The optimum recovery-control manipulation will depend on the mass loading of the specific configuration. (See ref. 1.)

For specific configurations, when the spin-estimation method or spin-tunnel-model results indicate that fairly steady developed spins can be maintained, complementary calculations may also be made, if desired, to determine whether these spins can be obtained from any poststall gyration and potential incipient spin motions which the craft may be capable of executing, starting from normal flight regimes, and using methods equivalent to those of references 6, 7, and 8. Correlation should be made, if possible, with experimental results.

CONCLUSIONS

An analytical study has been made of fairly steady developed spins and recoveries of a sweptback-wing aircraft configuration by using rotation-balance

aerodynamic wind-tunnel data and a digital computer. Changes in aerodynamic, inertia, and relative-density factors were made to obtain varied developed spins. Recoveries from each of these developed spins were attempted by application of an external antispin yawing or rolling moment. The results of the investigation indicate the following conclusions:

1. The addition of positive yawing-moment coefficient C_n led to more rapidly rotating, higher angle of attack spins having a higher spin energy factor and a need for increased magnitudes of recovery moments.

2. Multiplying the measured rolling-moment coefficient C_l values by either 0.1 or 1.5 caused only very small variations in rotation rate, angle of attack, and spin-energy factor. However, multiplying the measured C_l by 0.1 led to decreased magnitudes of recovery moments and multiplying the measured C_l by 1.5 led to increased magnitudes of recovery moments compared with the recovery moments needed for the basic C_l.

3. Multiplying the measured pitching-moment coefficient C_m values by 1.5 generally led to spins having a higher rotation rate, lower angle of attack, higher spin energy factor, and a need for increased magnitudes of recovery moments.

4. In one case, when the measured C_m values were multiplied by 1.5, two spinning conditions were obtained from a single original spin; each of the new spins had higher rates of rotation than did the original, one of the new spins had a lower angle of attack, and the other had a higher angle of attack than did the original spin.

5. For a given mass loading, increasing values of relative density generally led to more rapidly rotating, higher angle of attack spins, having a higher spin energy factor and a need for increased magnitudes of recovery moments.

6. A nondimensional spin-energy factor based on the kinetic energy of spin rotation was devised. The antispin yawing-moment coefficient required to provide a satisfactory recovery was shown to be related to this factor. The antispin rolling moment required to provide a satisfactory recovery was found to depend on both this spin-energy factor and upon the moment of inertia about the longitudinal axis.

7. A method is presented for estimating the approximate nature of steady developed spin characteristics by using certain aerodynamic and inertia factors.

Langley Research Center,
National Aeronautics and Space Administration,
Langley Station, Hampton, Va., October 23, 1962.

APPENDIX A

EQUATIONS OF MOTION AND ASSOCIATED FORMULAS

The equations of motion used in the computer calculations were

$$\dot{p} = \frac{I_Y - I_Z}{I_X} qr + \frac{\rho V_R^2 Sb}{2I_X}\left(C_{l,rb} + C_{l_p}\frac{p_o b}{2V_R} + C_{l_r}\frac{r_o b}{2V_R}\right) + \frac{Z_R y}{I_X}$$

$$\dot{q} = \frac{I_Z - I_X}{I_Y} pr + \frac{\rho V_R^2 Sb}{2I_Y}\left(C_{m,rb} + C_{m_q}\frac{q_o b}{2V_R}\right)$$

$$\dot{r} = \frac{I_X - I_Y}{I_Z} pq + \frac{\rho V_R^2 Sb}{2I_Z}\left(C_{n,rb} + C_{n_p}\frac{p_o b}{2V_R} + C_{n_r}\frac{r_o b}{2V_R}\right) - \frac{X_R y}{I_Z}$$

$$\dot{u} = -g \sin\theta_e + vr - wq + \frac{\rho V_R^2 S}{2m} C_{X,rb}$$

$$\dot{v} = g \cos\theta_e \sin\phi_e + wp - ur + \frac{\rho V_R^2 S}{2m} C_{Y,rb}$$

$$\dot{w} = g \cos\theta_e \cos\phi_e + uq - vp + \frac{\rho V_R^2 S}{2m} C_{Z,rb}$$

In addition, the following formulas were used:

$$\alpha = \tan^{-1}\left(\frac{w}{u}\right)$$

$$\beta = \sin^{-1}\left(\frac{v}{V_R}\right)$$

$$V_R = \sqrt{u^2 + v^2 + w^2}$$

$$\Omega = \sqrt{p^2 + q^2 + r^2}$$

$$h = h_0 - \Delta t V$$

$$V = -u \sin \theta_e + v \cos \theta_e \sin \phi_e + w \cos \theta_e \cos \phi_e$$

$$\dot{\theta}_e = q \cos \phi_e - r \sin \phi_e$$

$$\dot{\phi}_e = p + r \tan \theta_e \cos \phi_e + q \tan \theta_e \sin \phi_e$$

$$\dot{\psi}_e = \frac{\dot{\phi}_e - p}{\sin \theta_e}$$

$$\phi_e = \sin^{-1}\left(\frac{\sin \phi}{\cos \theta_e}\right)$$

$$\text{Turns in spin} = \frac{\int \dot{\psi}_e \, dt}{2\pi}$$

$$p_o = \dot{\phi}_e$$

$$q_o = \dot{\theta}_e \cos \phi_e$$

$$r_o = -\dot{\theta}_e \sin \phi_e$$

By using these equations, time histories of the variables acting were computed. The aerodynamic coefficients used in the equations of motion were programed for the digital computer as functions of the variables shown in the following table:

Function of -	α	β	$\frac{\Omega b}{2V}$	Constant
$C_{l,rb}$	X	X	X	
$C_{m,rb}$	X	X	X	
$C_{n,rb}$	X	X	X	
$C_{X,rb}$	X	X	X	
$C_{Y,rb}$	X	X	X	
$C_{Z,rb}$	X	X	X	
C_{l_p}	X			
C_{l_r}				0
C_{m_q}				-1.5
C_{n_p}				0
C_{n_r}	X			

The following discussion gives the reasoning behind the use of the oscillatory aerodynamic coefficients in the form shown in the equations of motion.

If static-force test aerodynamic data had been used (as in refs. 6, 7, and 8), this method would have called also for conventional use of oscillatory-type derivatives such as C_{l_p}, C_{l_r}, C_{m_q}, C_{n_p}, and C_{n_r} in the equations of motion to account for the effects of angular motions. However, in utilizing rotation-balance aerodynamic data as a function of $\Omega b/2V_R$ and in obtaining these data from steady nonoscillating rotations, there arises the problem of how to include the effects of oscillations superimposed on the steady spinning motion. The effects of the steady rotation are, of course, included in the C_l, C_m, and C_n measured coefficients (terms in equations of motion with subscript rb). Conventional oscillatory-type derivatives, when used along with such rotation-balance data, should be used in such a way as to account only for the effects of oscillations superimposed on the steady rotation, and the effects of these oscillations should be determined separately and added to the C_l, C_m, and C_n coefficients obtained from the steady rotation.

Reference 9 shows that

$$p = \dot{\phi}_e - \dot{\psi}_e \sin \theta_e$$

$$q = \dot{\theta}_e \cos \phi_e + \dot{\psi}_e \cos \theta_e \sin \phi_e$$

and

$$r = -\dot{\theta}_e \sin \phi_e + \dot{\psi}_e \cos \theta_e \cos \phi_e$$

In these total relationships for p, q, and r, the p_r, q_r, and r_r components due to steady rotation and the p_o, q_o, and r_o components due to oscillations superimposed on this steady rotation are:

$$p_o = \dot{\phi}_e \qquad p_r = -\dot{\psi}_e \sin \theta_e$$

$$q_o = \dot{\theta}_e \cos \phi_e \qquad q_r = \dot{\psi}_e \cos \theta_e \sin \phi_e$$

$$r_o = -\dot{\theta}_e \sin \phi_e \qquad r_r = \dot{\psi}_e \cos \theta_e \cos \phi_e$$

If a notation scheme is used in which $C_{l,s}$ and $C_{l,rb}$ represent, respectively, rolling-moment coefficients from static-force-test data and from rotation-balance data, the total aerodynamic factors acting when static-force-test data and oscillatory-type derivatives are used (not done in present investigation) would be represented by:

$$C_{l,s} + C_{l_r} \frac{rb}{2V_R} + C_{l_p} \frac{pb}{2V_R}$$

$$C_{m,s} + C_{m_q} \frac{qb}{2V_R}$$

$$C_{n,s} + C_{n_r} \frac{rb}{2V_R} + C_{n_p} \frac{pb}{2V_R}$$

The total aerodynamic factors acting when rotation-balance data and oscillatory-type derivatives are used, as in the present investigation, are assumed to be represented by:

$$C_{l,rb} + C_{l_r} \frac{r_o b}{2V_R} + C_{l_p} \frac{p_o b}{2V_R}$$

$$C_{m,rb} + C_{m_q} \frac{q_o b}{2V_R}$$

$$C_{n,rb} + C_{n_r} \frac{r_o b}{2V_R} + C_{n_p} \frac{p_o b}{2V_R}$$

where

$$C_{l,rb} = C_{l,s} + C_{l_r} \frac{r_r b}{2V_R} + C_{l_p} \frac{p_r b}{2V_R}$$

$$C_{m,rb} = C_{m,s} + C_{m_q} \frac{q_r b}{2V_R}$$

$$C_{n,rb} = C_{n,s} + C_{n_r} \frac{r_r b}{2V_R} + C_{n_p} \frac{p_r b}{2V_R}$$

APPENDIX B

SPIN-ESTIMATION METHOD

Basis for Spin-Estimation Method

An attempt was made to estimate the nature of any possible steady developed spinning conditions by an examination of aerodynamic and inertia input factors. The primary reason for doing this was to save valuable digital computer time by enabling initial computer-input conditions to be chosen at or near the final potential spin conditions so that calculations of large-angle transient motions could be avoided. The method used to make these estimates is presented in detail, along with an illustration of its use, based on the reasoning as follows:

Regardless of angle of attack or rate of rotation, a developed spin is generally described as smooth and steady, moderately oscillatory, or violently oscillatory. In smooth, steady spins, the resultant yawing, rolling, and pitching moments acting on the airplane are approximately zero. Otherwise, the airplane would be continually changing its rate of yawing, rolling, and pitching velocity and the motion would not be smooth and steady. In a smooth spin, the wing generally remains oriented in a nearly horizontal attitude as the craft rotates. In oscillatory spins, the three resultant moments continue to oscillate in such a manner that all three moments are never zero together.

In steady spins with the wing about in a level attitude, three of the basic conditions which must be satisfied are as follows: A negative (nose-down) aerodynamic pitching moment must be equal and opposite to a positive (nose-up) inertia pitching moment; the aerodynamic and inertia rolling moments must be such that the airplane is stable in roll while spinning; and there should be a stabilizing variation of aerodynamic yawing moment with any change in rate of spin rotation, that is, a curve of $C_{n,rb}$ plotted against $\Omega b/2V_R$ at the angle of attack of the spin should indicate a negative slope where $C_{n,rb}$ is zero. See figure 5 for examples of such $C_{n,rb}$ curves.

If a steady spin exists for a particular combination of aerodynamic and inertia inputs, the estimation method should indicate the characteristics of that spin. This method, however, does not consider the nature of rolling moments and it may indicate spins for cases where the roll stability characteristics will cause the configuration to achieve an oscillatory developed spin or to oscillate out of the spin following even a very small disturbance in roll. Also, there possibly might be oscillatory spins for cases in which the estimation method predicts no spin, but where stability in roll can cope with the oscillations of limited magnitude set up by lack of balance in the pitching and yawing moments.

Rotation-balance aerodynamic data (figs. 3 to 8) for 0° sideslip were used on the assumption that any spin indicated would be at or near a wing-level attitude with a corresponding sideslip near 0°, or would be oscillating slightly above and below 0° sideslip. This assumption means that discrepancies may appear

between any estimated spin and a spin obtained by free-model tests or computer calculations in which the configuration is free to oscillate and/or to choose its own sideslip angle while spinning.

Description of Spin-Estimation Method

The detailed steps of the spin-estimation method are as follows:

(1) By using rotation-balance data plots of $C_{n,rb}$ plotted against $\Omega b/2V_R$ and $C_{m,rb}$ plotted against $\Omega b/2V_R$, tabulate combinations of $\Omega b/2V_R$ and α for which $C_{n,rb} = 0$. For these combinations, read and record $C_{m,rb}$ values. These values should represent potential equilibrium wing-level spinning conditions (potential due to dependency on results of steps (2) and (3) below, as well as on subsequent determination of roll stability).

(2) For the combinations of $\Omega b/2V_R$ and α obtained in step (1), compute $C_{m,rb}$ from

$$-C_{m,rb} = K \frac{\Omega^2}{V_R^2} \sin 2\alpha \tag{B1}$$

where

$$K = \frac{I_Z - I_X}{\rho S b} \tag{B2}$$

and

$$\frac{\Omega^2}{V_R^2} = \left(\frac{\Omega b}{2V_R} \frac{2}{b}\right)^2 \tag{B3}$$

Equation (B1) for $C_{m,rb}$ was derived from the pitching equation of motion for an equilibrium spin as follows; from reference 1 or the pitching equation of motion (appendix A of this paper), it can be shown that

$$\Omega^2 = \frac{-M_{aero}}{\frac{1}{2}(I_Z - I_X)\sin 2\alpha} = \frac{-C_{m,rb}\rho V_R^2 S b}{(I_Z - I_X)\sin 2\alpha}$$

therefore

$$-C_{m,rb} = \frac{I_Z - I_X}{\rho S b} \frac{\Omega^2}{V_R^2} \sin 2\alpha$$

If it is assumed that

$$K = \frac{I_Z - I_X}{\rho S b}$$

then

$$-C_{m,rb} = K \frac{\Omega^2}{V_R^2} \sin 2\alpha$$

(3) Plot a curve of the variation of $C_{m,rb}$ with α from the results of step (1). On the same figure, plot another such curve from the results of step (2). The intersection of the two curves indicates the estimated α and $C_{m,rb}$ of a potential spin.

(4) Determine $\frac{\Omega}{V_R}$ of the spin from

$$\frac{\Omega}{V_R} = \sqrt{\frac{-C_{m,rb}}{K \sin 2\alpha}} \tag{B4}$$

which is derived from the same formula that was used in step (2). Multiply Ω/V_R by $b/2$ to obtain $\Omega b/2V_R$.

(5) Determine V_R of the spin by first obtaining C_D from rotation-balance test data at the α and $\Omega b/2V_R$ of the spin. Since C_D was not measured directly, compute it from

$$C_D = -C_Z \sin \alpha - C_X \cos \alpha \tag{B5}$$

Then V_R may be computed from

$$V_R = \sqrt{\frac{W}{\frac{1}{2} \rho S C_D}} \tag{B6}$$

(6) Determine Ω of spin from

$$\Omega = \frac{\Omega b}{2V_R} \frac{2V_R}{b} \tag{B7}$$

Illustration of Spin-Estimation Method

A numerical illustration of the application of the spin-estimation method is presented in the following paragraphs. The values of several of the parameters obtained by the use of this method are given in the following table:

① α	② $\frac{\Omega b}{2V_R}$	③ $C_{m,rb}$ from step 1	④ $C_{m,rb}$ from step 2
0			
10	0.275	-0.008	-0.14836
20	.115	.004	-.04878
30	.135	-.065	-.09057
40	.135	-.140	-.10299
50	.085	-.169	-.04082
60	.035	-.211	-.00606
70	.015	-.255	-.00682
80	0	-.279	0

Columns ① and ② show the values of α and $\Omega b/2V_R$ where $C_{n,rb} = 0$. The values are taken from figure 5(a). For these combinations of α and $\Omega b/2V_R$, values of $C_{m,rb}$ were obtained from figure 4(a) and are given in column ③.

Solving for K for the subject configuration with equation (B2) yields $K = \frac{64,302 - 17,374}{(0.001496)(350)(39.67)} = 2,259.28$ for loading II at an altitude of 15,000 feet.

For a sample $C_{m,rb}$ computation, let $\alpha = 10^\circ$ and $\Omega b/2V_R = 0.275$ (as shown in columns ① and ②). Then Ω^2/V_R^2 is obtained from equation (B3) which gives

$$\frac{\Omega^2}{V_R^2} = \left(\frac{\Omega b}{2V_R}\frac{2}{b}\right)^2 = \left(0.275 \times \frac{2}{39.67}\right)^2 = (0.01386)^2 = 0.000192$$

Computing $C_{m,rb}$ from equation (B1) yields

$$-C_{m,rb} = (2259.3)(0.000192)(0.34202) = 0.14836$$

or

$$C_{m,rb} = -0.14836$$

Values of $C_{m,rb}$ for each combination of α and $\Omega b/2V_R$ were determined in this manner and are shown in column ④.

The variations in $C_{m,rb}$ with α from steps (1) and (2) are plotted in figure 23. The point where these two curves intersect represents the estimated α and $C_{m,rb}$ which should be present for an equilibrium spinning motion. In this example, $\alpha = 37.0$ and $C_{m,rb} = -0.12$.

From equation (B4), Ω/V_R becomes

$$\frac{\Omega}{V_R} = \sqrt{\frac{0.12}{(2259.3)(0.95)}} = \sqrt{0.0000557} = 0.00746$$

$$\frac{\Omega b}{2V_R} = (0.00746)\frac{39.67}{2} = 0.148$$

The value of V_R of the spin is determined from equation (B6) after C_D is found. From figures 6(a) and 8(a) and equation (B5) C_D becomes

$$C_D = (1.25)(0.602) - (-0.038)(0.799) = 0.783$$

and V_R is given by

$$V_R = \sqrt{\frac{16,801}{\frac{1}{2}(0.001492)(350)(0.783)}} = \sqrt{81,996} = 286 \text{ ft/sec}$$

If V_R is known from step (5), Ω is now determined from equation (B7) as follows:

$$\Omega = \frac{\Omega b}{2V_R} \times \frac{2V_R}{b} = 0.148\left(\frac{2 \times 286}{39.67}\right) = 2.13 \text{ radians/sec}$$

In summation, the parameters for the estimated spin for this example are:

$$\alpha = 37^\circ$$

$$\phi = 0^\circ$$

$$V_R = 286 \text{ ft/sec}$$

$$\Omega = 2.13 \text{ radians/sec}$$

A comparison of estimated spin parameters with those obtained by computer calculations is given in table I where the numerical example shown above corresponds to calculation 19.

The spin-estimation method was devised specifically for this investigation, although it may also be derived by starting from a spin-prediction method presented in reference 10, with the assumption that the sideslip angles of all spins would be zero. The complete method of reference 10 was designed to predict exact values for α, β, V_R, and $\Omega b/2V_R$ for equilibrium spins in which the rolling, yawing, and pitching moments all were in simultaneous balance. The complete

method insofar as its usefulness for obtaining spin parameters for computer inputs is concerned is unnecessarily exacting and relatively more unwieldy to apply than is the method of the present investigation.

APPENDIX C

DERIVATION OF FORMULA FOR I_V

In order to obtain a formula for computing a moment of inertia I_V about a vertical axis, the case was considered where the XZ body plane was rotated through the angle θ_e followed by a rotation of the YZ body plane through the angle ϕ_e.

The equations of transformation of coordinates under these two angular rotations about the center of gravity are:

$$x_v = x \cos \theta_e + y \sin \phi_e \sin \theta_e + z \sin \theta_e \cos \phi_e$$

$$y_v = y \cos \phi_e - z \sin \phi_e$$

$$z_v = -x \sin \theta_e + y \cos \theta_e \sin \phi_e + z \cos \theta_e \cos \phi_e$$

The formulas for the moments of inertia about the body axes due to mass arrangement within the body are:

$$I_X = \int \left(y^2 + z^2\right) dm$$

$$I_Y = \int \left(x^2 + z^2\right) dm$$

$$I_Z = \int \left(y^2 + x^2\right) dm$$

Therefore

$$I_V = \int \left(y_v^2 + x_v^2\right) dm$$

$$I_V = \int \Big[\left(y \cos \phi_e - z \sin \phi_e\right)^2 + \left(x \cos \theta_e + y \sin \theta_e \sin \phi_e \right.$$

$$\left. + z \sin \theta_e \cos \phi_e\right)^2\Big] dm$$

$$I_V = \int \left(x^2\cos^2\theta_e + y^2\sin^2\phi_e \sin^2\theta_e + y^2\cos^2\phi_e + z^2\sin^2\theta_e \cos^2\phi_e + z^2\sin^2\phi_e \right) dm$$

$$+ \int 2 \sin\theta_e \cos\theta_e \sin\phi_e \, xy \, dm + \int 2 \sin\theta_e \cos\theta_e \cos\phi_e \, xz \, dm$$

$$+ \int 2 \sin^2\theta_e \sin\phi_e \cos\phi_e \, yz \, dm - \int 2 \sin\phi_e \cos\phi_e \, yz \, dm$$

$$I_V = \int \Big[x^2 \left(\cos^2\theta_e \sin^2\phi_e + \cos^2\theta_e \cos^2\phi_e \right) + y^2 \left(\sin^2\theta_e \sin^2\phi_e + \sin^2\theta_2 \cos^2\phi_e \right.$$

$$\left. + \cos^2\theta_e \cos^2\phi_e \right) + z^2 \left(\sin^2\theta_e \cos^2\phi_e + \sin^2\theta_e \sin^2\phi_e + \cos^2\theta_e \sin^2\phi_e \right) \Big] dm$$

$$+ \sin 2\theta_e \sin\phi_e I_{XY} + \sin 2\theta_e \cos\phi_e I_{XZ} + \sin^2\theta_e \sin 2\phi_e I_{YZ} - \sin 2\phi_e I_{YZ}$$

$$I_V = \cos^2\theta_e \sin^2\phi_e I_Y + \cos^2\theta_e \cos^2\phi_e I_Z + \sin^2\theta_e \sin^2\phi_e I_X + \sin^2\theta_e \cos^2\phi_e I_X$$

$$+ \sin 2\theta_e \sin\phi_e I_{XY} + \sin 2\theta_e \cos\phi_e I_{XZ} - \cos^2\theta_e \sin 2\phi_e I_{YZ}$$

$$I_V = \sin^2\theta_e I_X + \cos^2\theta_e \sin^2\phi_e I_Y + \cos^2\theta_e \cos^2\phi_e I_Z + \sin 2\theta_e \sin\phi_e I_{XY}$$

$$+ \sin 2\theta_e \cos\phi_e I_{XZ} - \cos^2\theta_e \sin 2\phi_e I_{YZ}$$

When $\phi_e = 0^\circ$, it will be noted that $I_V = \sin^2\theta_e I_X + \cos^2\theta_e I_Z + \sin 2\theta_e I_{XZ}$, which corresponds to the formula normally used in transferring I_Z from body axes to stability axes.

Figure 24 shows the variation of I_V with ϕ_e and θ_e for loading II. For angles of ϕ_e of less than 5°, such as were encountered in this investigation, the effect of ϕ_e on I_V may be neglected. As noted in the main text, figure 20 gives I_V as a function of θ_e for the three loadings used.

REFERENCES

1. Neihouse, Anshal I., Klinar, Walter J., and Scher, Stanley H.: Status of Spin Research for Recent Airplane Designs. NASA TR R-57, 1960. (Supersedes NACA RM L57F12.)

2. Stone, Ralph W., Jr., Burk, Sanger M., Jr., and Bihrle, William, Jr.: The Aerodynamic Forces and Moments on a $\frac{1}{10}$-Scale Model of a Fighter Airplane in Spinning Attitudes As Measured on a Rotary Balance in the Langley 20-Foot Free-Spinning Tunnel. NACA TN 2181, 1950.

3. Stone, Ralph W., Jr., and Klinar, Walter J.: The Influence of Very Heavy Fuselage Mass Loadings and Long Nose Lengths Upon Oscillations in the Spin. NACA TN 1510, 1948.

4. Campbell, John P., and McKinney, Marion O., Jr.: A Study of the Problem of Designing Airplanes With Satisfactory Inherent Damping of the Dutch Roll Oscillation. NACA Rep. 1199, 1954. (Supersedes NACA TN 3035.)

5. Berman, Theodore: Spin-Tunnel Investigation of a Model of a Swept-Wing Fighter Airplane Over a Wide Range of Fuselage-Heavy Loadings. NACA RM L50L08, 1950.

6. Scher, Stanley H., Anglin, Ernie L., and Lawrence, George F.: Analytical Investigation of Effect of Spin Entry Technique on Spin and Recovery Characteristics for a 60° Delta-Wing Airplane. NASA TN D-156, 1959.

7. Wykes, John H., Casteel, Gilbert R., and Collins, Richard A.: An Analytical Study of the Dynamics of Spinning Aircraft. Part I - Flight Test Data Analyses and Spin Calculations. WADC Tech. Rep. 58-381, Pt. I (ASTIA Doc. No. AD 203788), U.S. Air Force, Dec. 1958.

8. Grantham, William D., and Scher, Stanley H.: Analytical Investigation and Prediction of Spin and Recovery Characteristics of the North American X-15 Airplane. NASA TM X-294, 1960.

9. Scher, Stanley H.: An Analytical Investigation of Airplane Spin-Recovery Motion by Use of Rotary-Balance Aerodynamic Data. NACA TN 3188, 1954.

10. Bamber, M. J., and House, R. O.: Spinning Characteristics of the XN2Y-1 Airplane Obtained From the Spinning Balance and Compared With Results From the Spinning Tunnel and From Flight Tests. NACA Rep. 607, 1937.

TABLE I.- SPINS OBTAINED FROM COMPUTER AND ESTIMATION METHOD RESULTS

Calculation	Relative density, μ	Aerodynamic changes	Computer results				Estimation-method results			
			α, deg	Ω, radians/sec	V_R, ft/sec	E_s	α, deg	Ω, radians/sec	V_R, ft/sec	E_s
Loading I; $\frac{I_X - I_Y}{mb^2}(10^4) = -637$										
1	25.6	Basic	36.0	1.88	294	0.05309	38.2	1.90	285	0.06790
2	25.6	C_n + 0.028	57.6	1.96	217	.18630	58.5	2.00	215	.20312
3	25.6	C_n + 0.028	78-80	3.12	189	.81600	79.0	3.00	184	.78749
4	25.6	C_n + 0.0375	64.1	2.14	205	.27990	63.4	2.10	206	.26247
5	25.6	C_n + 0.0375	78-80	3.16	189	.30938	78.0	3.00	185	.73397
6	25.6	C_n + 0.05	66.8	2.22	201	.32430	68.7	2.30	200	.36574
7	43.1	Basic	37.0	1.92	372	.03620	45.1	1.83	327	.08804
8	43.1	C_n + 0.028	62.5	2.08	272	.24800	63.2	2.00	271	.26609
9	43.1	C_n + 0.0375	68.0	2.29	261	.28010	69.0	2.20	261	.37409
10	43.1	C_n + 0.05	80.0	3.17	246	.84090				
11	83.5	Basic	Oscillated out of spin condition				48.2	1.89	453	.10685
12	83.5	C_n + 0.028	80.0	3.38	347	.93010	70.0	2.40	360	.42500
13	83.5	C_n + 0.0375	81.7	3.44	348	.96520				
14	83.5	C_n + 0.05	84-87	4.92	336	1.92890				
15	171.1	Basic	Oscillated out of spin condition				51.6	1.90	618	.13357
16	171.1	C_n + 0.028	82.0	3.74	500	1.13540				
17	171.1	C_n + 0.0375		>5						
18	171.1	C_n + 0.05		>5						
Loading II; $\frac{I_X - I_Y}{mb^2}(10^4) = -394$										
19	25.6	Basic	37.0	2.10	287	0.0826	37.0	2.13	286	0.08479
20	25.6	C_n + 0.028	57.0	2.15	218	.2354	56.0	2.18	221	.23141
21	25.6	C_n + 0.028	79.0	3.47	194	.9645	80.5	3.47	182	1.13400
22	25.6	C_n + 0.0375	61.7	2.25	208	.3018	61.5	2.20	210	.29962
23	25.6	C_n + 0.05	65.7	2.39	202	.3786	67.0	2.43	200	.42362
24	43.1	Basic	40.3	2.15	357	.1304	43.0	2.20	335	.14032
25	43.1	C_n + 0.028	62.0	2.28	273	.3052	61.5	2.23	273	.29962
26	43.1	C_n + 0.028	79.0	3.35	243	.9621	77.5	3.10	245	.83780
27	43.1	C_n + 0.0375	66.0	2.45	263	.3971	66.3	2.41	265	.39462
28	43.1	C_n + 0.0375	78-80	3.33-3.52	244	.9891	73.0	2.80	252	.59744
29	43.1	C_n + 0.05	81.6	3.53	244	1.0716				
30	83.5	Basic	44.4	2.16	475	.1310	47.3	1.95	455	.13998
31	83.5	C_n + 0.028	68.0	2.59	371	.4398	68.0	2.58	370	.42909
32	83.5	C_n + 0.028	79.0	3.55	346	1.0322	73.0	2.74	354	.58263
33	83.5	C_n + 0.0375	80.5	3.52	347	1.0156				
34	83.5	C_n + 0.05		>5						
35	171.1	Basic	51.8	2.18	619	.1850	50.5	2.18	620	.16895
36	171.1	C_n + 0.028	80.4	3.72	504	1.0976				
37	171.1	C_n + 0.0375	82.2	4.13	502	1.3779				
38	171.1	C_n + 0.05		>5						

TABLE I.- SPINS OBTAINED FROM COMPUTER AND ESTIMATION METHOD RESULTS - Concluded

Calculation	Relative density, μ	Aerodynamic changes	Computer results				Estimation-method results			
			α, deg	Ω, radians/sec	V_R, ft/sec	E_s	α, deg	Ω, radians/sec	V_R, ft/sec	E_s
		Loading III; $\frac{I_X - I_Y}{mb^2}(10^4) = 93$								
39	25.6	Basic	26.0	2.34	350	0.0915	29.7	2.50	337	0.12149
40	25.6	C_n + 0.028	49.7	2.75	234	.3402	50.0	2.70	230	.35974
41	25.6	C_n + 0.0375	54.9	2.80	221	.4297	55.0	2.79	218	.43349
42	25.6	C_n + 0.05	60.3	2.92	208	.5588	60.0	2.92	207	.60099
43	43.1	Basic	36.5	2.80	380	.2065	37.4	2.69	365	.19514
44	43.1	C_n + 0.028	57.0	2.87	286	.4674	55.5	2.80	287	.44676
45	43.1	C_n + 0.0375	61.8	2.98	272	.5669	62.0	2.89	270	.57483
46	43.1	C_n + 0.05	67.0	3.19	260	.7357	66.5	3.21	258	.76165
47	83.5	Basic	43.3	2.80	480	.2760	44.0	2.62	462	.26219
48	83.5	C_n + 0.028	64.3	3.23	384	.6582	62.8	3.00	377	.59685
49	83.5	C_n + 0.028	79.0	4.60	339	1.8288	80.0	3.82	330	2.59240
50	83.5	C_n + 0.0375	66.7	3.30	372	.7421	67.5	3.10	365	.68030
51	83.5	C_n + 0.05	82.4	4.84	340	2.0223				
52	171.1	Basic	47.0	2.82	651	.3118	47.5	2.83	655	.30956
53	171.1	C_n + 0.028	80.0	4.72	494	.8687	70.0	3.50	515	.88538
54	171.1	C_n + 0.0375		>5						
55	171.1	C_n + 0.05		>5						
		Loading II; $\frac{I_X - I_Y}{mb^2}(10^4) = -394$								
56	25.6	1.5 (C_l and C_{l_p})	37.5	2.09	287	0.08871	37.0	2.13	286	0.08479
57	25.6	0.1 (C_l and C_{l_p})	37.9	2.08	285	.08989	37.0	2.13	286	.08479
58	43.1	1.5 (C_l and C_{l_p})	39.9	2.15	358	.10189	43.0	2.20	335	.14032
59	43.1	0.1 (C_l and C_{l_p})	41.8	2.13	349	.11507	43.0	2.20	335	.14032
60	83.5	1.5 (C_l and C_{l_p})	43.8	2.13	473	.12586	47.3	1.95	455	.13998
61	83.5	0.1 (C_l and C_{l_p})	46.1	2.13	463	.13756	47.3	1.95	455	.13998
62	171.1	1.5 (C_l and C_{l_p})	Oscillated out of spin condition				50.5	2.18	620	.16895
63	171.1	0.1 (C_l and C_{l_p})	51.5	2.13	616	.17596	50.5	2.18	620	.16895
64	25.6	1.5 (C_m and C_{m_q})	36.9	2.55	286	.13123	30.5	2.45	322	.08183
65	43.1	1.5 (C_m and C_{m_q})	39.8	2.63	359	.15884	39.5	2.36	342	.13971
66	83.5	1.5 (C_m and C_{m_q})	41.8	2.62	485	.17375	38.7	2.66	505	.15439
67	171.1	1.5 (C_m and C_{m_q})	48.2	2.60	642	.22749	45.2	2.71	670	.16646
		Loading I; $\frac{I_X - I_Y}{mb^2}(10^4) = -637$								
68	43.1	1.5 (C_m and C_{m_q})	65.9	2.66	264	0.44987	62.7	2.56	271	0.37760
68	43.1	C_n + 0.0375								
69	43.1	1.5 (C_m and C_{m_q})	78.7	3.95	247	1.28620	77.6	3.58	245	1.06480
69	43.1	C_n + 0.0375								

TABLE II.- RECOVERIES OBTAINED FROM COMPUTED SPINS BY APPLICATION OF CONSTANT YAWING MOMENTS

Calculation	Relative density, μ	Aerodynamic changes	Force, lb	ΔC_n	Turns for recovery	Force, lb	ΔC_n	Turns for recovery	Force, lb	ΔC_n	Turns for recovery
1	25.6	Basic	-1,000	-0.022	0.7	-750	-0.017	1.2	-500	-0.011	∞
2	25.6	C_n + 0.028	-2,000	-.081	.9	-1,750	-.071	1.0	-1,500	-.061	∞
3	25.6	C_n + 0.028	-2,000	-.107	1.5	-1,500	-.080	2.5			
4	25.6	C_n + 0.0375	-2,000	-.091	1.1	-1,750	-.080	1.5			
5	25.6	C_n + 0.0375	-2,000	-.107	1.8	-1,750	-.094	2.4			
6	25.6	C_n + 0.05	-2,500	-.118	1.0	-2,250	-.106	1.4	-750	-.035	∞
7	43.1	Basic	-1,000	-.023	.8	-800	-.019	1.4	-750	-.017	∞
8	43.1	C_n + 0.028	-2,000	-.087	1.0	-1,750	-.076	1.2	-1,500	-.065	∞
9	43.1	C_n + 0.0375	-2,500	-.118	.9	-2,000	-.094	1.4	-1,750	-.083	∞
10	43.1	C_n + 0.05	-3,000	-.159	1.3	-2,500	-.133	1.7	-2,250	-.119	2.1
12	83.5	C_n + 0.028	-3,000	-.155	1.0	-2,000	-.103	1.9	-1,500	-.078	3.1
13	83.5	C_n + 0.0375	-3,500	-.180	1.0	-2,000	-.103	2.4	-1,500	-.077	∞
14	83.5	C_n + 0.05	-3,500	-.193	1.2	-3,000	-.165	2.0	-2,500	-.138	3.4
16	171.1	C_n + 0.028	-3,000	-.153	1.4	-2,500	-.128	1.8	-2,000	-.102	3.9
19	25.6	Basic	-750	-.017	1.2	-700	-.016	1.3	-500	-.012	∞
20	25.6	C_n + 0.028	-2,000	-.080	.8	-1,750	-.070	1.1	-1,500	-.060	∞
21	25.6	C_n + 0.028	-2,000	-.101	1.5	-1,500	-.076	2.4	-1,000	-.051	∞
22	25.6	C_n + 0.0375	-2,000	-.088	.9	-1,750	-.077	1.7	-1,500	-.066	∞
23	25.6	C_n + 0.05	-2,500	-.117	.9	-2,250	-.105	1.3	-2,000	-.094	∞
24	43.1	Basic	-1,000	-.025	.9	-750	-.019	1.6	-700	-.018	∞
25	43.1	C_n + 0.028	-2,000	-.086	1.0	-1,750	-.075	1.3	-1,500	-.065	∞
26	43.1	C_n + 0.028	-3,000	-.163	1.0	-2,000	-.109	1.8	-1,500	-.082	2.9
27	43.1	C_n + 0.0375	-2,000	-.093	1.3	-1,750	-.081	2.0	-1,500	-.070	∞
28	43.1	C_n + 0.0375	-3,000	-.162	1.0	-2,000	-.108	1.9	-1,750	-.094	2.6
29	43.1	C_n + 0.05	-3,000	-.162	1.3	-2,500	-.135	1.7	-2,250	-.121	2.1
30	83.5	Basic	-1,000	-.028	1.2	-750	-.021	2.2	-500	-.014	∞
31	83.5	C_n + 0.028	-2,000	-.090	1.2	-1,500	-.068	2.4	-1,000	-.045	∞
32	83.5	C_n + 0.028	-3,000	-.156	1.3	-2,000	-.104	2.2	-1,500	-.078	2.4
33	83.5	C_n + 0.0375	-3,500	-.181	1.0	-2,000	-.103	2.4	-1,500	-.078	∞
35	171.1	Basic	-1,000	-.033	1.3	-750	-.025	2.4	-500	-.017	∞
36	171.1	C_n + 0.028	-3,500	-.176	1.0	-2,000	-.100	2.4	-1,500	-.075	3.9
37	171.1	C_n + 0.0375	-4,000	-.202	1.1	-2,500	-.127	2.4	-2,000	-.101	3.4
39	25.6	Basic	-500	-.008	.2	-100	-.002	2.1			
40	25.6	C_n + 0.028	-2,000	-.070	1.1	-1,500	-.052	2.2	-1,400	-.049	2.9
41	25.6	C_n + 0.0375	-2,500	-.098	1.1	-2,000	-.078	1.6	-1,750	-.068	2.4
42	25.6	C_n + 0.05	-3,000	-.132	1.0	-2,250	-.099	1.7	-2,000	-.088	∞
43	43.1	Basic	-1,000	-.022	1.2	-750	-.017	1.9	-500	-.011	3.6
44	43.1	C_n + 0.028	-2,000	-.079	1.4	-1,500	-.059	2.9	-1,000	-.039	∞
45	43.1	C_n + 0.0375	-2,500	-.109	1.1	-2,000	-.087	1.7	-1,750	-.076	3.0
46	43.1	C_n + 0.05	-3,000	-.143	1.1	-2,500	-.119	1.7	-2,250	-.107	2.0
47	83.5	Basic	-1,500	-.041	1.0	-1,000	-.027	1.9	-750	-.020	3.0
48	83.5	C_n + 0.028	-3,000	-.127	1.0	-2,000	-.084	1.8	-1,500	-.063	3.7
49	83.5	C_n + 0.028				-2,250	-.122	2.6	-2,000	-.108	3.0
50	83.5	C_n + 0.0375	-3,500	-.157	.8	-2,000	-.090	2.0	-1,750	-.079	3.2
51	83.5	C_n + 0.05	-4,500	-.242	1.5	-3,500	-.188	2.1	-2,500	-.135	3.3
52	171.1	Basic	-1,500	-.045	1.3	-1,000	-.030	2.3	-750	-.023	3.9
56	25.6	1.5 (C_l and C_{l_p})	-1,000	-.023	.9	-750	-.017	1.4	-500	-.012	∞
57	25.6	0.1 (C_l and C_{l_p})	-1,000	-.024	.5	-750	-.018	.7	-500	-.012	∞
58	43.1	1.5 (C_l and C_{l_p})	-1,000	-.025	1.0	-750	-.019	1.8	-500	-.013	∞
59	43.1	0.1 (C_l and C_{l_p})	-1,000	-.026	.9	-750	-.020	1.2	-500	-.013	∞
60	83.5	1.5 (C_l and C_{l_p})	-1,000	-.028	1.2	-750	-.021	2.1	-500	-.014	2.8
61	83.5	0.1 (C_l and C_{l_p})	-1,000	-.029	1.1	-750	-.022	1.6	-500	-.015	∞
63	171.1	0.1 (C_l and C_{l_p})	-1,000	-.034	1.4	-750	-.025	2.1	-500	-.017	∞
64	25.6	1.5 (C_m and C_{m_q})	-1,000	-.023	1.1	-750	-.018	1.3	-500	-.012	∞
65	43.1	1.5 (C_m and C_{m_q})	-1,000	-.025	1.5	-750	-.019	2.5	-500	-.012	∞
66	83.5	1.5 (C_m and C_{m_q})	-1,500	-.040	.8	-1,000	-.026	1.5	-750	-.020	∞
67	171.1	1.5 (C_m and C_{m_q})	-1,500	-.046	1.1	-750	-.023	3.1	-500	-.015	∞

TABLE III.- RECOVERIES OBTAINED FROM COMPUTED SPINS BY APPLICATION OF CONSTANT ROLLING MOMENTS

Calculation	Relative density, μ	Aerodynamic changes	Force, lb	ΔC_l	Turns for recovery	Force, lb	ΔC_l	Turns for recovery	Force, lb	ΔC_l	Turns for recovery
2	25.6	C_n + 0.028	900	0.037	0.4	600	0.024	1.2	500	0.020	∞
3	25.6	C_n + 0.028	700	.037	2.2	600	.032	2.5			
4	25.6	C_n + 0.0375	700	.032	1.3	600	.027	1.5			
5	25.6	C_n + 0.0375	800	.043	2.1	700	.037	2.5			
6	25.6	C_n + 0.05	900	.043	.7	700	.033	1.4	600	.028	1.8
7	43.1	Basic	600	.014	.6	500	.012	1.0	400	.009	1.4
8	43.1	C_n + 0.028	700	.030	1.3				600	.026	∞
9	43.1	C_n + 0.0375	800	.038	.7	700	.033	1.2			
10	43.1	C_n + 0.05	900	.048	2.2	800	.042	2.4			
12	83.5	C_n + 0.028	900	.047	2.2	800	.041	3.1	700	.036	4.0
13	83.5	C_n + 0.0375	1,000	.051	2.1	900	.046	3.2	800	.041	4.1
14	83.5	C_n + 0.05	2,250	.124	2.1	2,000	.110	2.4	1,750	.096	3.0
16	171.1	C_n + 0.028	1,750	.089	2.2	1,500	.077	3.0	1,250	.064	4.0
19	25.6	Basic	500	.012	1.1	400	.009	1.7	250	.006	∞
20	25.6	C_n + 0.028	1,000	.040	1.4	900	.036	2.6	800	.032	∞
21	25.6	C_n + 0.028	2,500	.127	2.2	2,000	.101	2.8			
22	25.6	C_n + 0.0375	1,500	.066	.8	1,100	.049	2.2	1,000	.044	∞
23	25.6	C_n + 0.05	1,500	.070	1.3	1,300	.061	2.5	1,100	.051	∞
24	43.1	Basic	750	.019	.9	600	.015	1.3	500	.013	∞
25	43.1	C_n + 0.028	1,500	.065	.7	1,000	.043	2.7			
26	43.1	C_n + 0.028				2,500	.136	2.0	1,500	.082	3.7
27	43.1	C_n + 0.0375	1,500	.070	1.6	1,200	.056	2.2	1,000	.046	∞
28	43.1	C_n + 0.0375				2,500	.135	2.1	1,500	.081	4.6
29	43.1	C_n + 0.05				3,500	.189	1.8	2,500	.135	3.4
30	83.5	Basic	750	.021	1.2	600	.017	2.5	500	.014	∞
31	83.5	C_n + 0.028	1,500	.068	1.8	1,400	.063	2.4	1,000	.045	∞
32	83.5	C_n + 0.028				3,000	.156	2.2	2,000	.104	4.2
33	83.5	C_n + 0.0375				3,000	.155	2.2	2,500	.129	3.3
35	171.1	Basic	750	.025	2.2	700	.023	2.3	500	.017	∞
36	171.1	C_n + 0.028	4,000	.201	1.8	3,500	.176	2.7	2,500	.126	∞

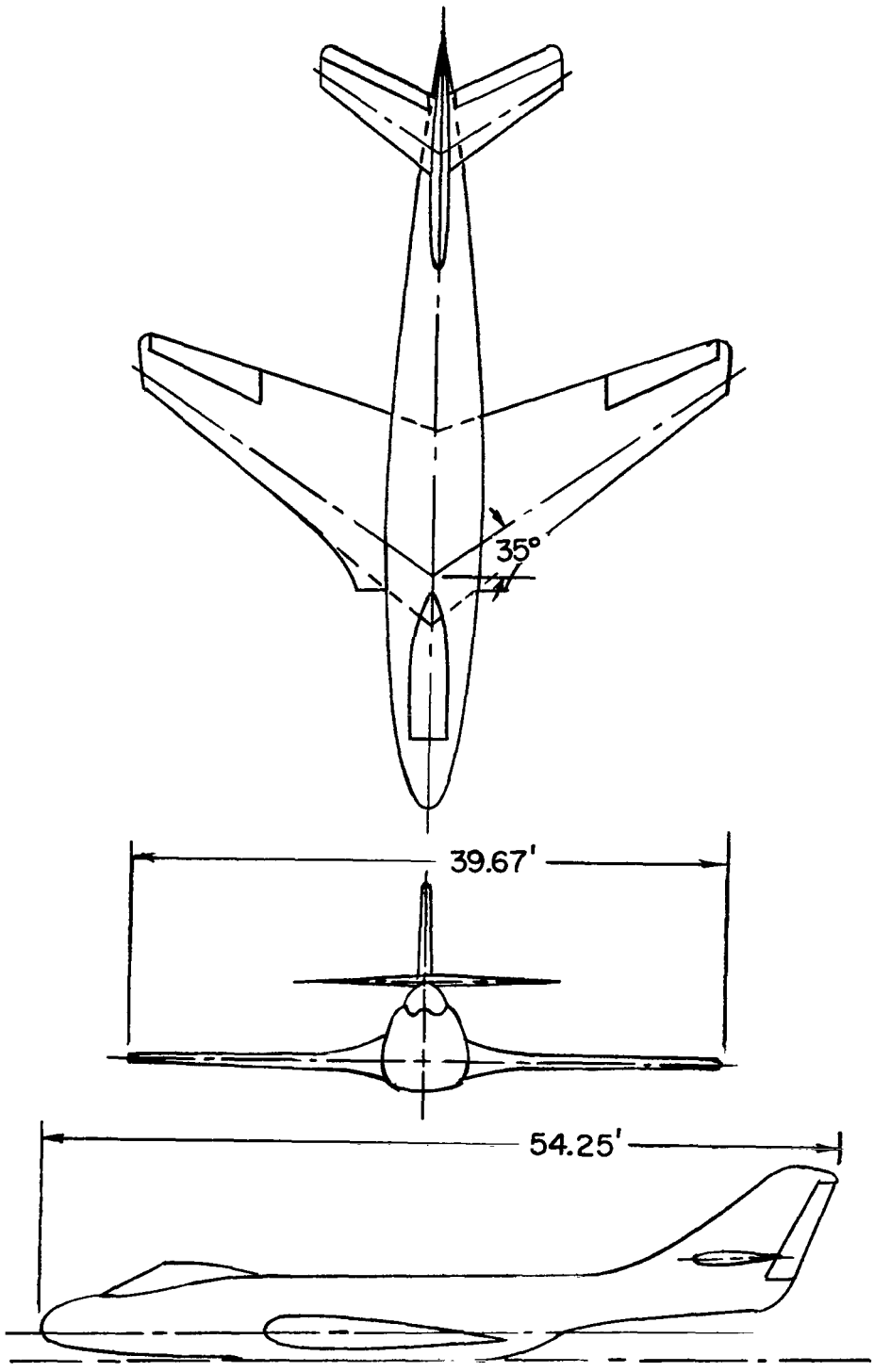

Figure 1.- Three-view sketch of configuration.

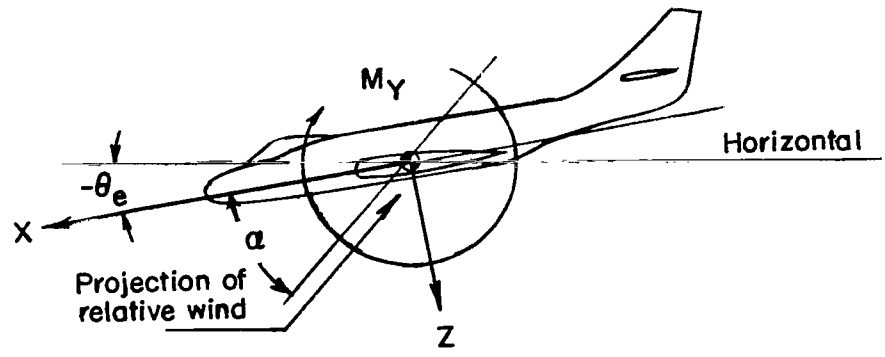

(a) ϕ_e and $\psi_e = 0$.

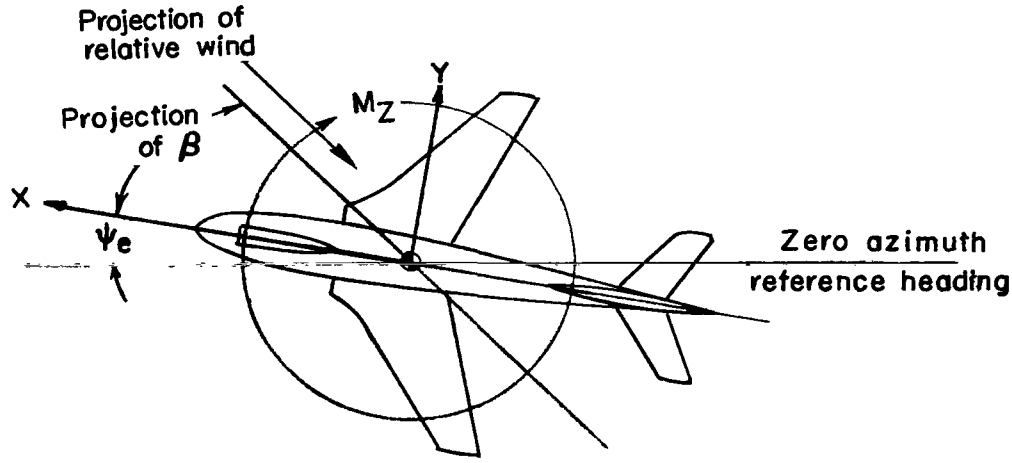

(b) θ_e and $\phi_e = 0$.

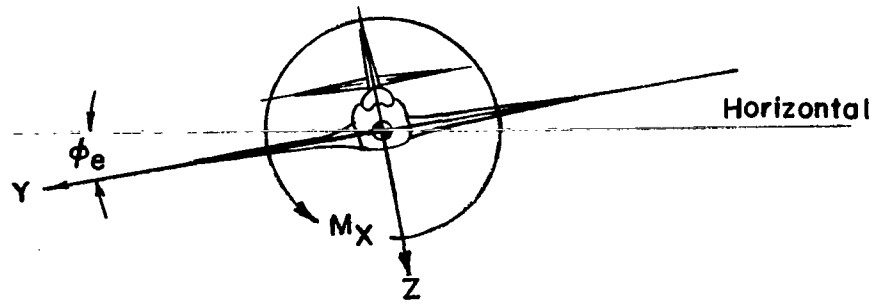

(c) θ_e and $\psi_e = 0$, and in this case $\phi = \phi_e$.

Figure 2.- Body system of axes and related angles.

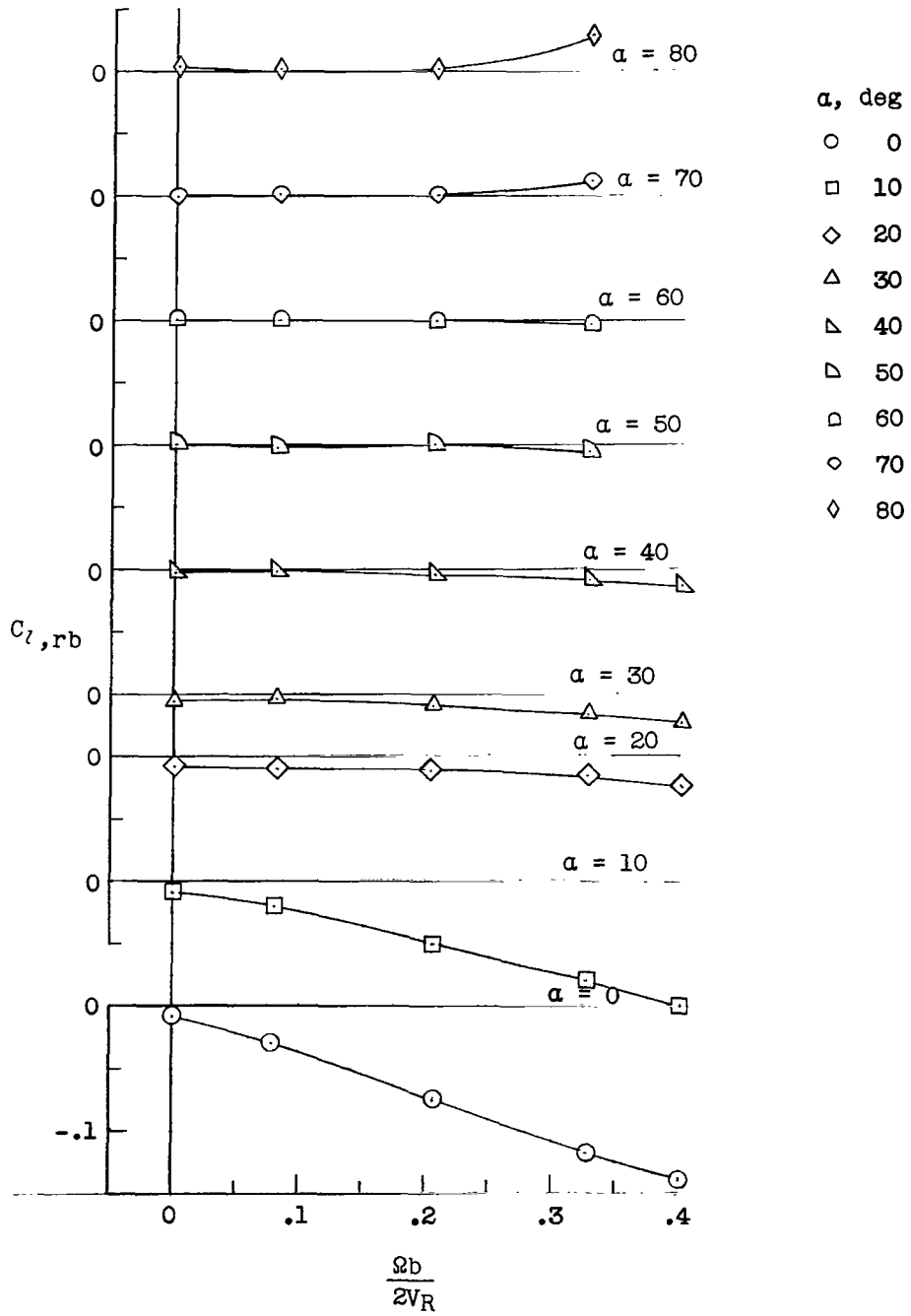

(a) $\beta = 0^{\circ}$.

Figure 3.- Variation of $C_{l,rb}$ with $\frac{\Omega b}{2V_R}$ for various angles of attack.

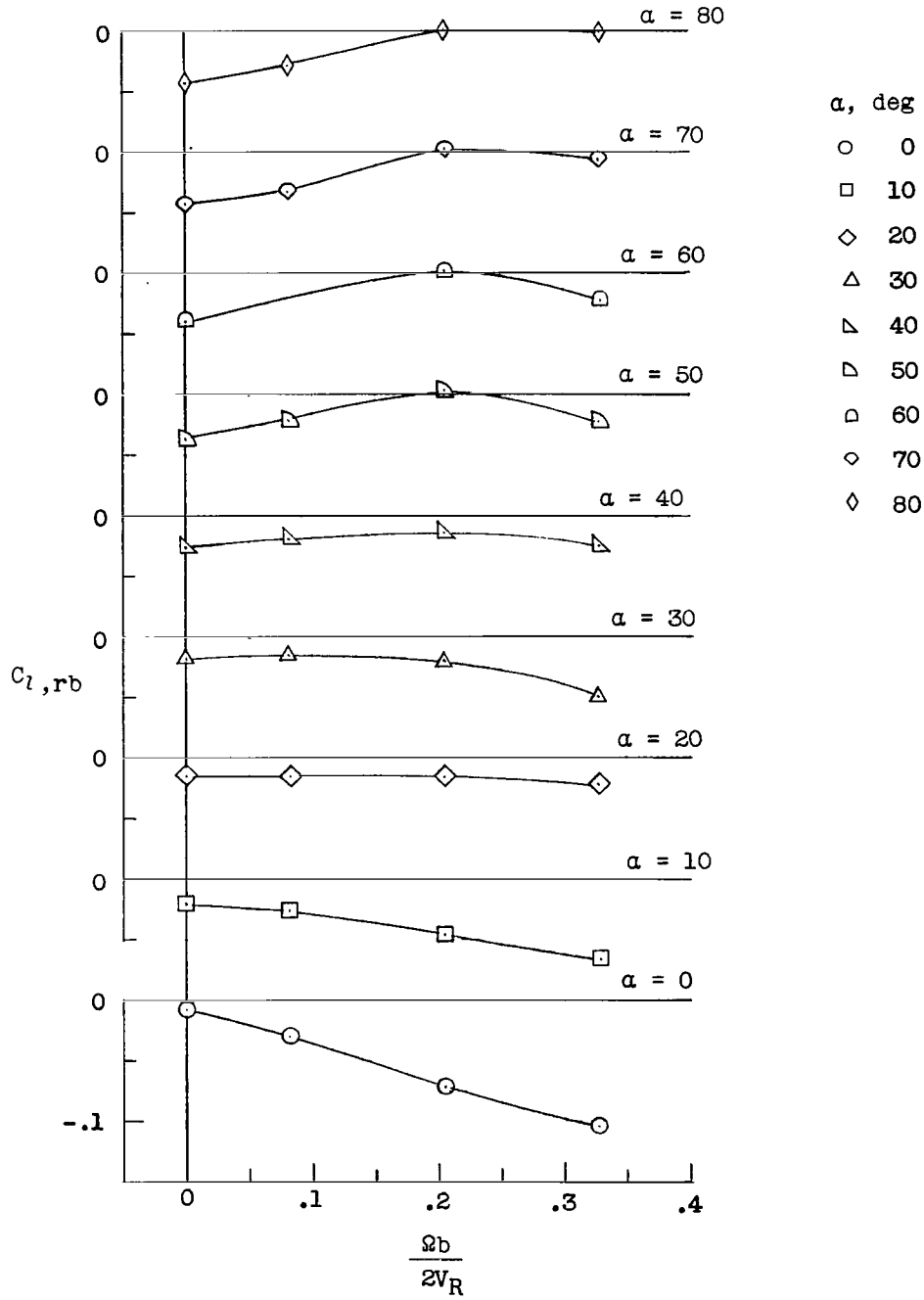

(b) $\beta = 10^{\circ}$.

Figure 3.- Continued.

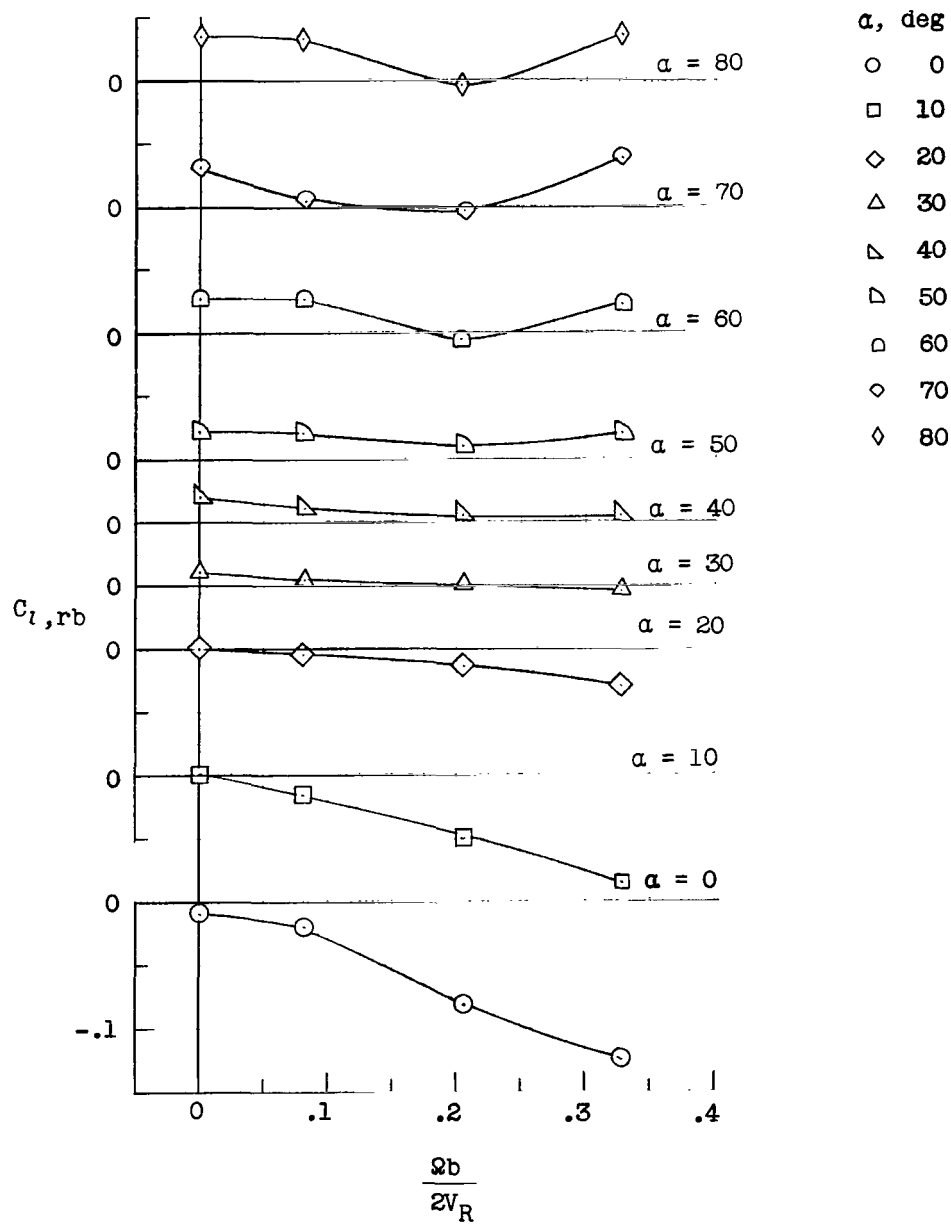

(c) $\beta = -10^{\circ}$.

Figure 3.- Concluded.

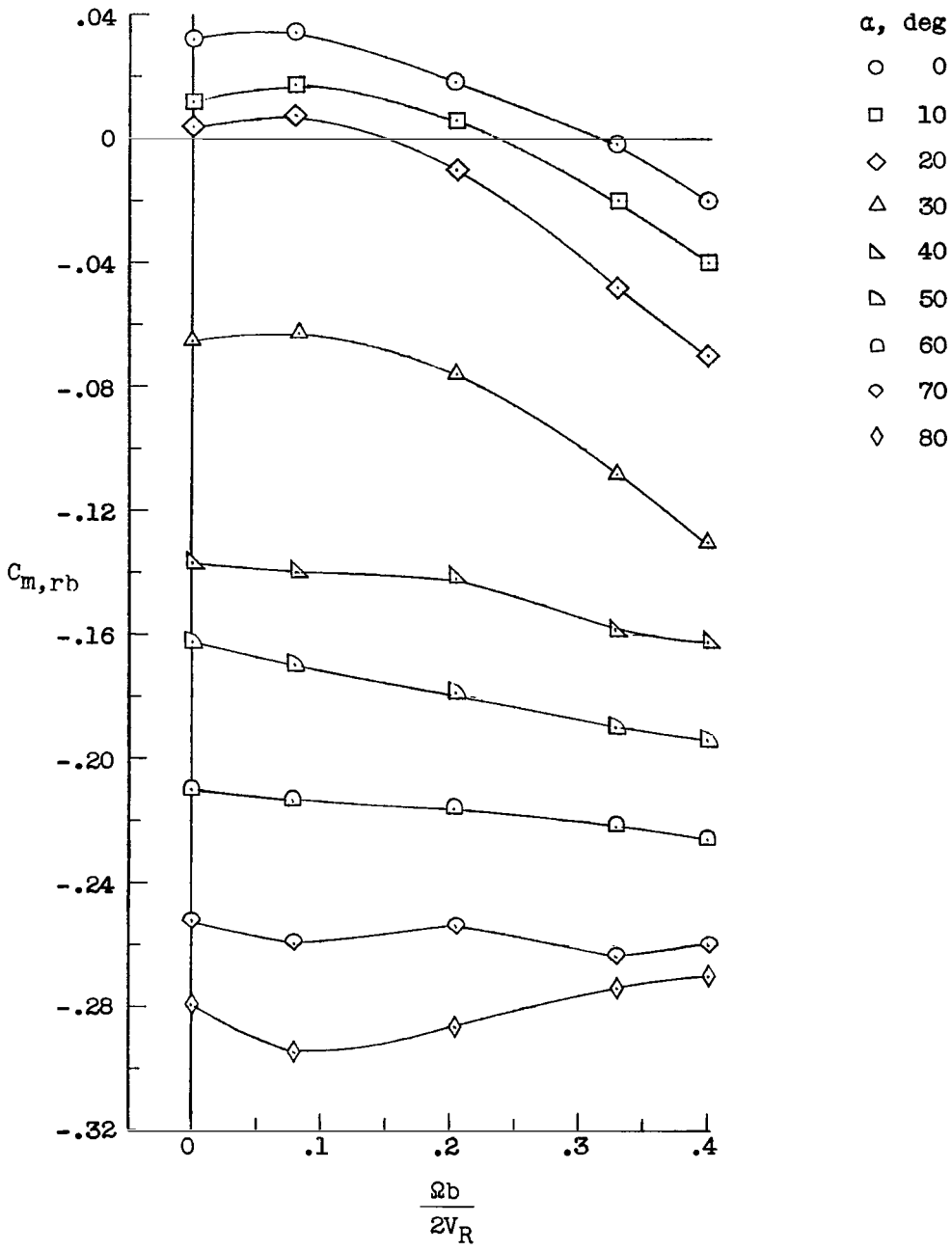

(a) $\beta = 0°$.

Figure 4.- Variation of $C_{m,rb}$ with $\frac{\Omega b}{2V_R}$ for various angles of attack. ($C_{m,rb}$ nondimensionalized with respect to wing span, b.)

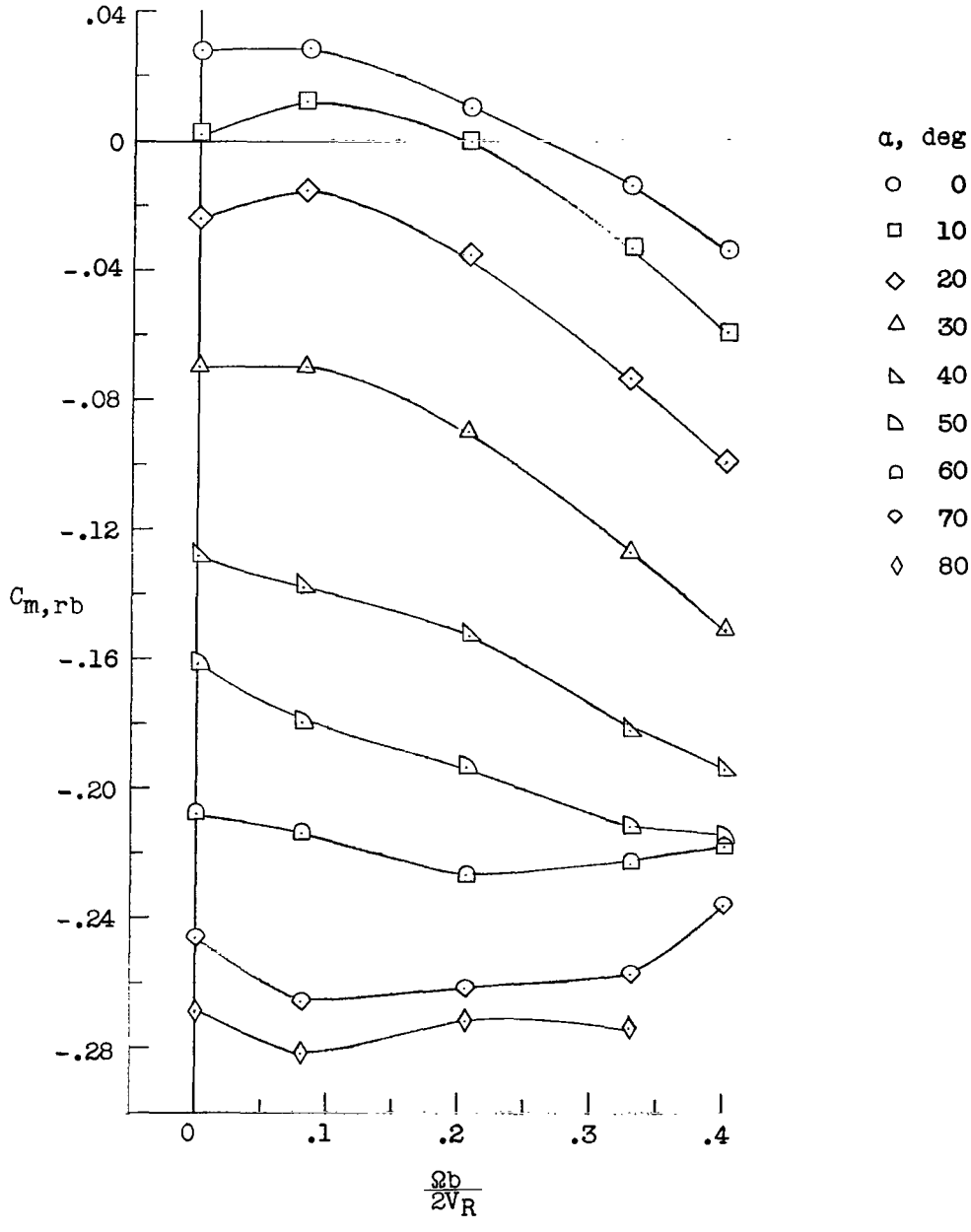

(b) $\beta = 10^{\circ}$.

Figure 4.- Continued.

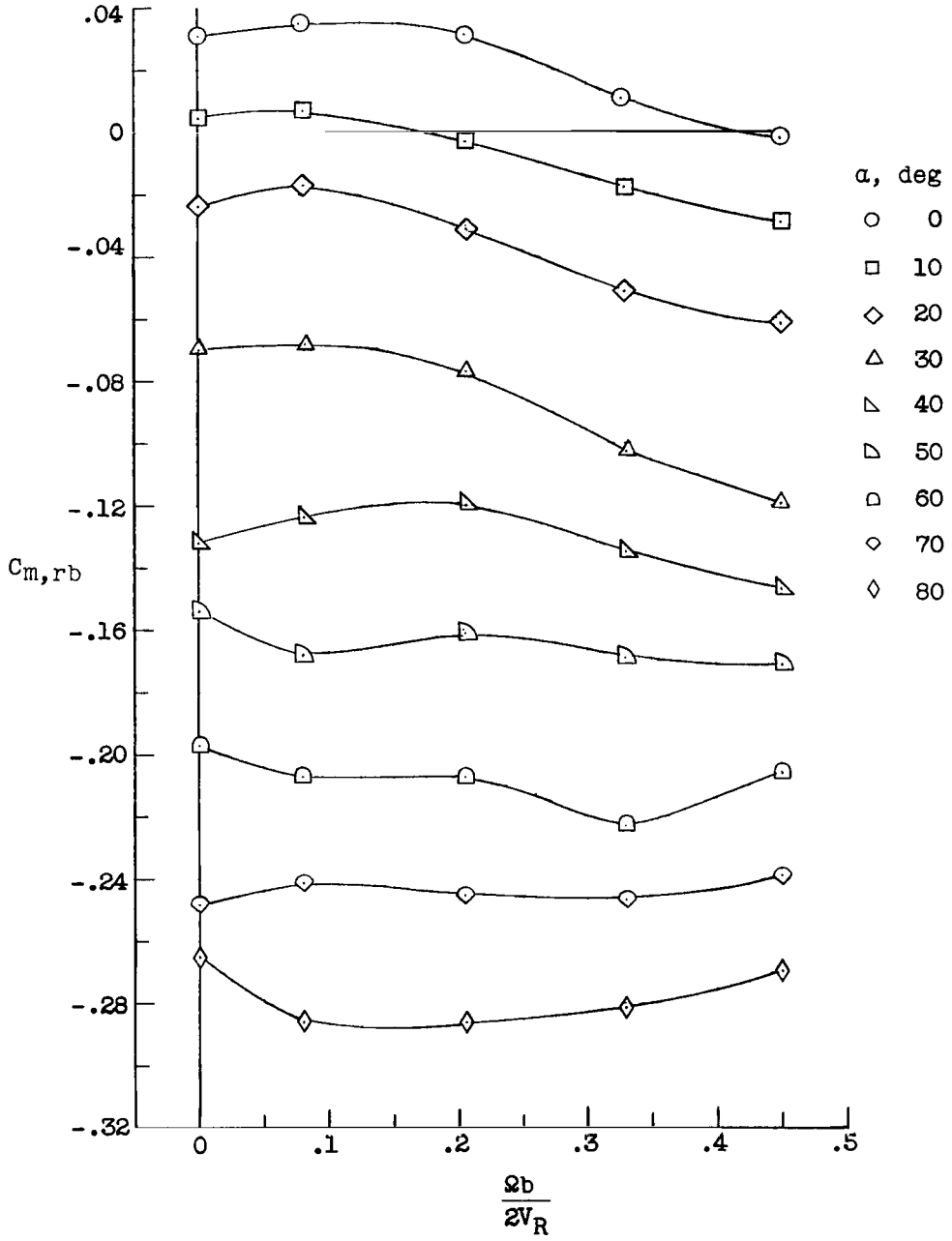

(c) $\beta = -10^{\circ}$.

Figure 4.- Concluded.

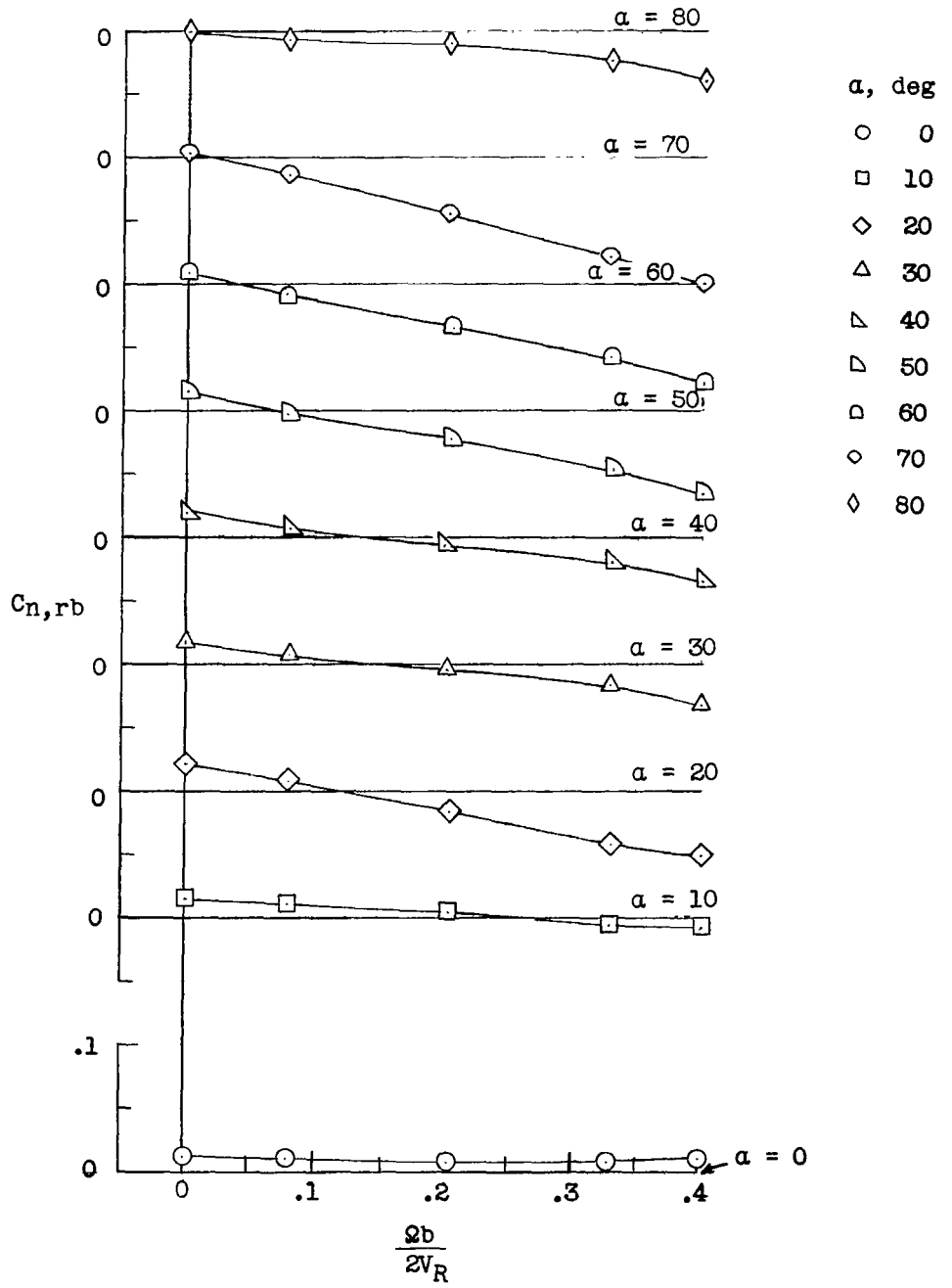

(a) $\beta = 0^{\circ}$.

Figure 5.- Variation of $C_{n,rb}$ with $\frac{\Omega b}{2V_R}$ for various angles of attack.

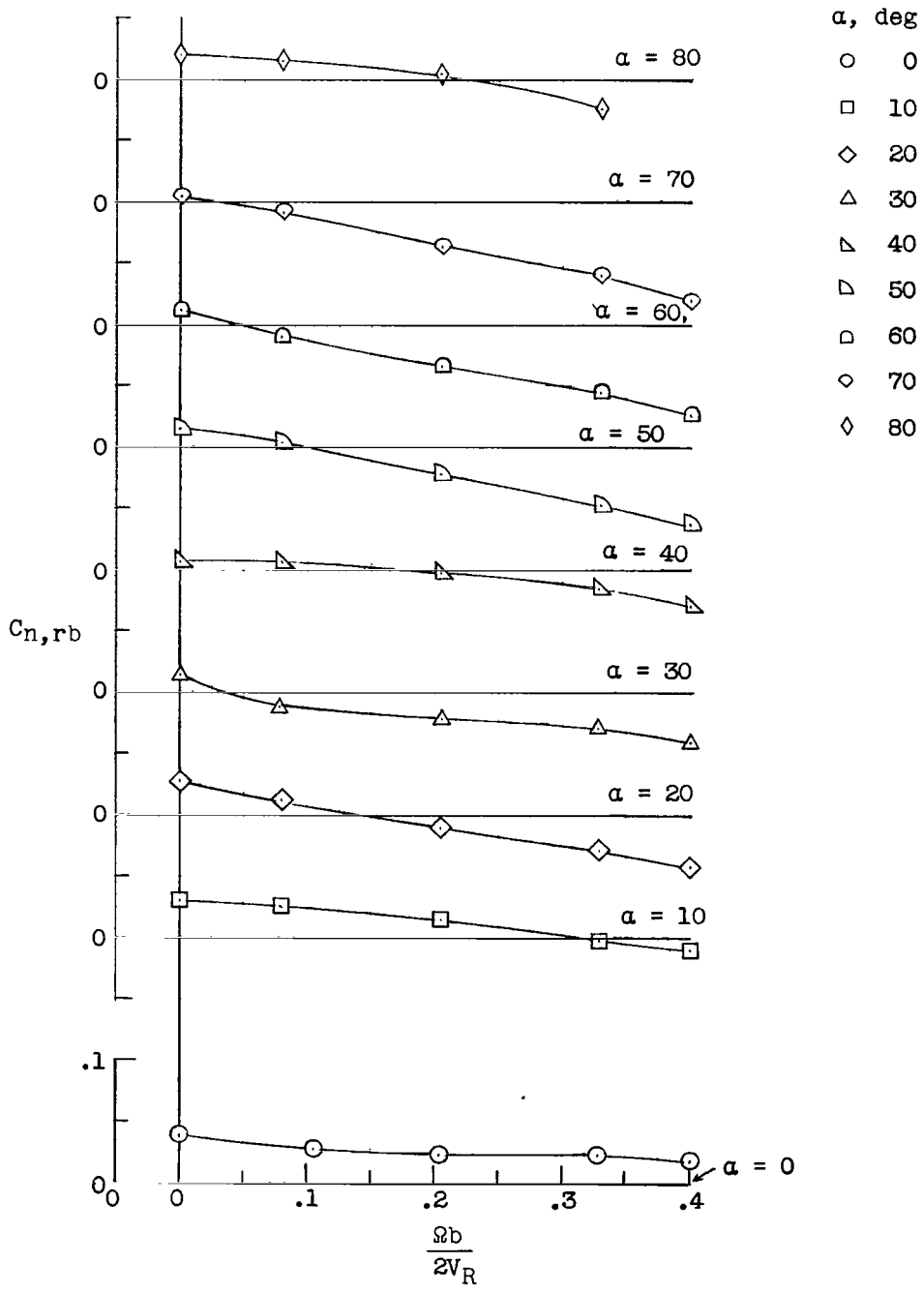

(b) $\beta = 10^{\circ}$.

Figure 5.- Continued.

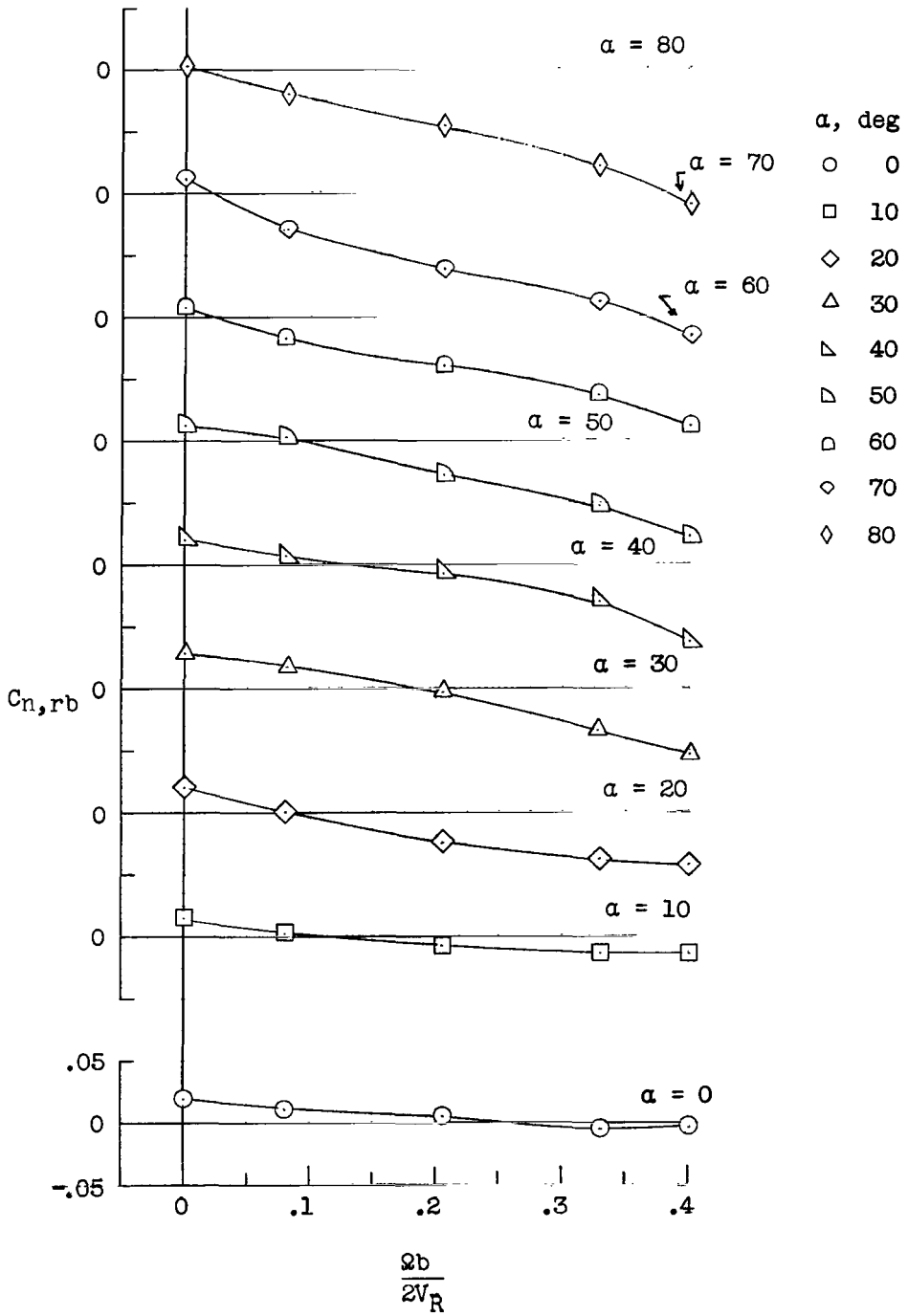

(c) $\beta = -10^\circ$.

Figure 5.- Concluded.

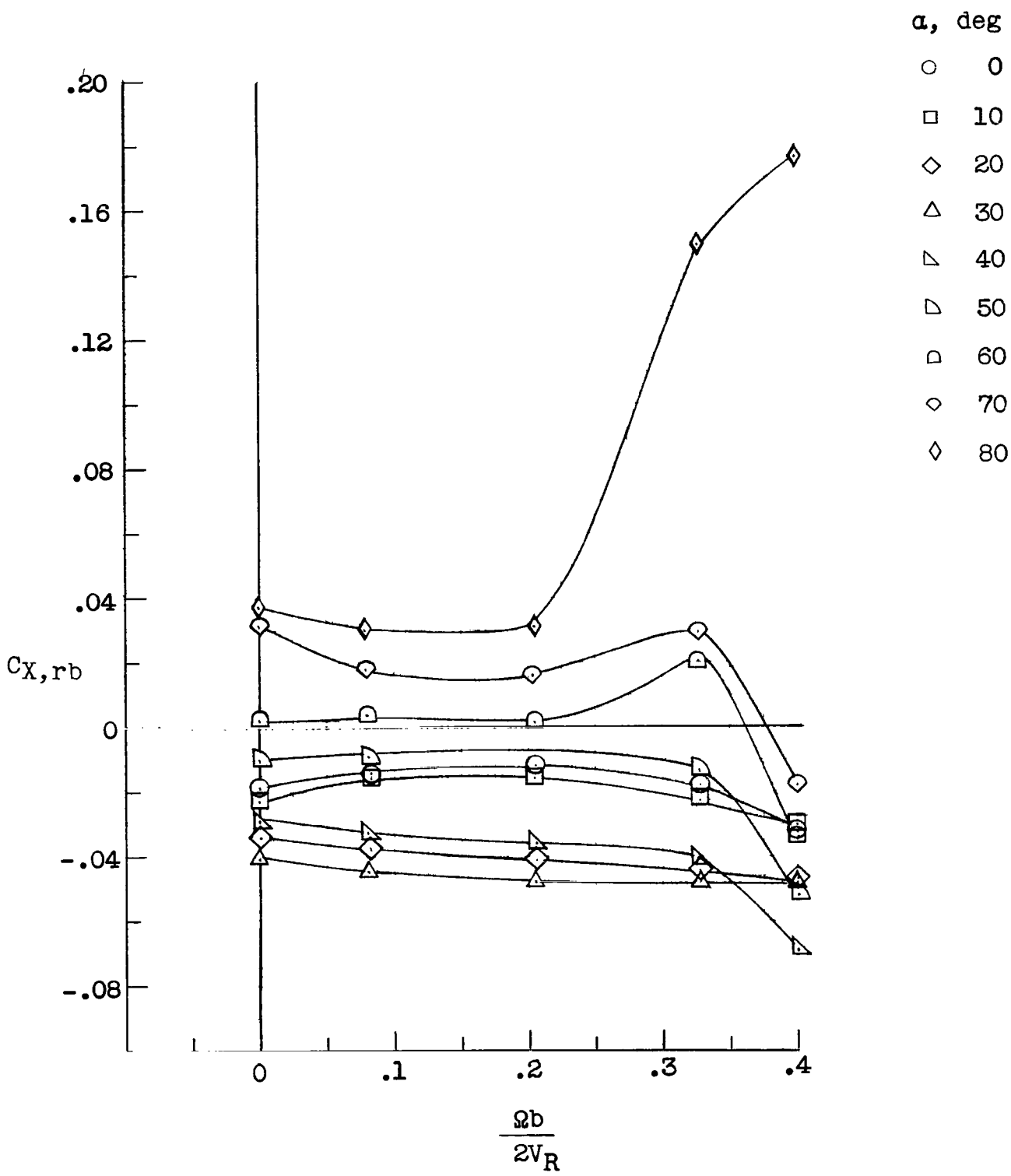

(a) $\beta = 0^{\circ}$.

Figure 6.- Variation of $C_{X,rb}$ with $\frac{\Omega b}{2V_R}$ for various angles of attack.

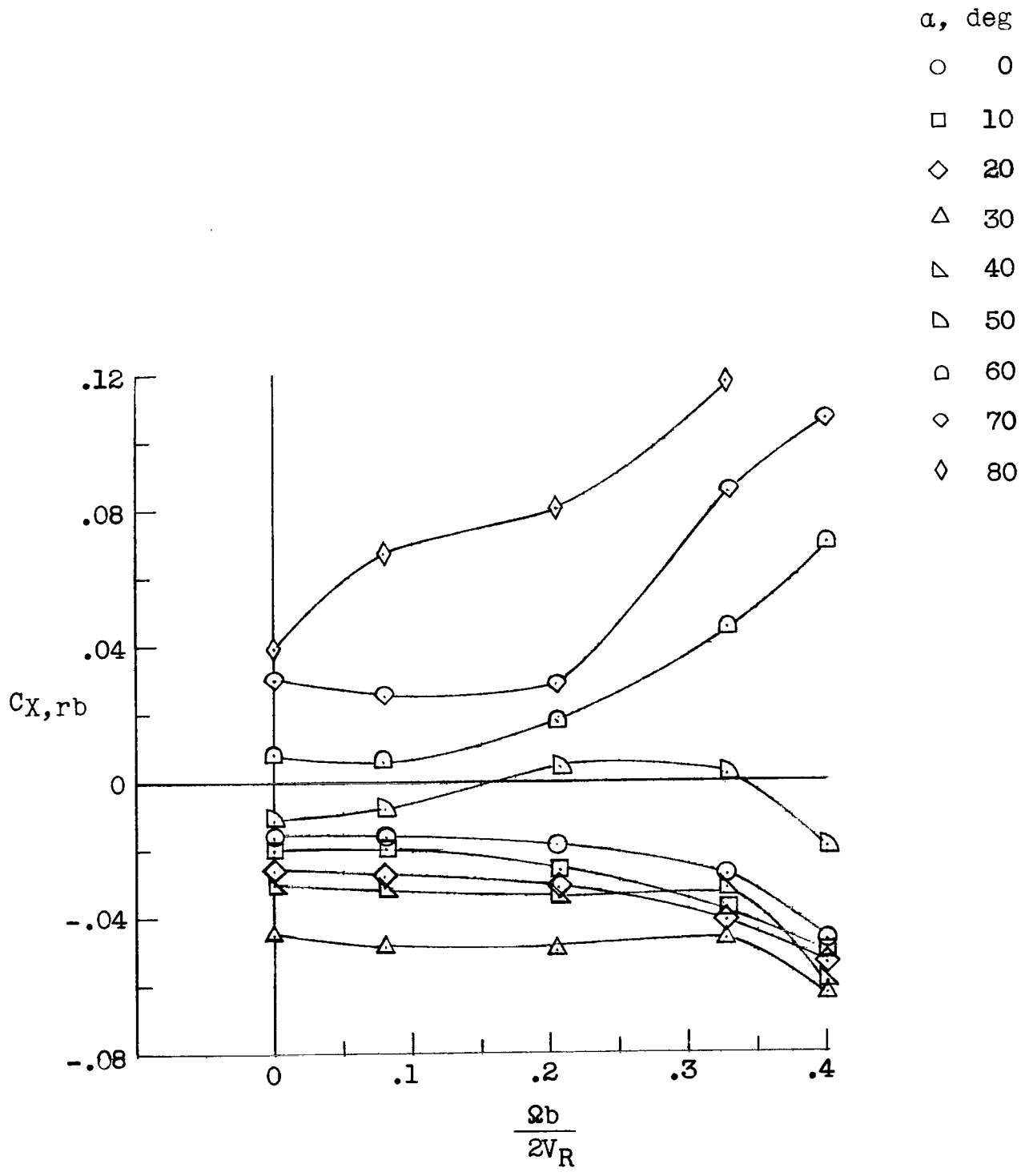

(b) $\beta = 10^{\circ}$.

Figure 6.- Continued.

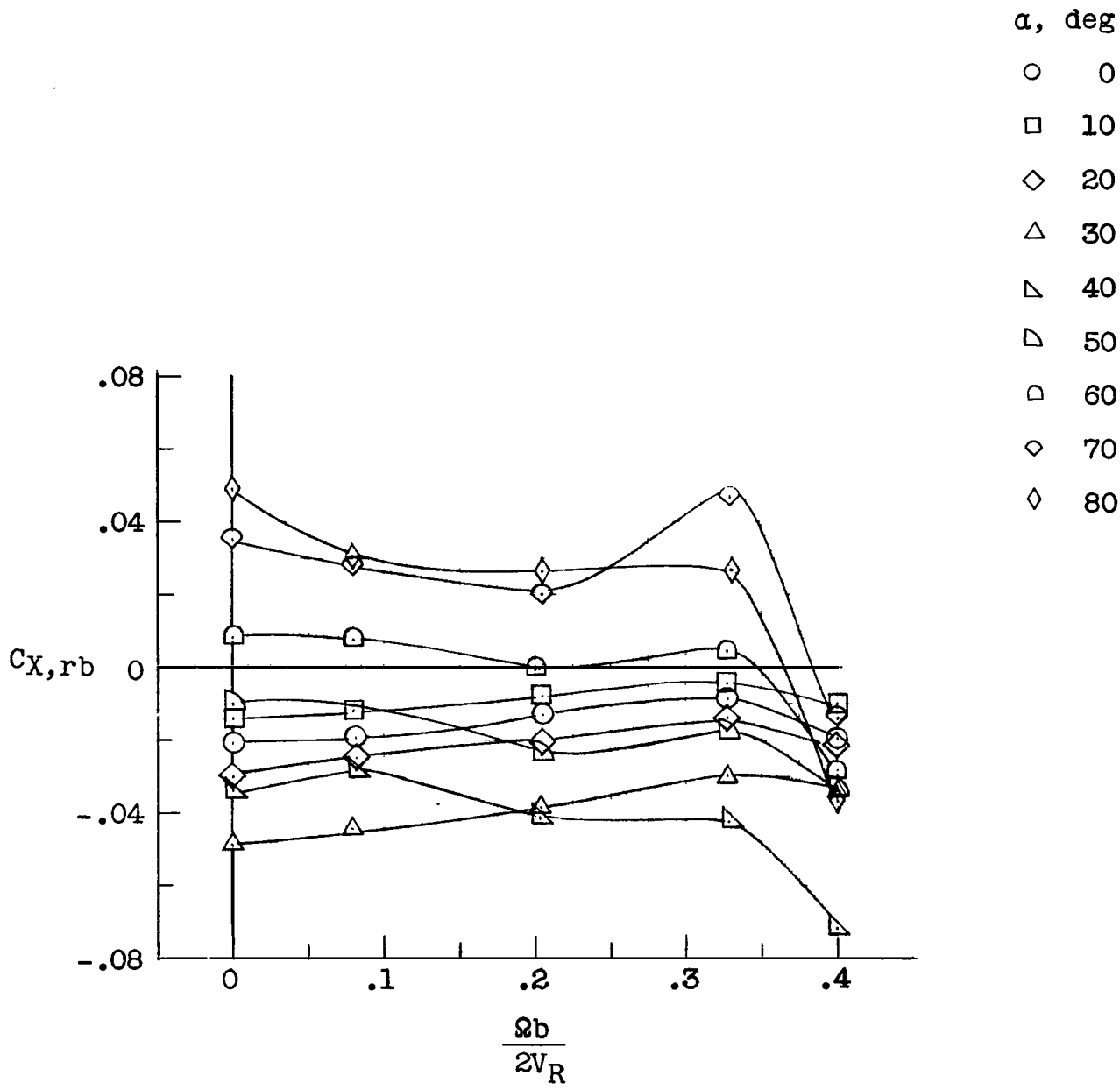

(c) $\beta = -10^{\circ}$.

Figure 6.- Concluded.

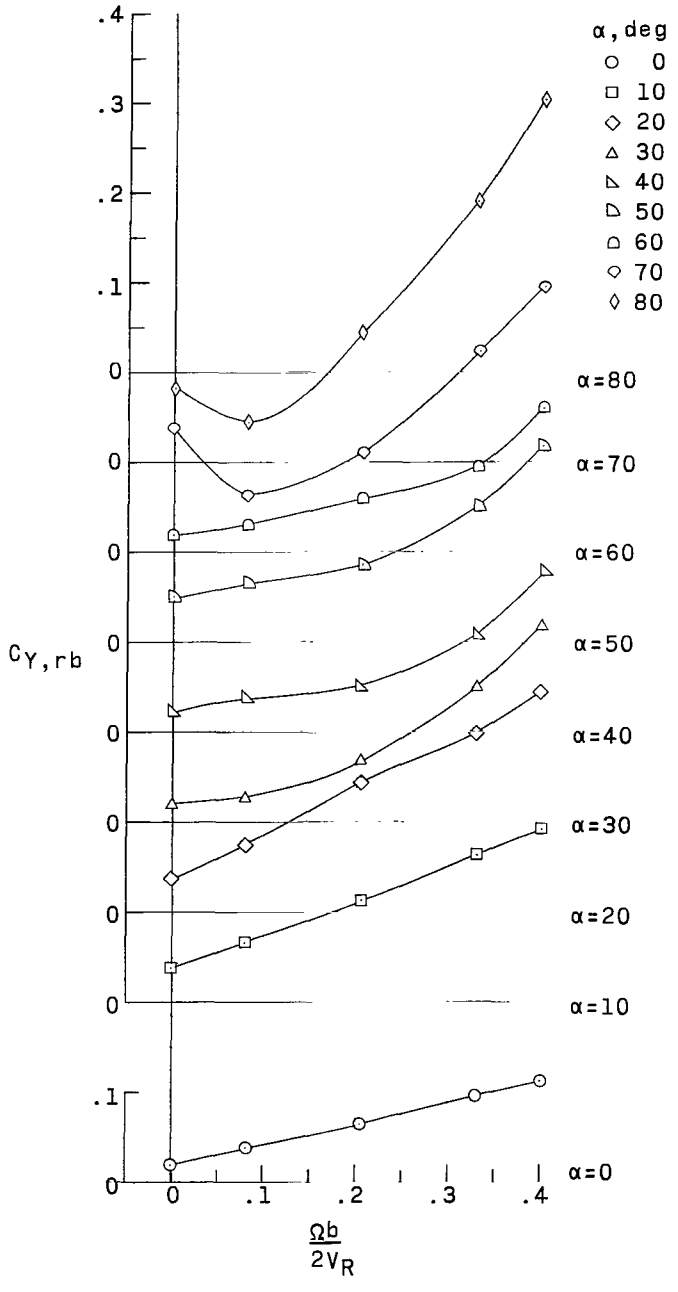

(a) $\beta = 0^\circ$.

Figure 7.- Variation of $C_{Y,rb}$ with $\frac{\Omega b}{2V_R}$ for various angles of attack.

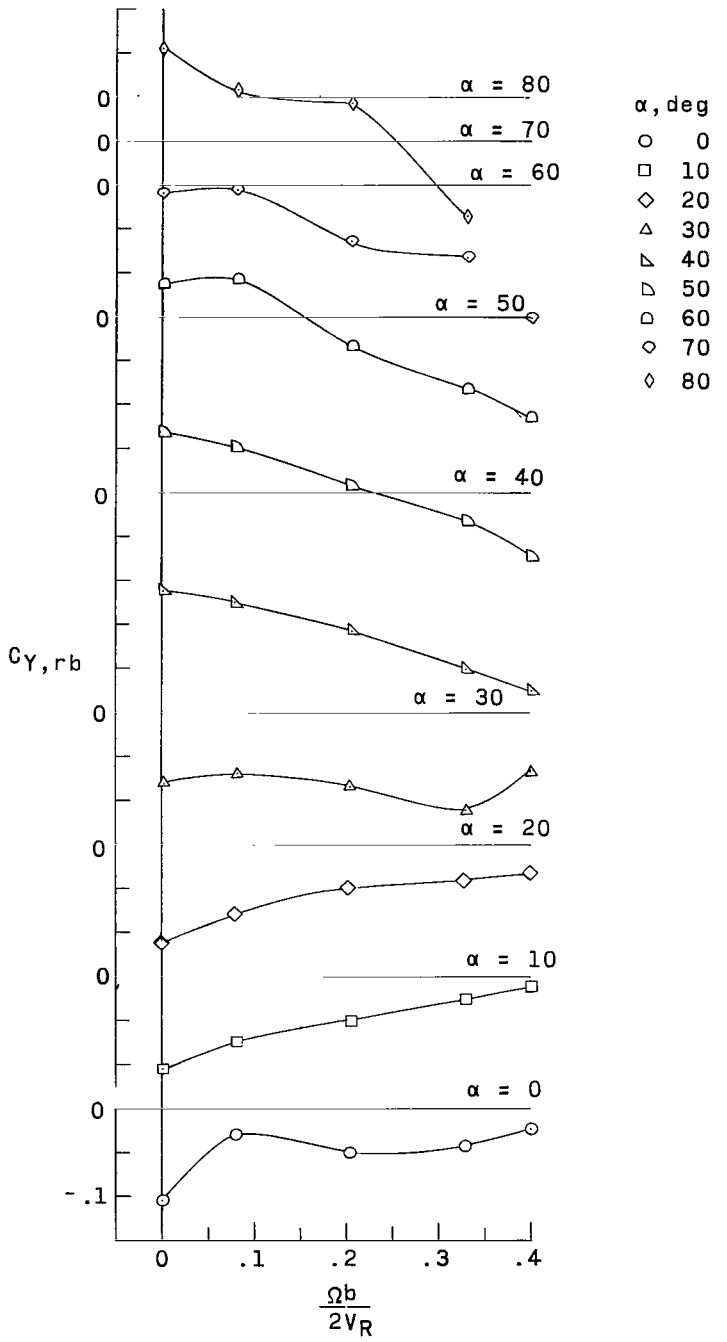

(b) $\beta = 10^{\circ}$.

Figure 7.- Continued.

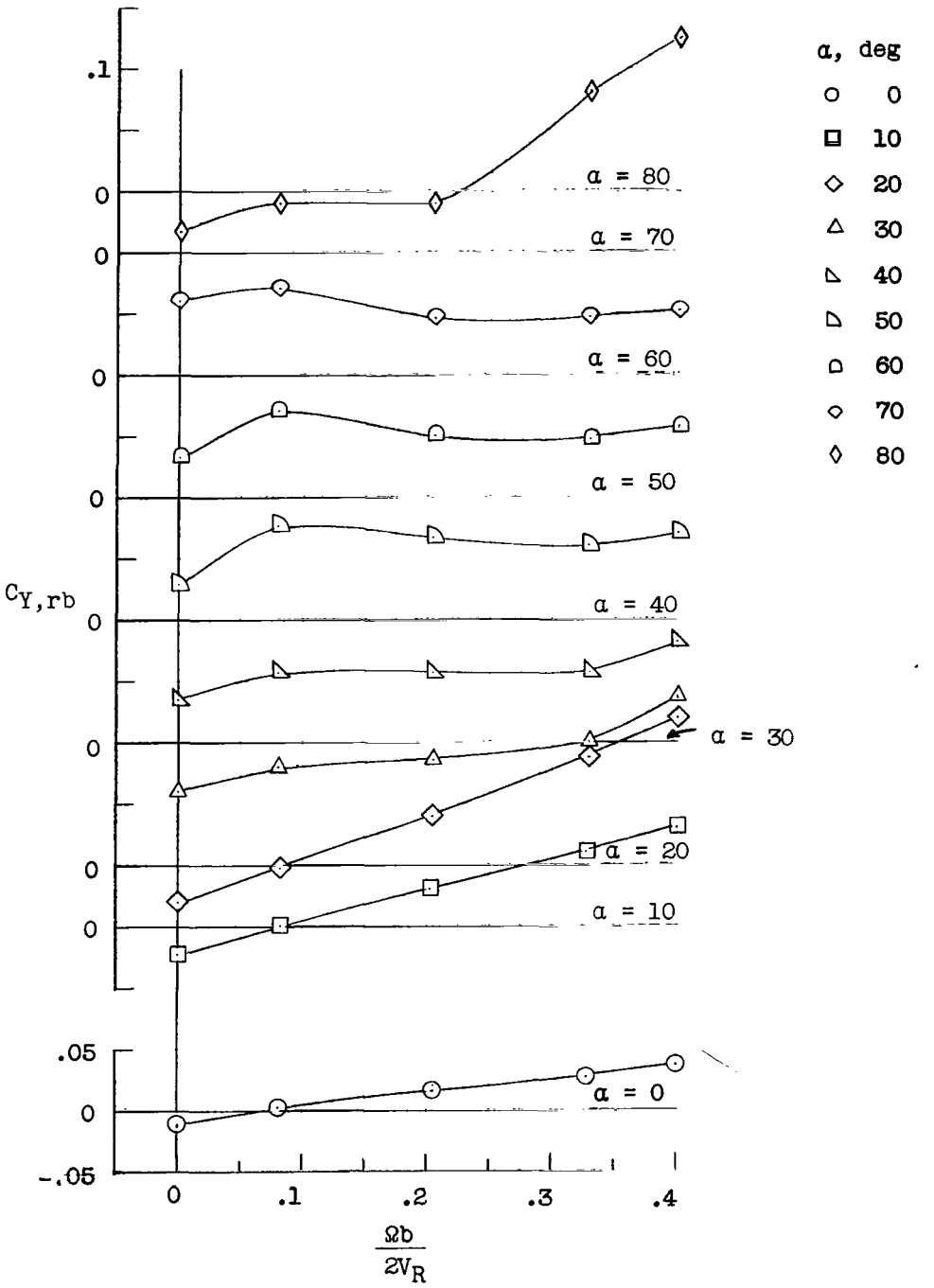

(c) $\beta = -10^{\circ}$.

Figure 7.- Concluded.

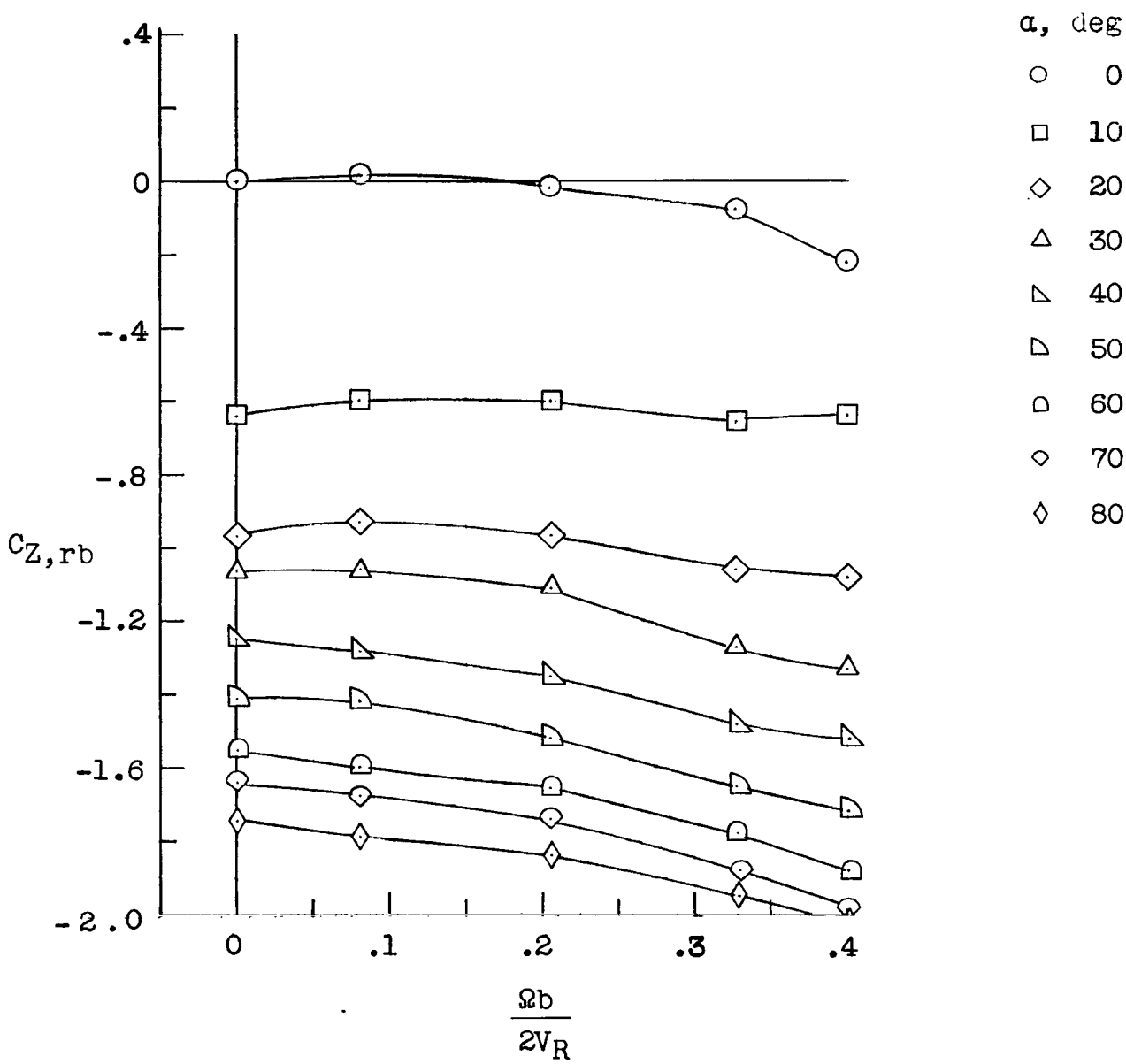

(a) $\beta = 0°$.

Figure 8.- Variation of $C_{Z,rb}$ with $\frac{\Omega b}{2V_R}$ for various angles of attack.

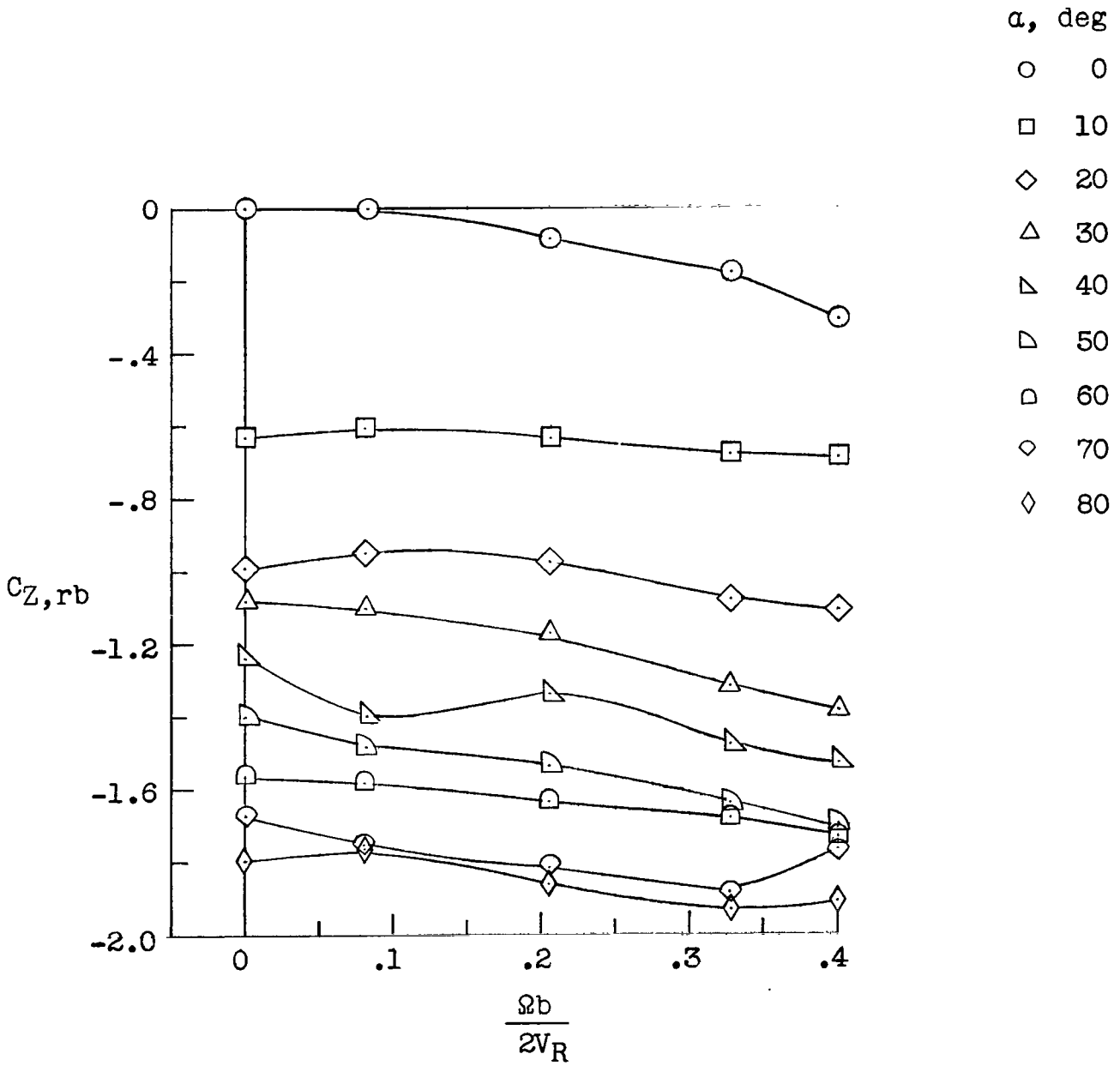

(b) $\beta = 10^{\circ}$.

Figure 8.- Continued.

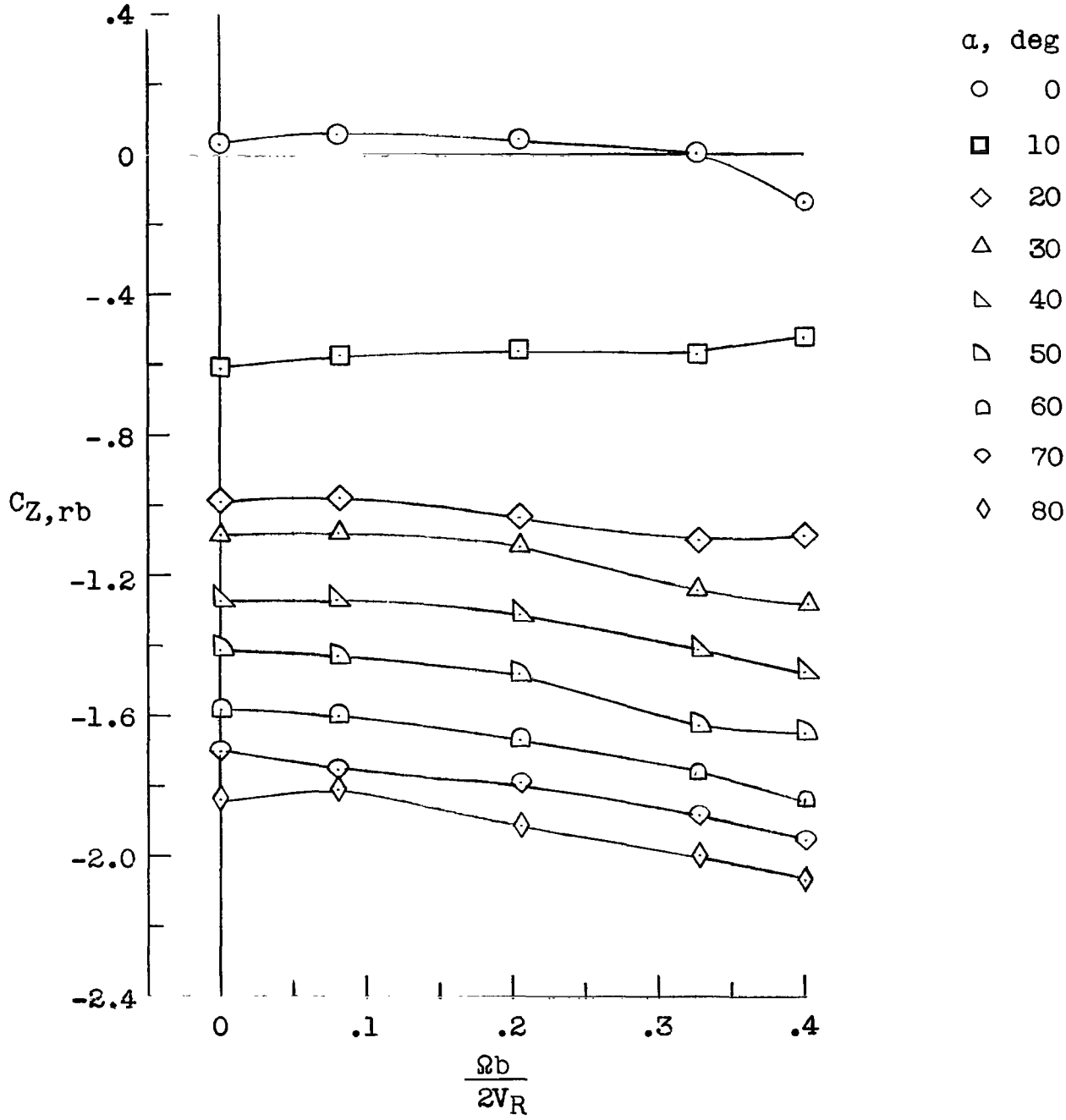

(c) $\beta = -10^{\circ}$.

Figure 8.- Concluded.

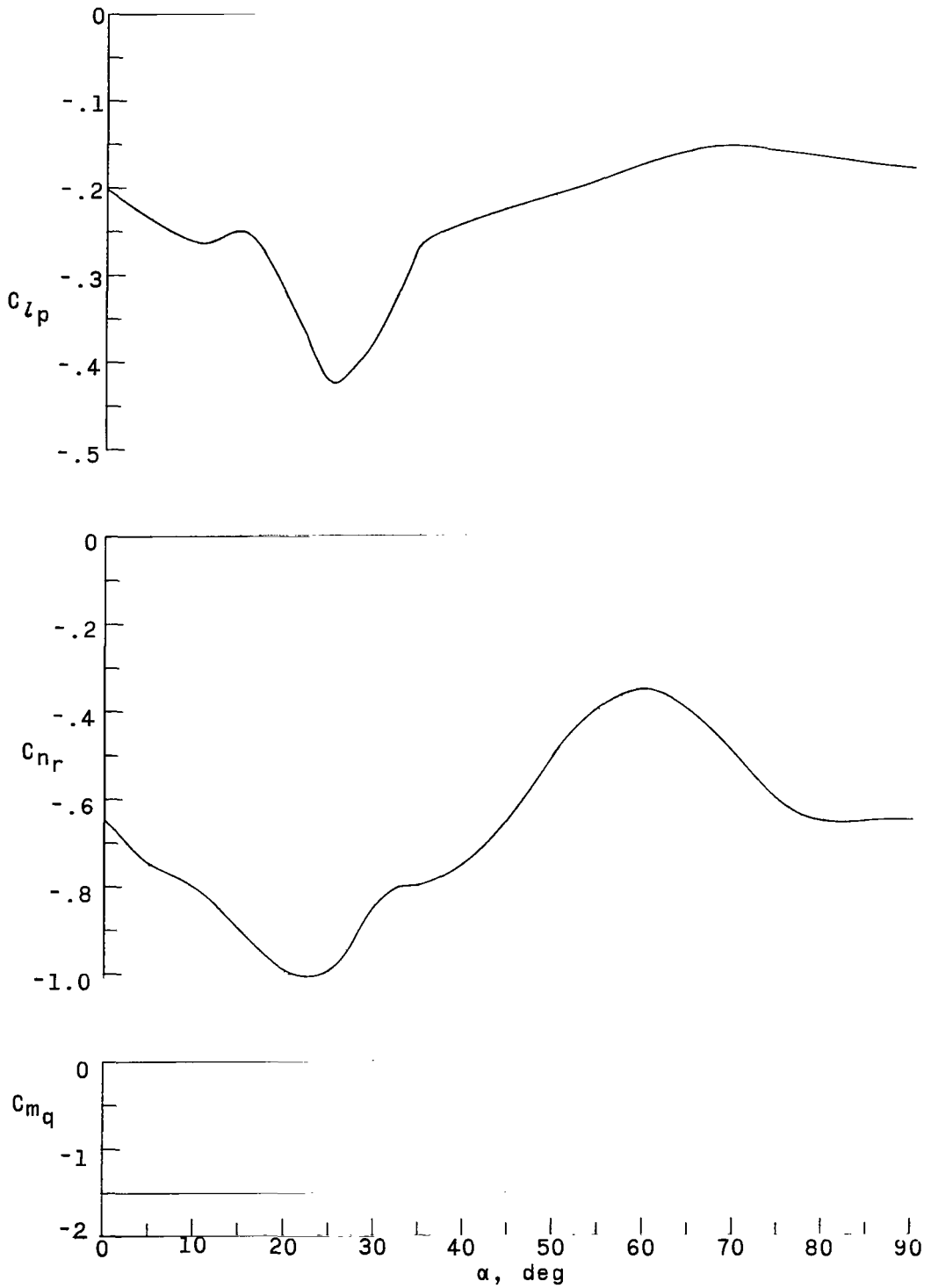

Figure 9.- Variations of the damping derivatives with angle of attack.

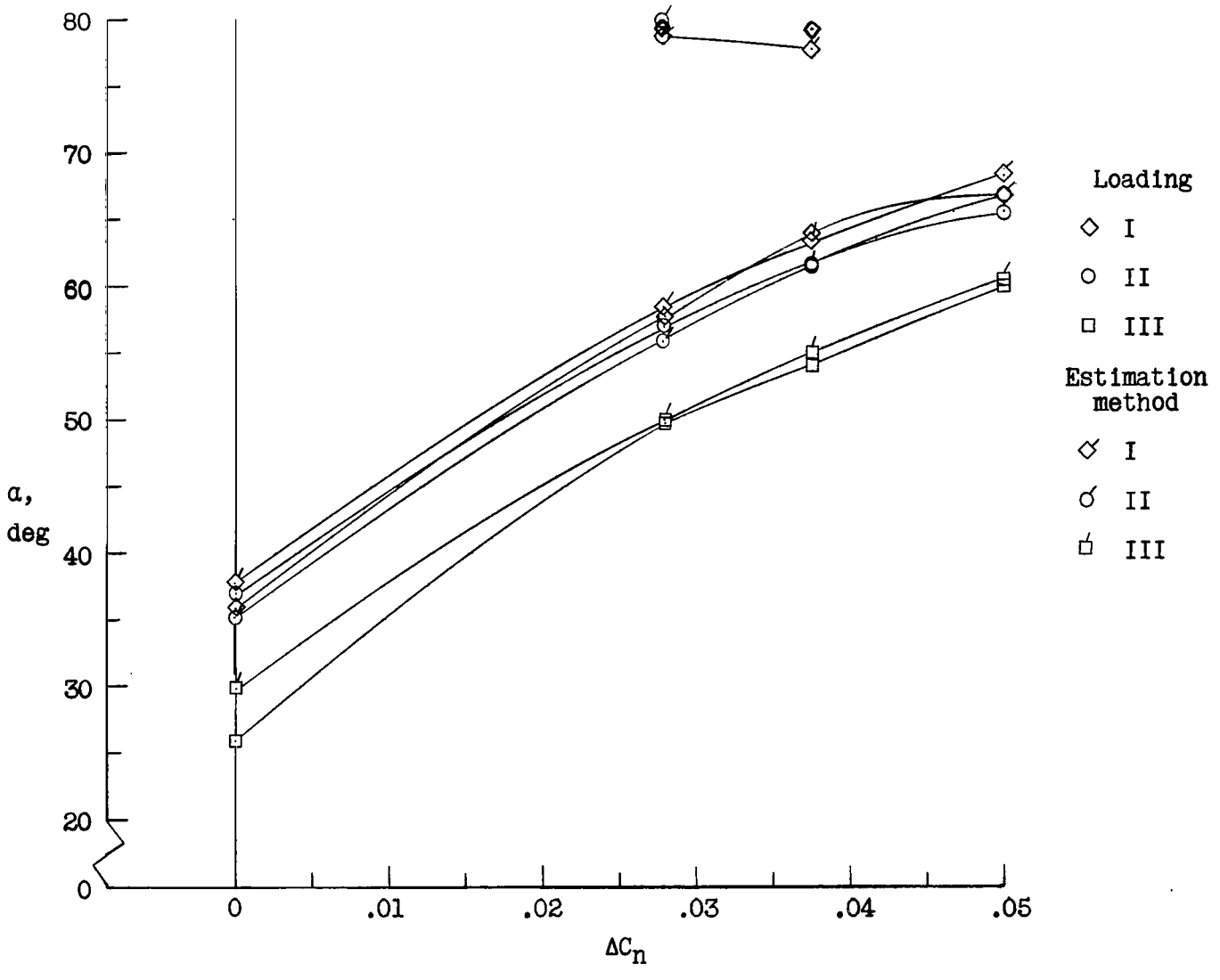

(a) α.

Figure 10.- Variations of α, Ω, and E_s with ΔC_n for all loadings and relative density of 25.6.

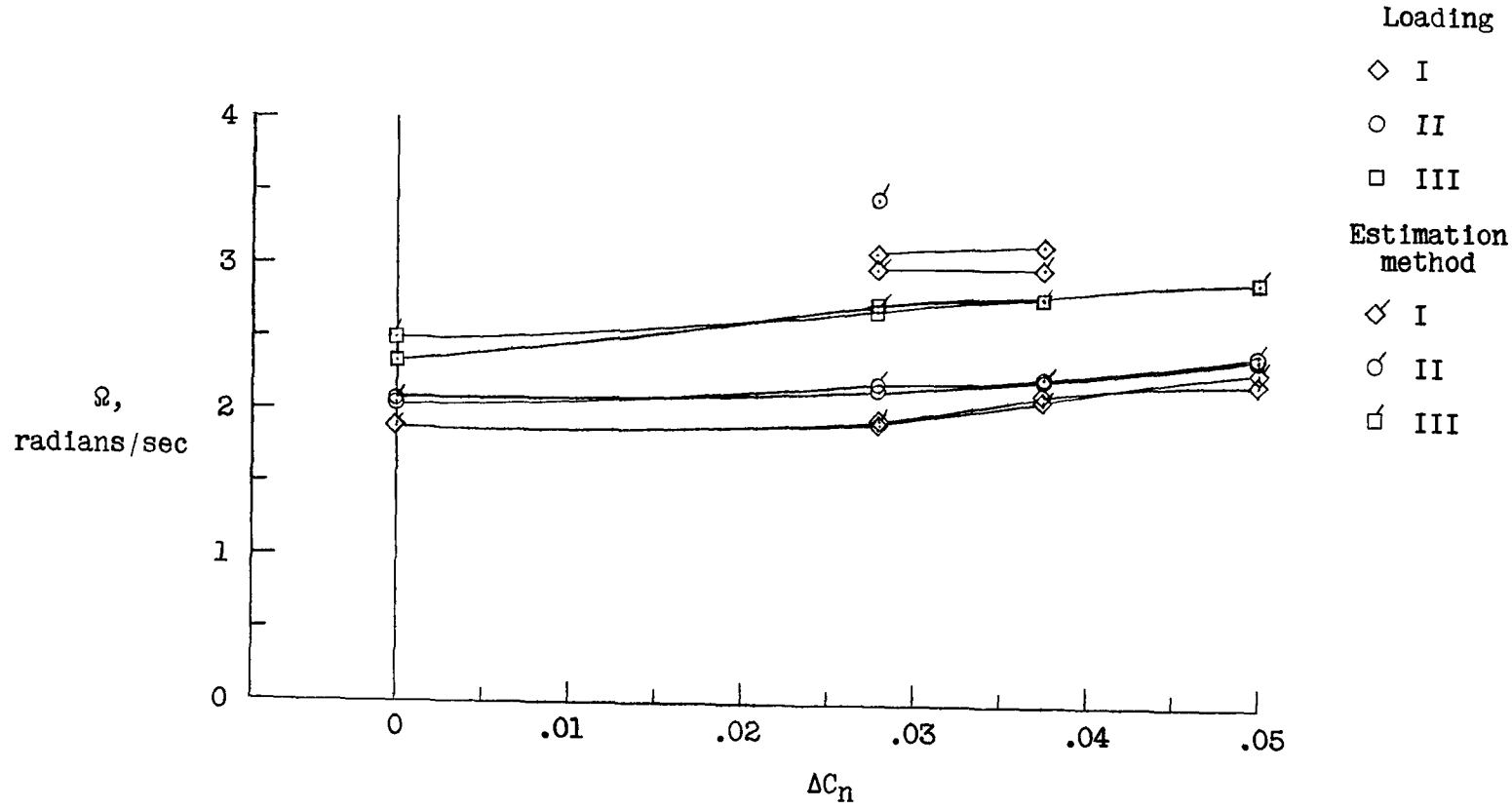

(b) Ω.

Figure 10.- Continued.

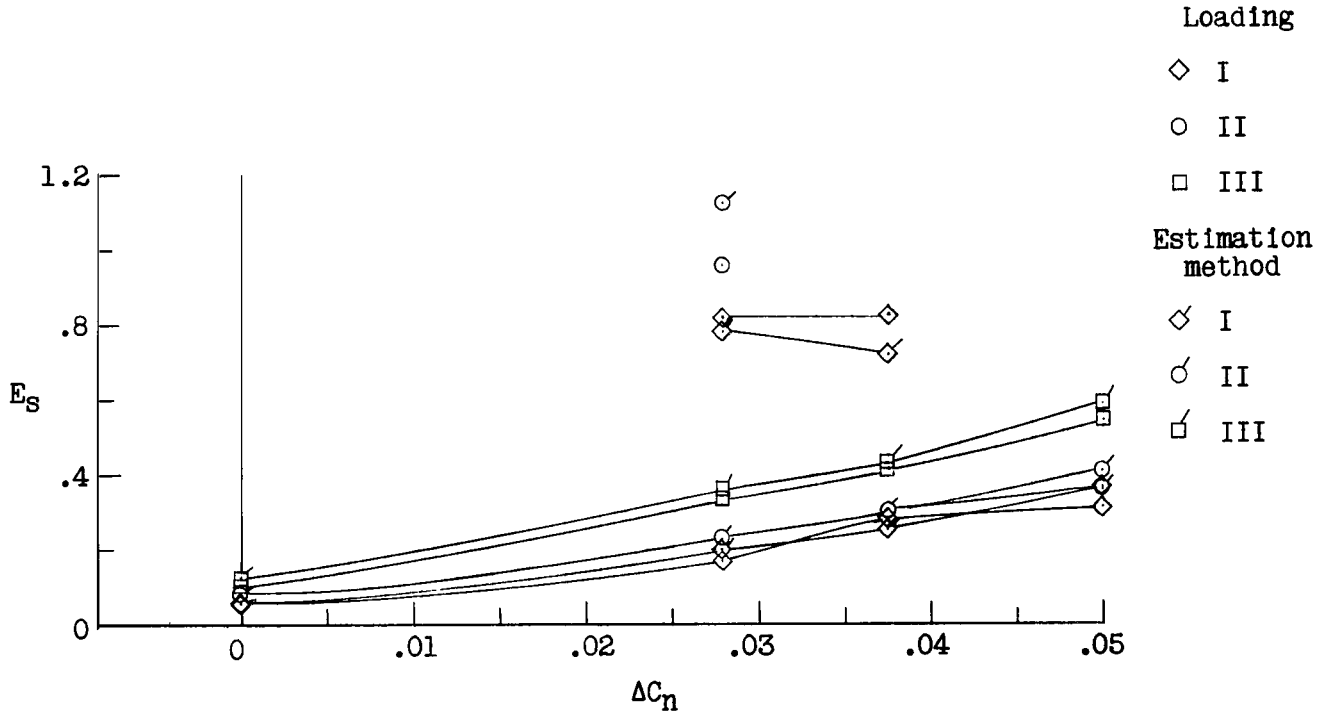

(c) E_s.

Figure 10.- Concluded.

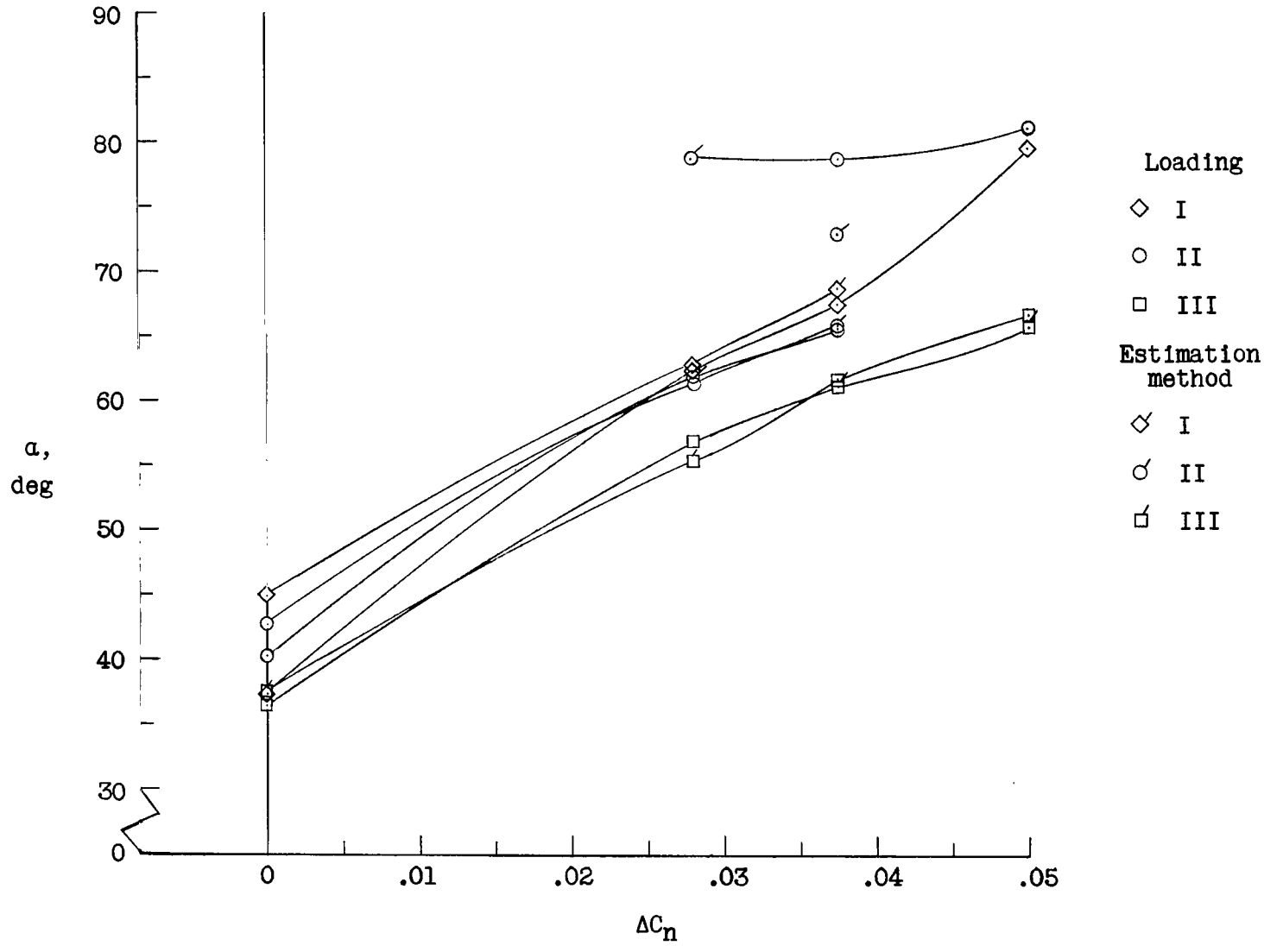

(a) α.

Figure 11.- Variation of α, Ω, and E_s with ΔC_n for all loadings and relative density of 43.1.

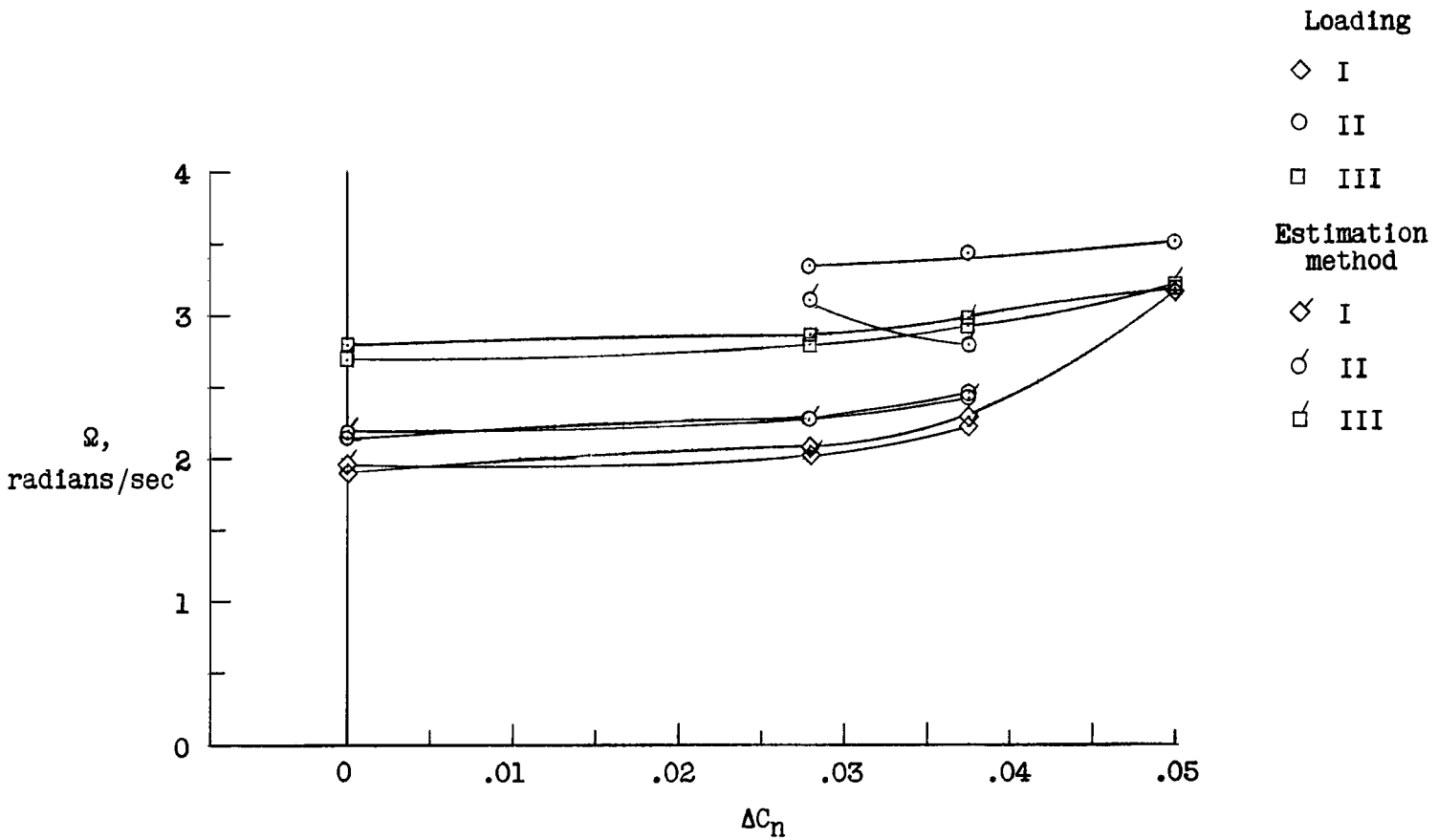

(b) Ω.

Figure 11.- Continued.

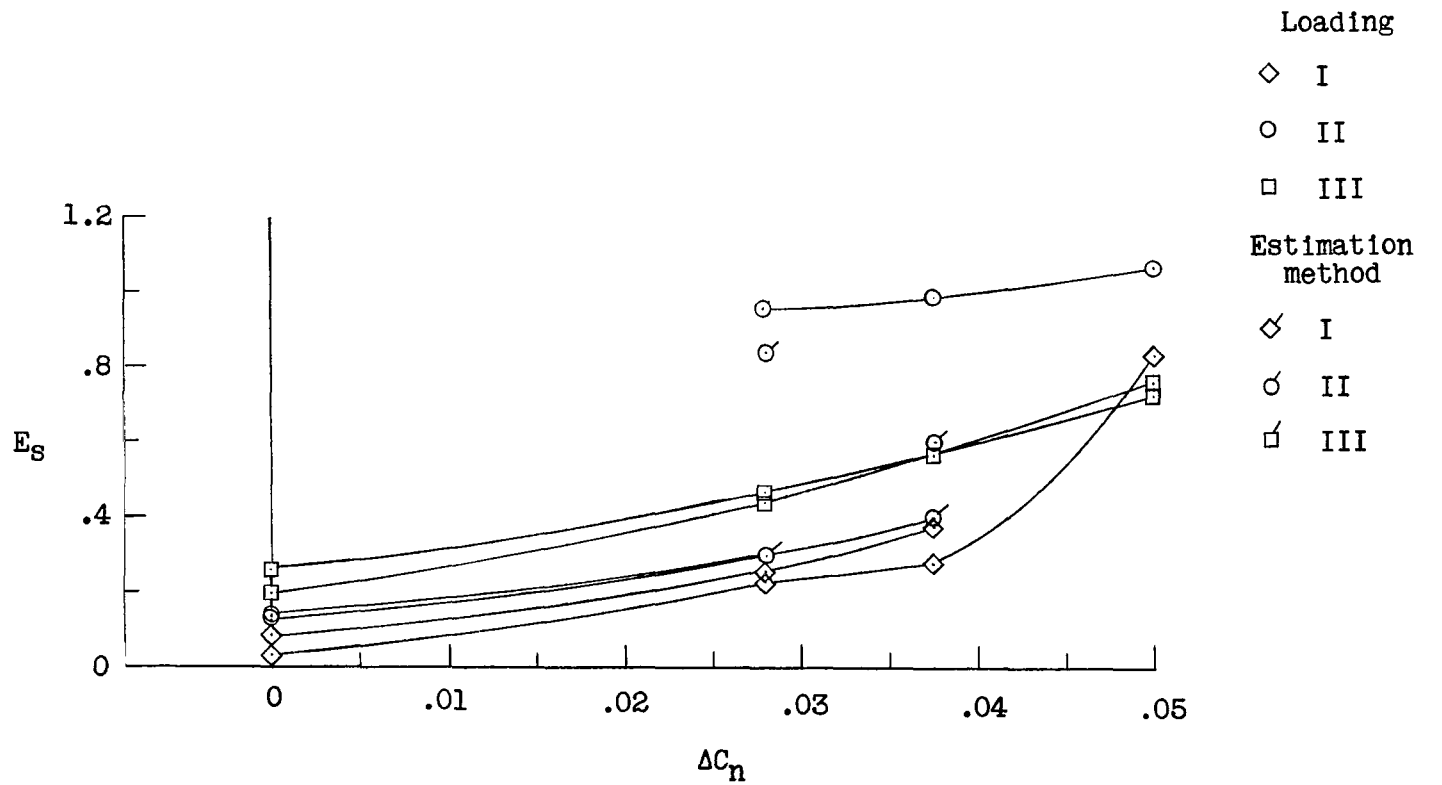

(c) E_s.

Figure 11.- Concluded.

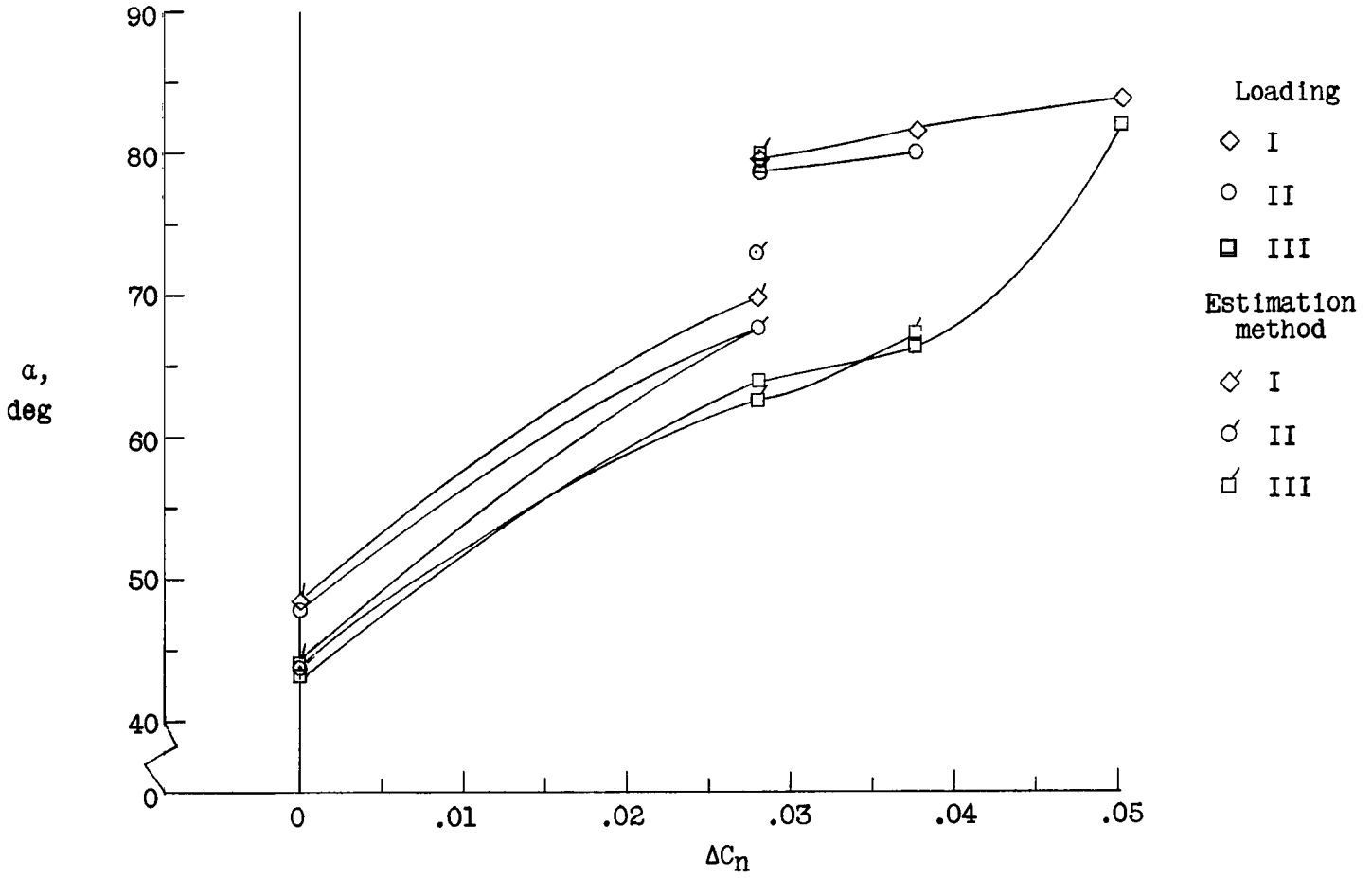

(a) α.

Figure 12.- Variation of α, Ω, and E_s with ΔC_n for all loadings and relative density of 83.5.

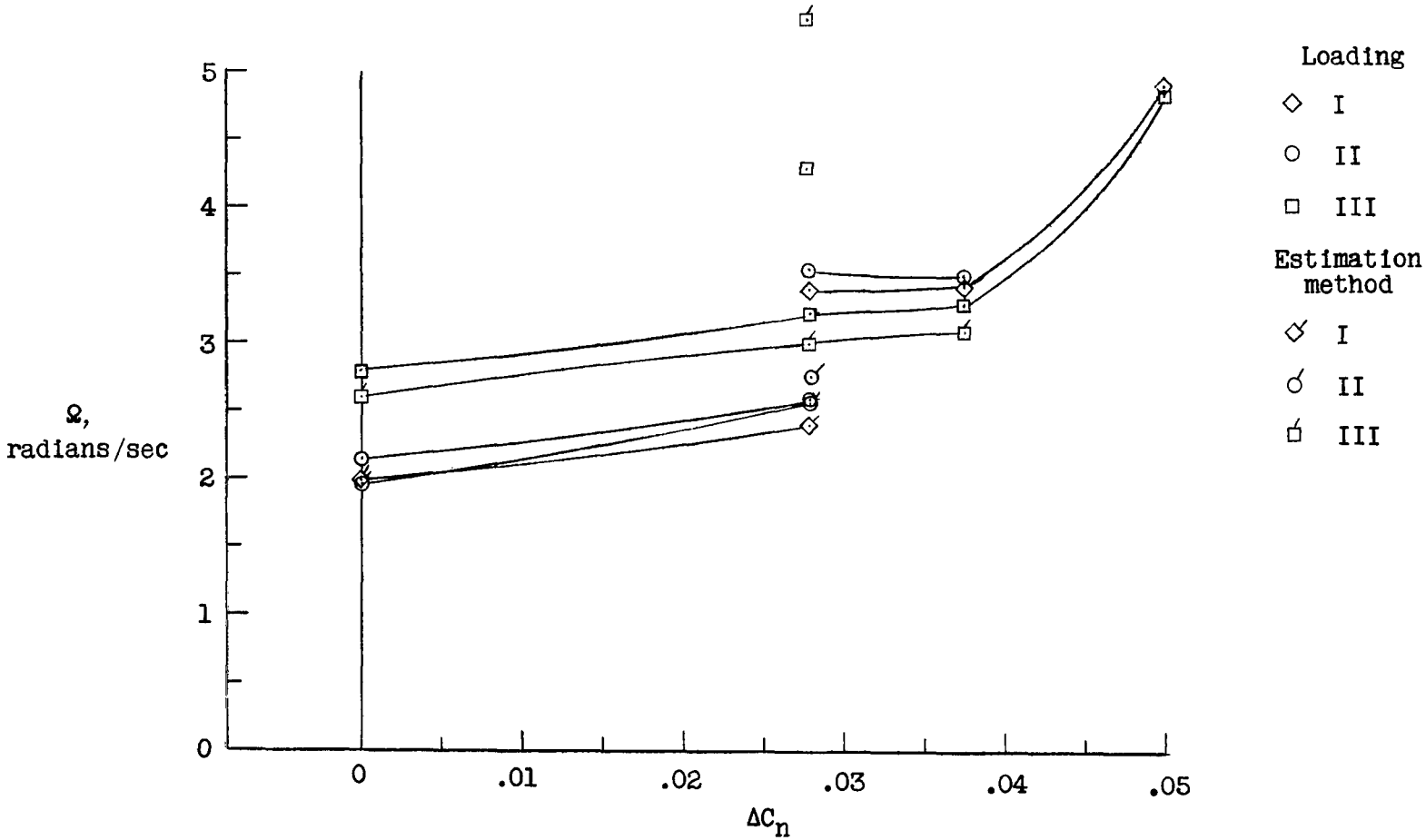

(b) Ω.

Figure 12.- Continued.

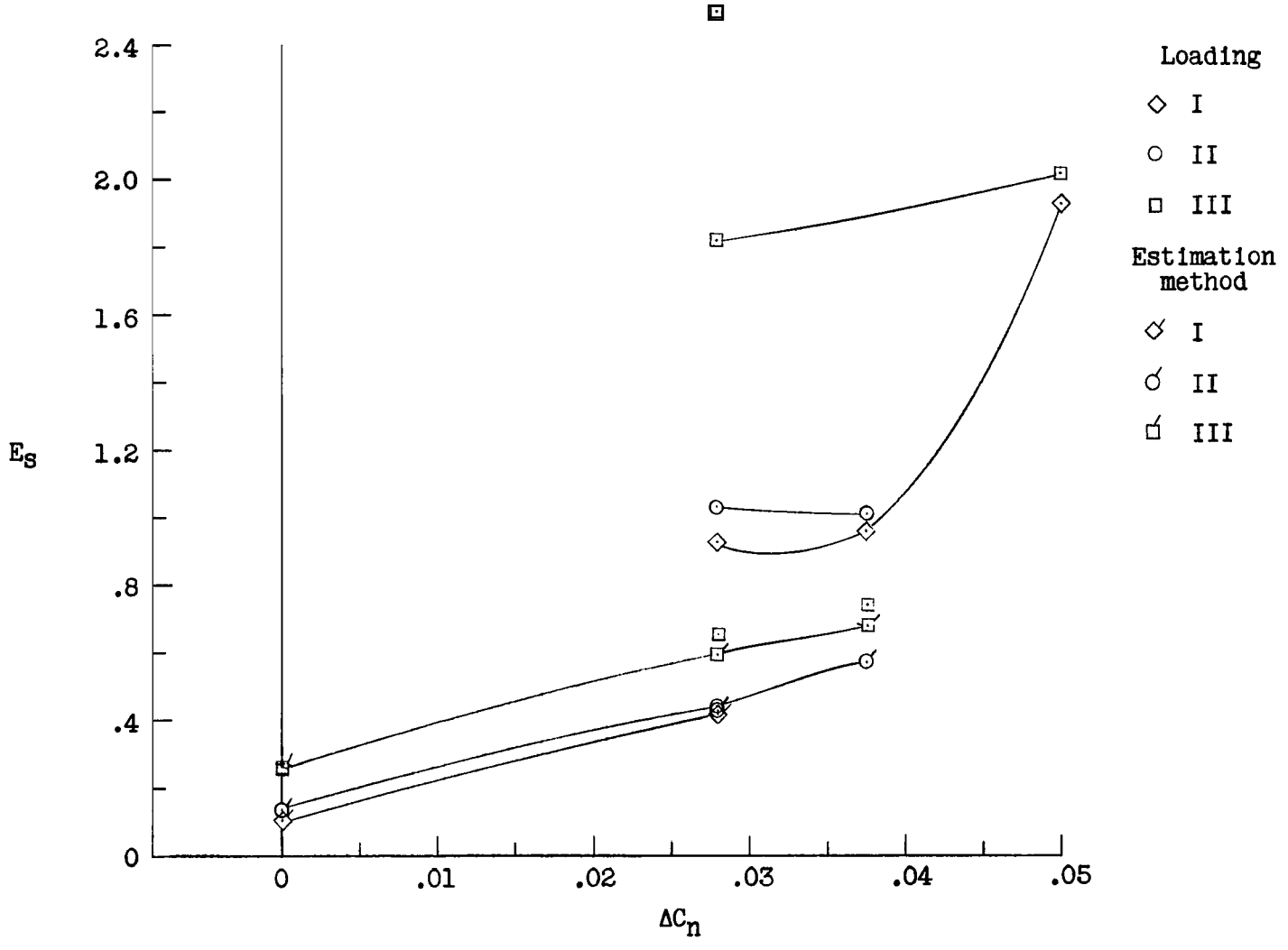

(c) E_s.

Figure 12.- Concluded.

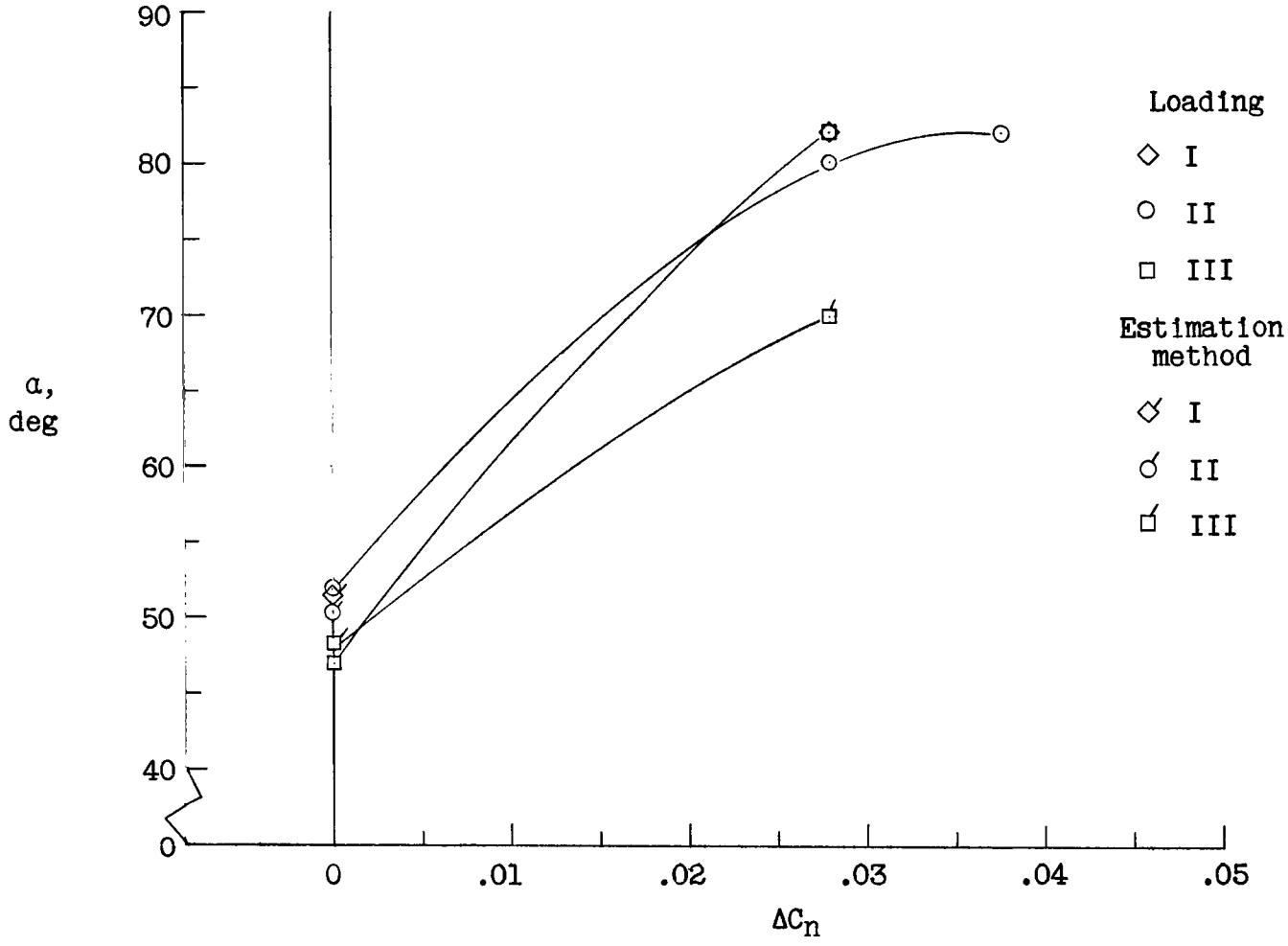

(a) α.

Figure 13.- Variation of α, Ω, and E_s with ΔC_n for all loadings and relative density of 171.1.

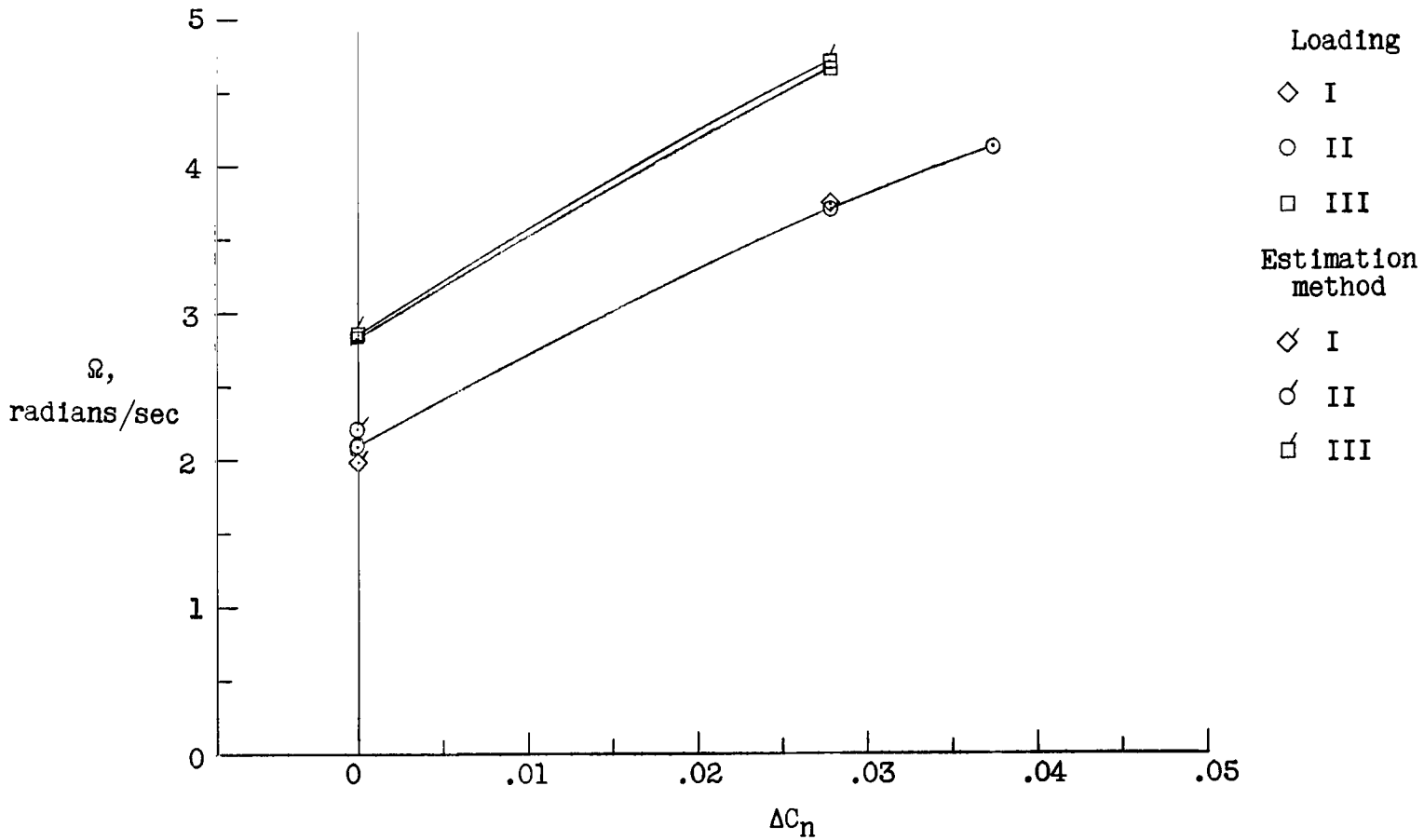

(b) Ω.

Figure 13.- Continued.

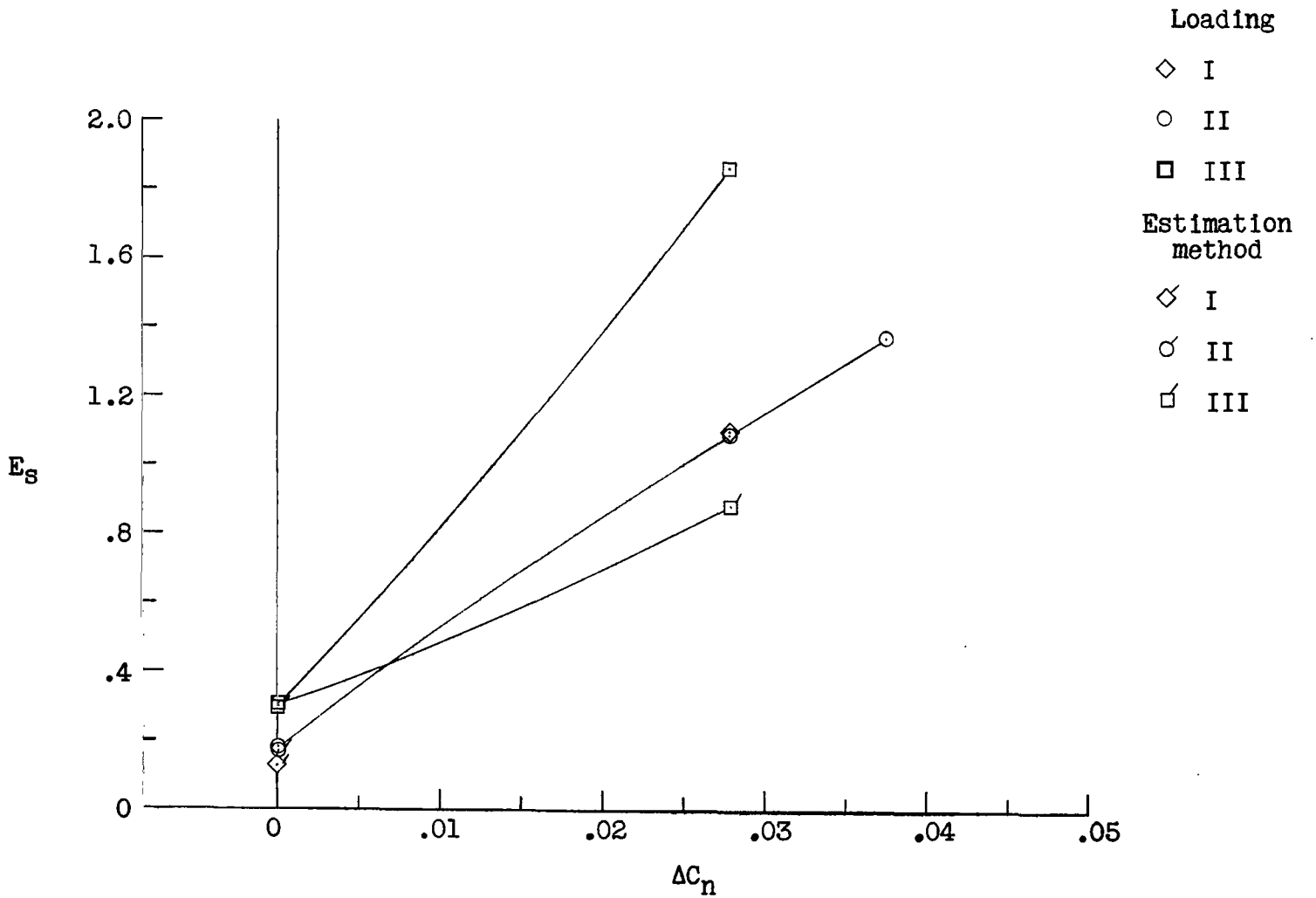

(c) E_s.

Figure 13.- Concluded.

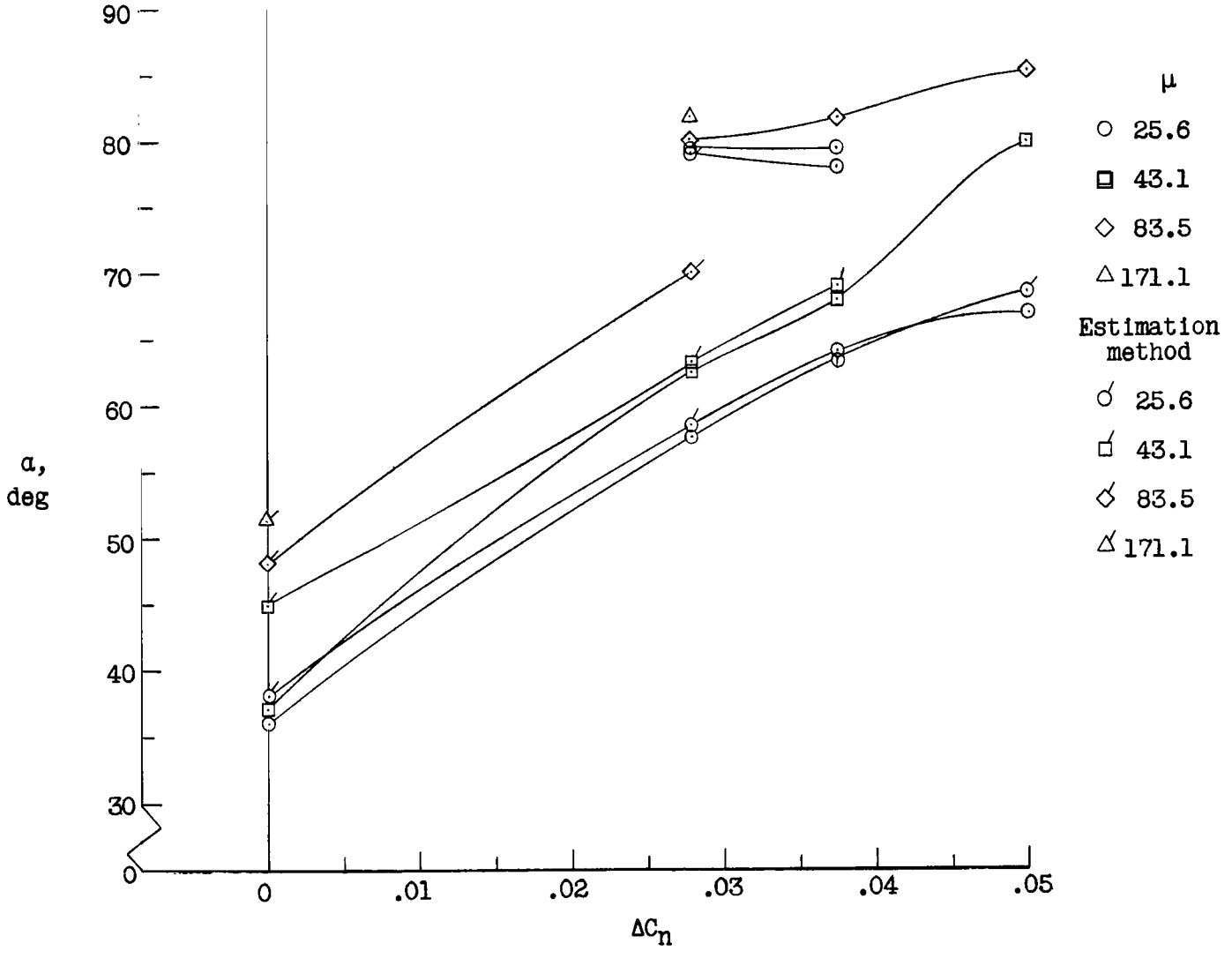

(a) α.

Figure 14.- Variation of α, Ω, and E_s with ΔC_n for all relative densities and loading I.

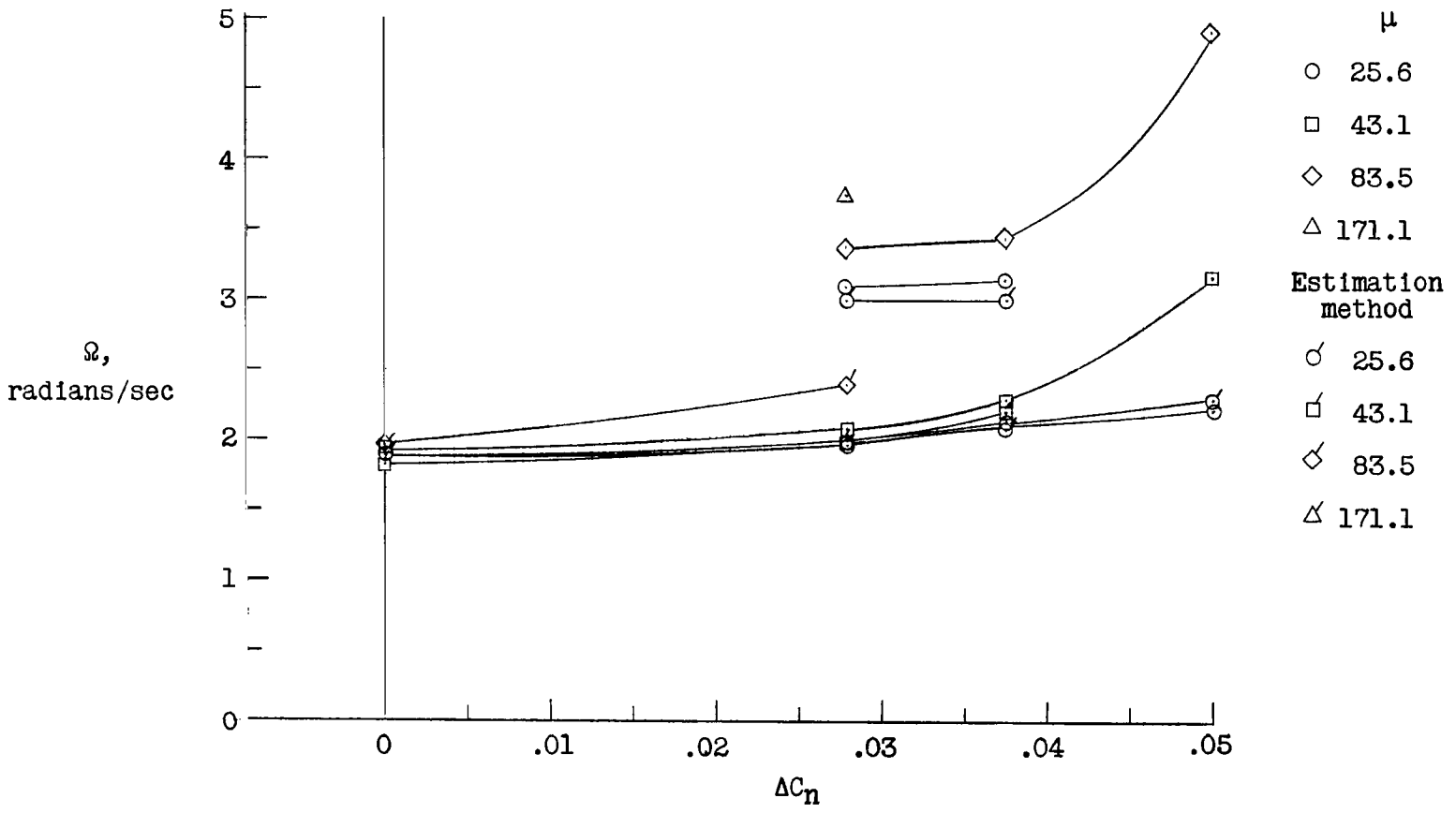

(b) Ω.

Figure 14.- Continued.

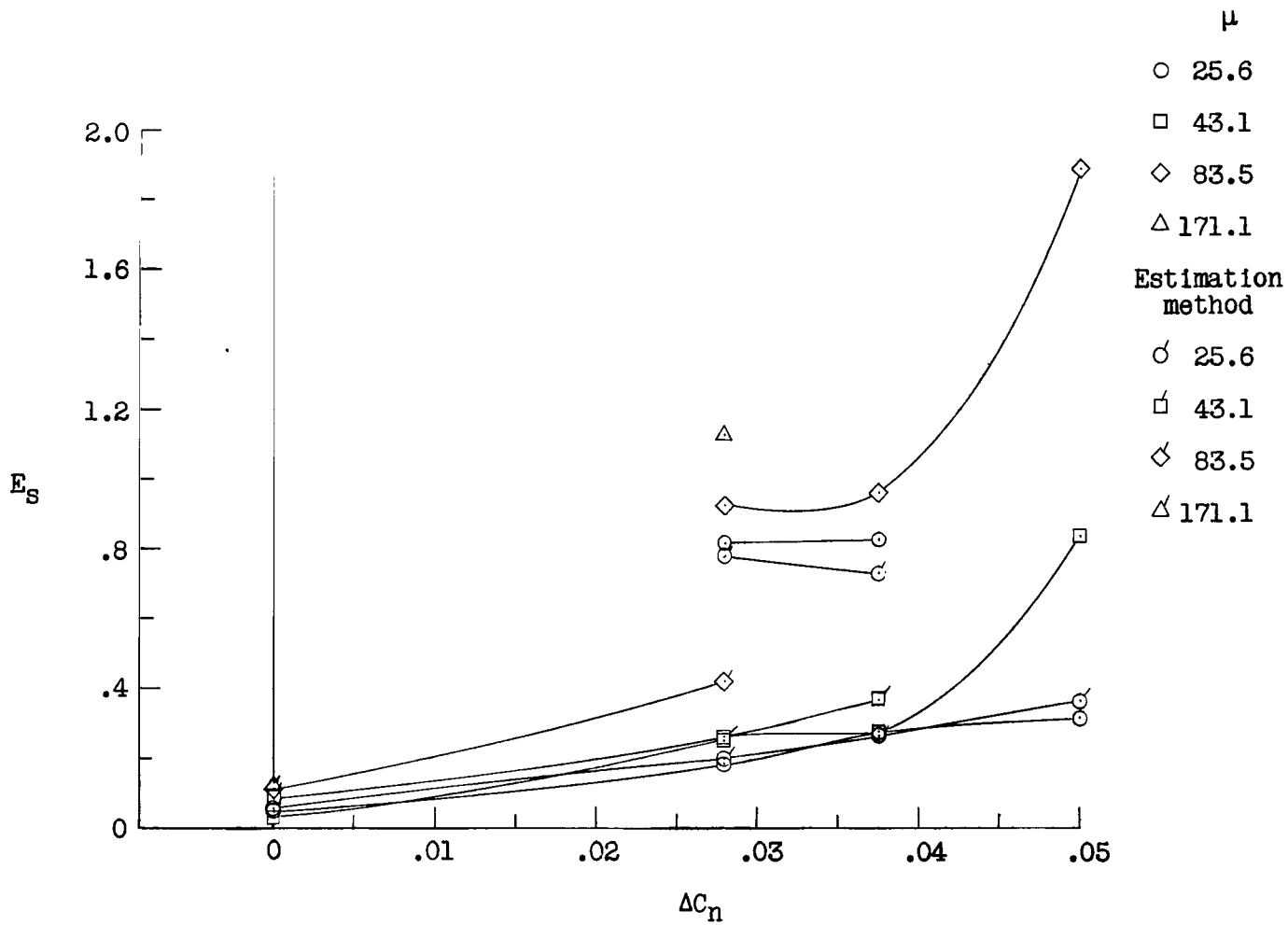

(c) E_s.

Figure 14.- Concluded.

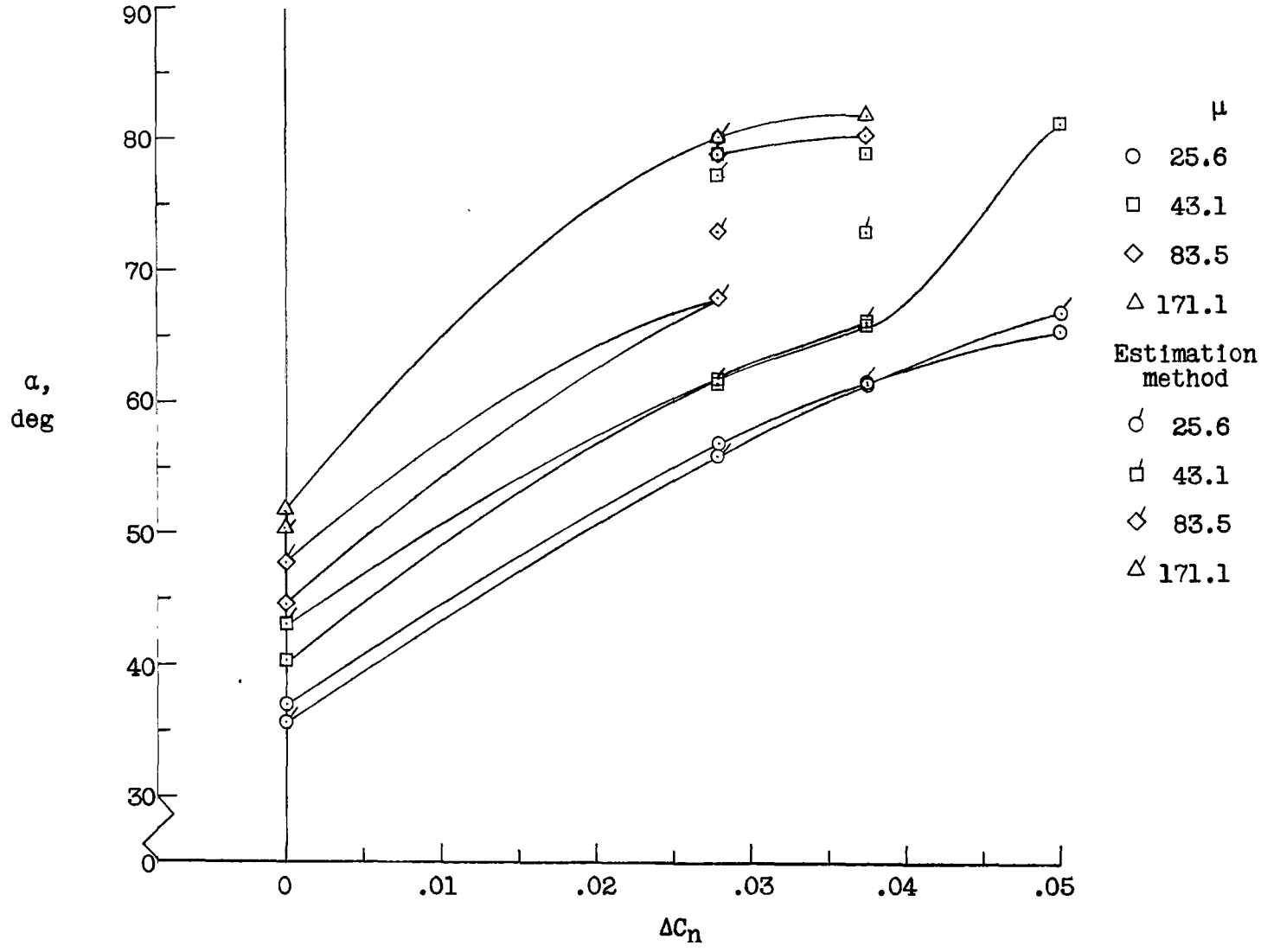

(a) α.

Figure 15.- Variation of α, Ω, and E_s with ΔC_n for all relative densities and loading II.

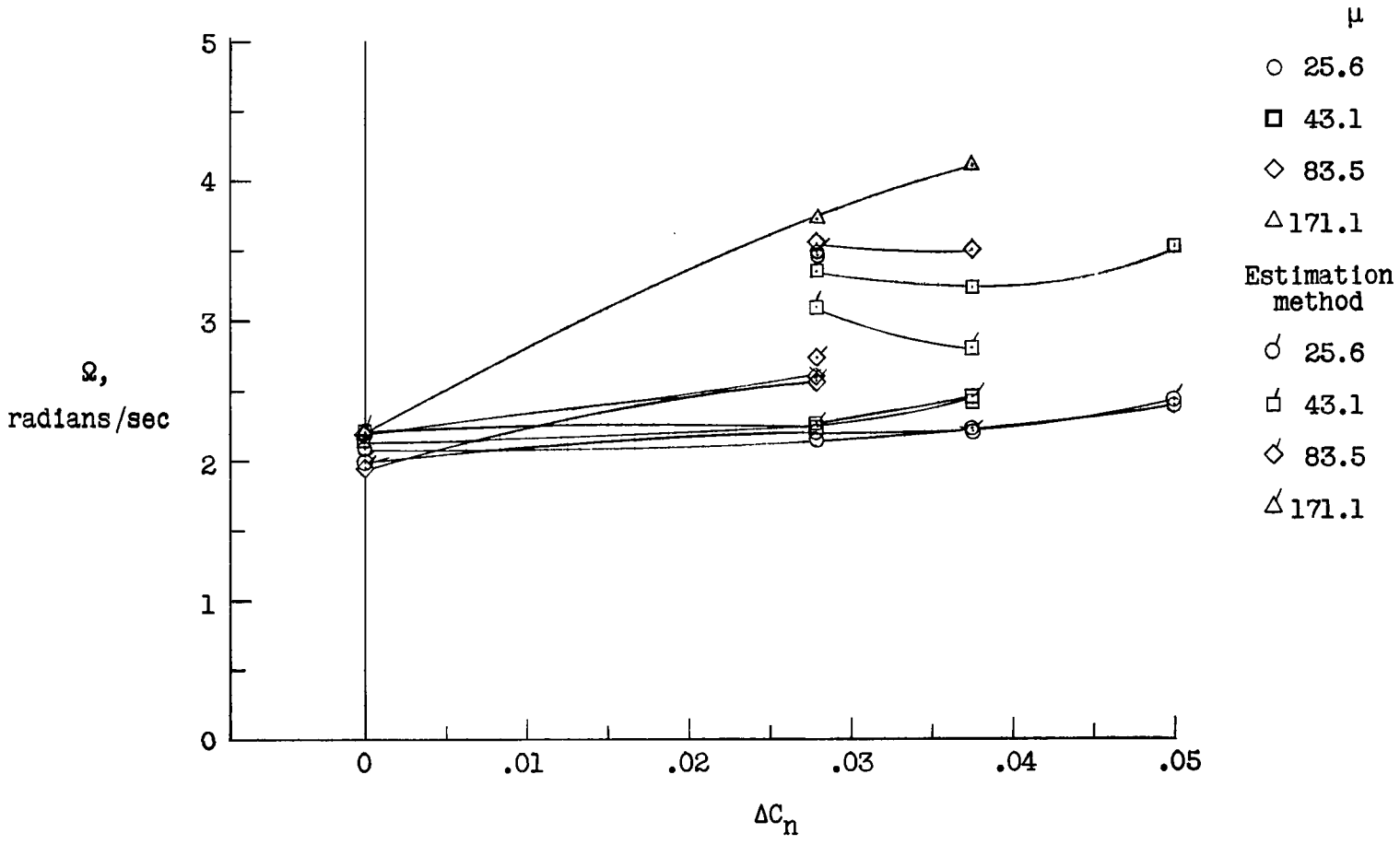

(b) Ω.

Figure 15.- Continued.

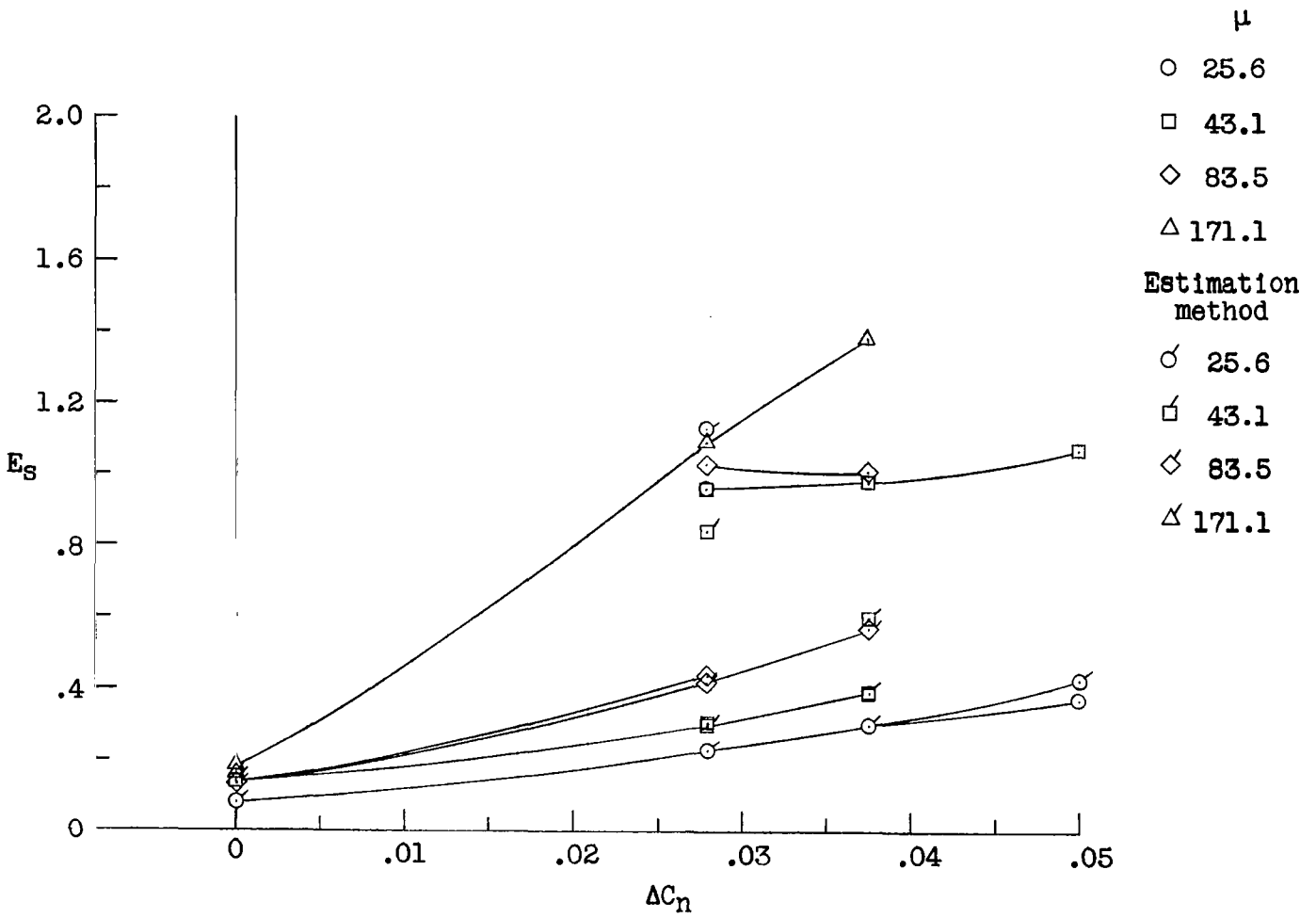

(c) E_s.

Figure 15.- Concluded.

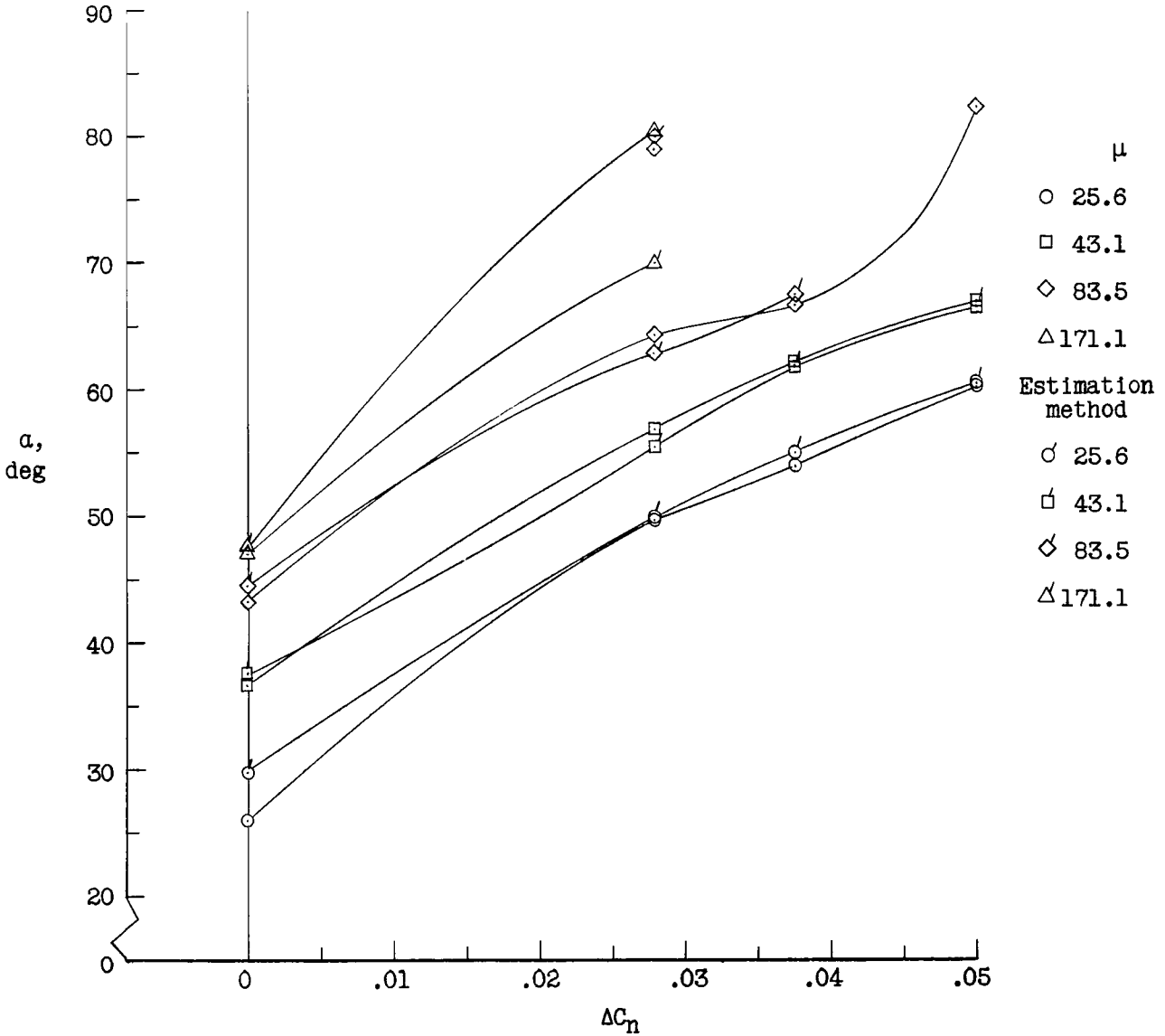

(a) α.

Figure 16.- Variation of α, Ω, and E_s with ΔC_n for all relative densities and loading III.

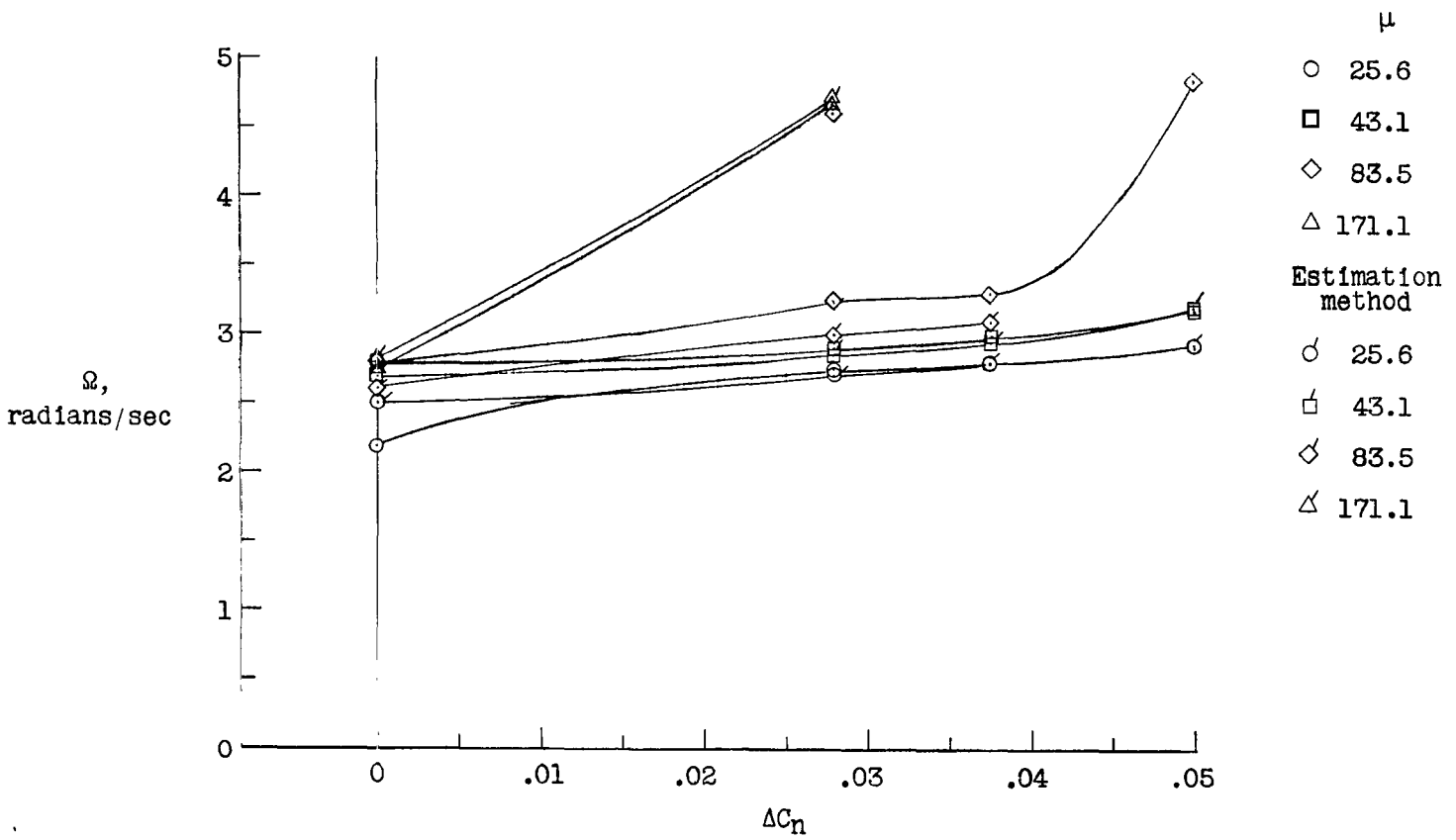

(b) Ω.

Figure 16.- Continued.

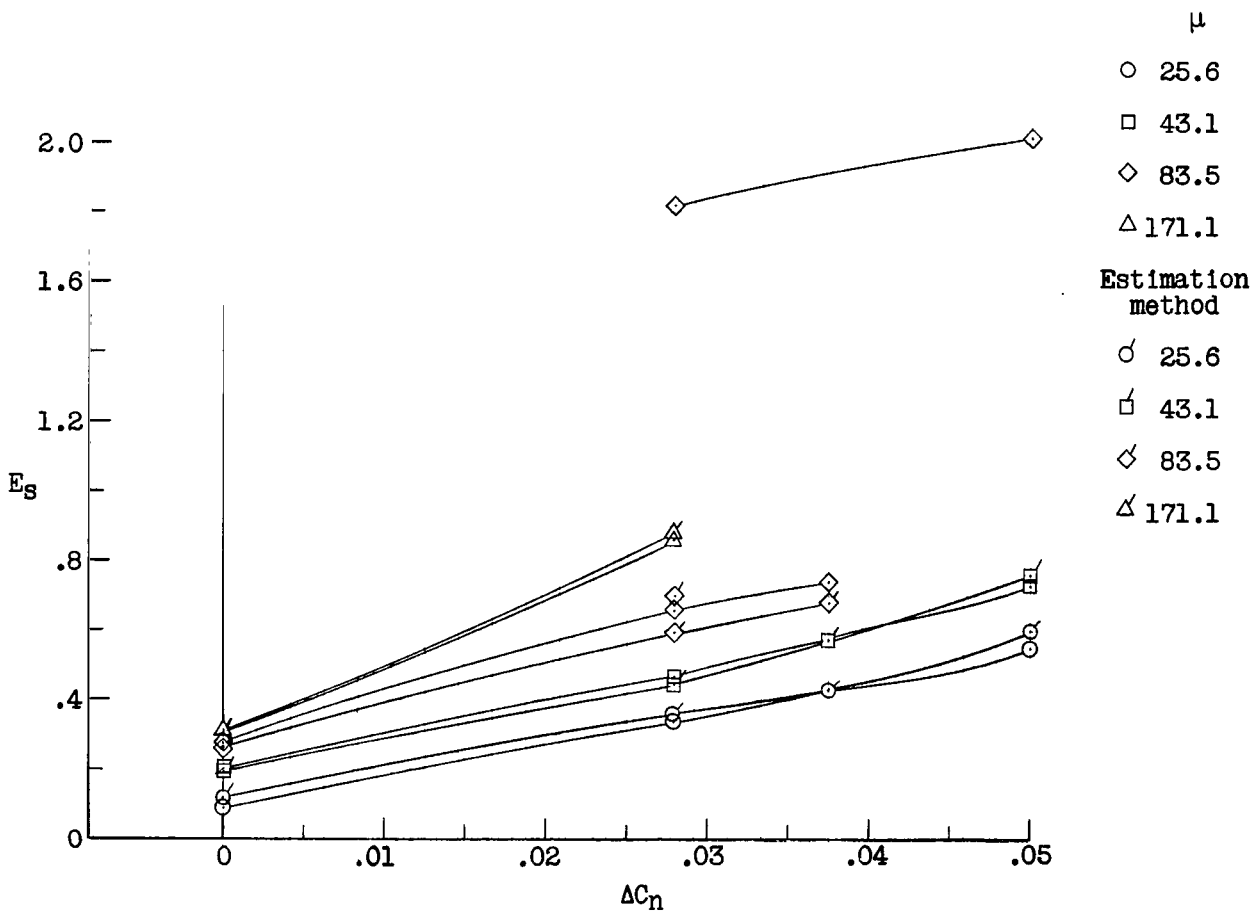

(c) E_s.

Figure 16.- Concluded.

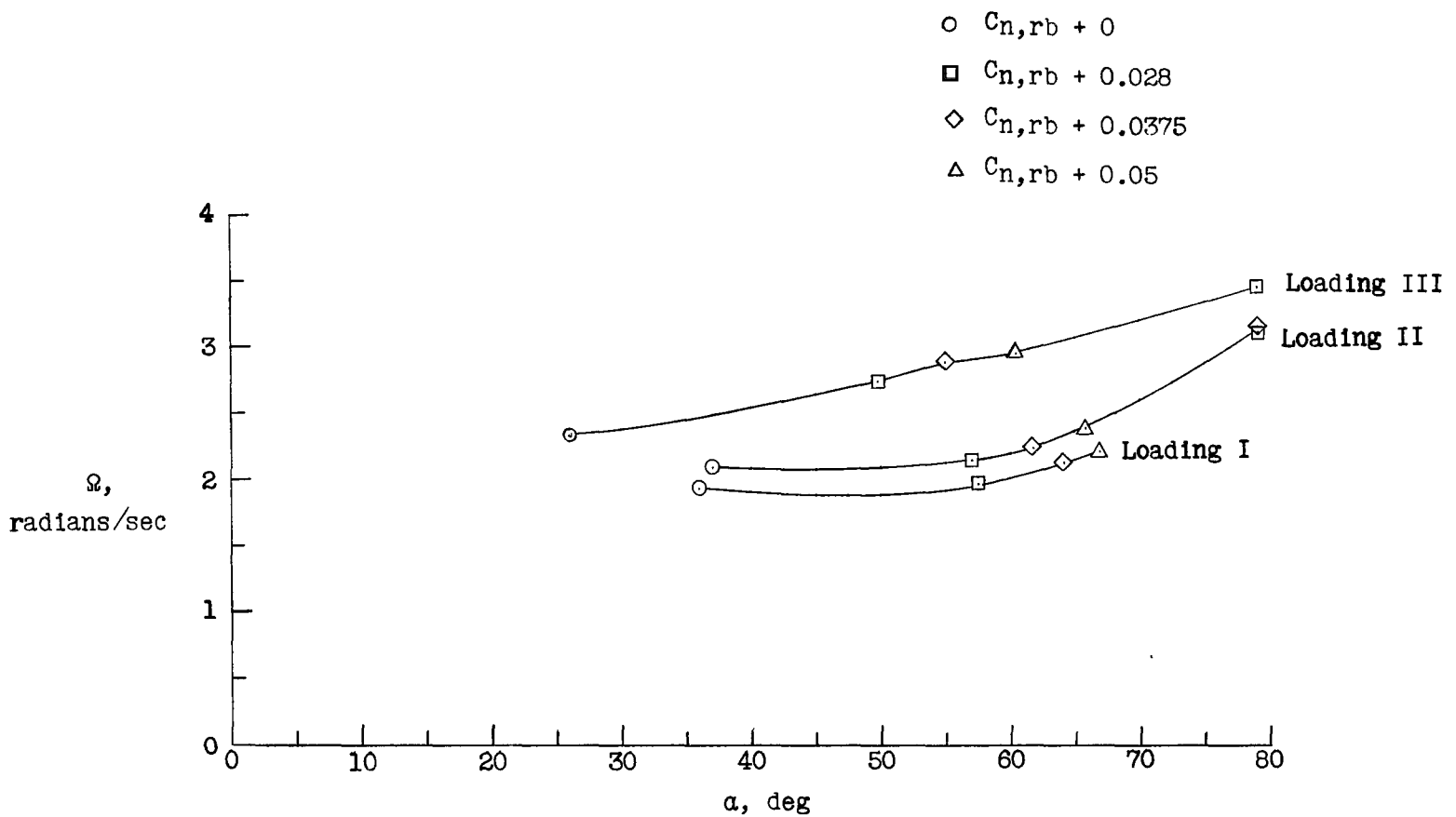

(a) $\mu = 25.6$.

Figure 17.- Variation of Ω with α for all loadings and ΔC_n values.

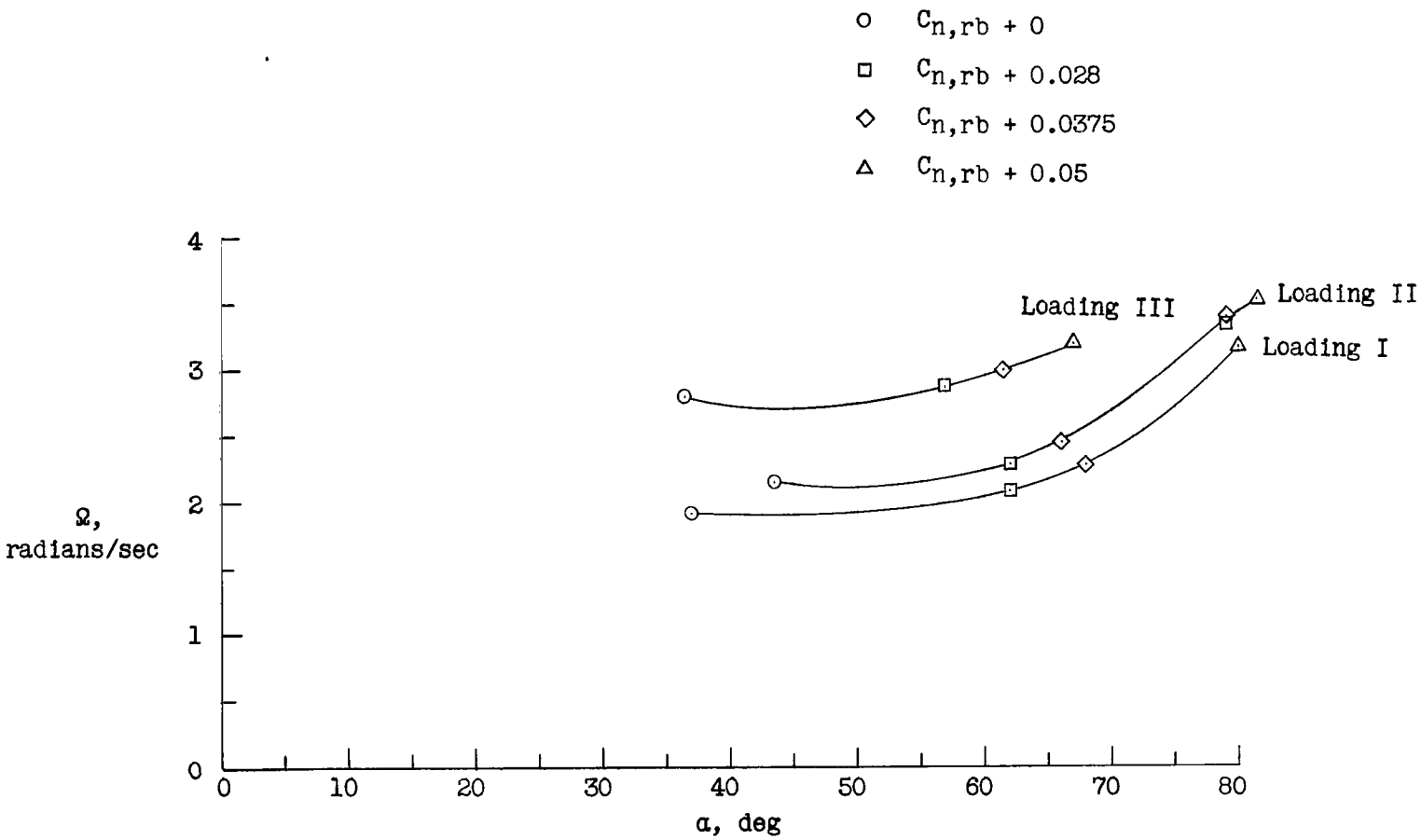

(b) $\mu = 43.1$.

Figure 17.- Continued.

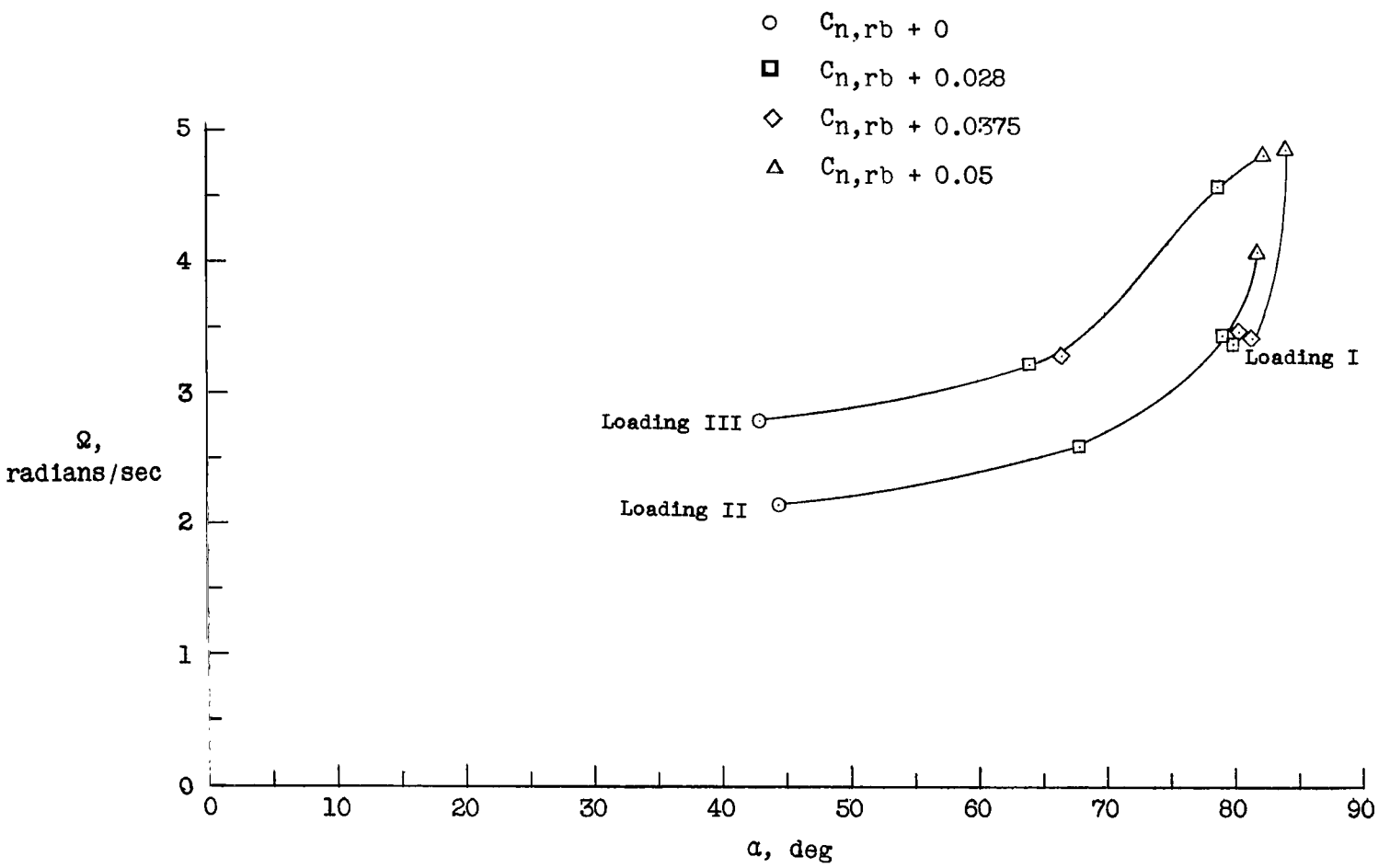

(c) $\mu = 83.5$.

Figure 17.- Continued.

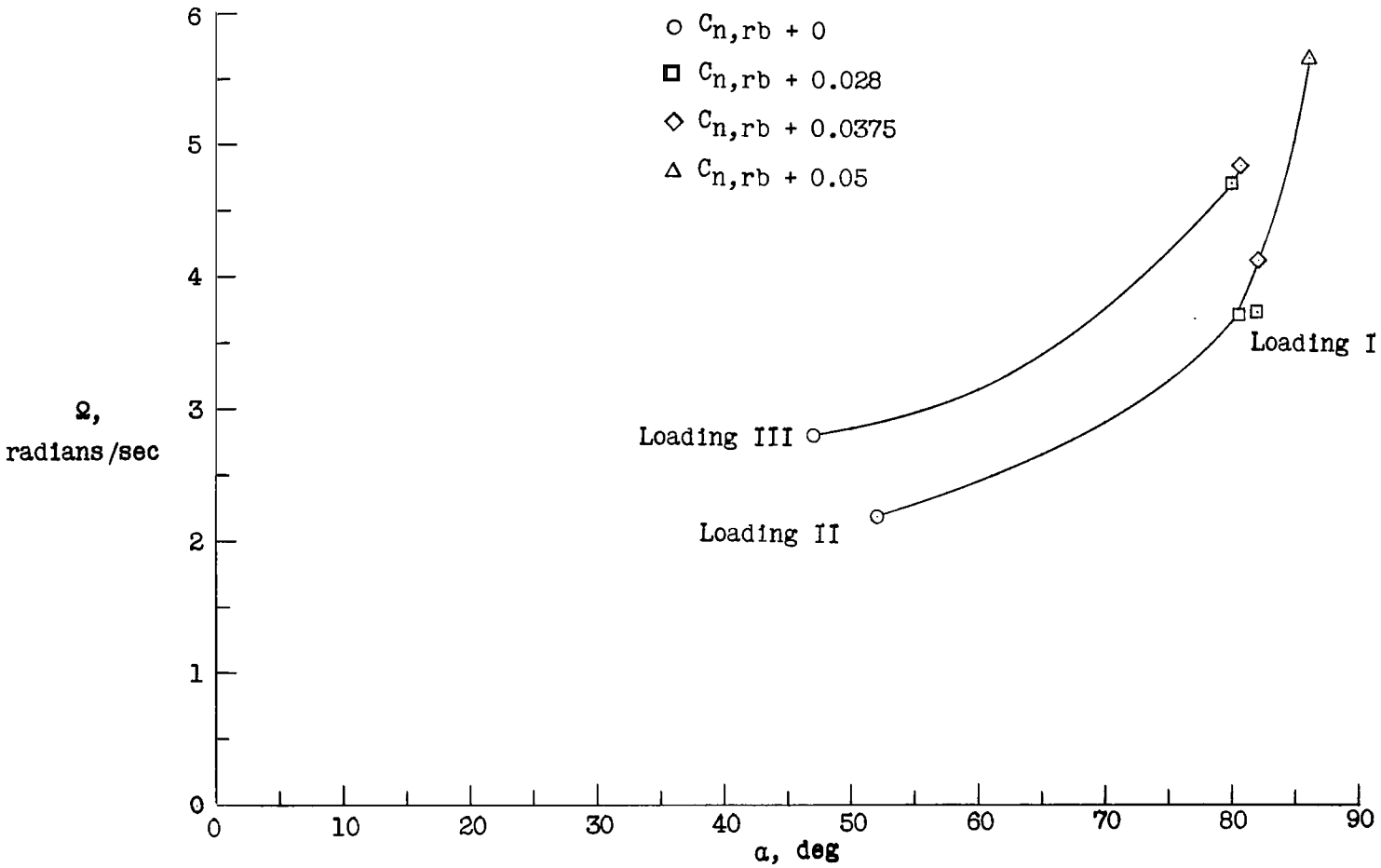

(d) μ = 171.1.

Figure 17.- Concluded.

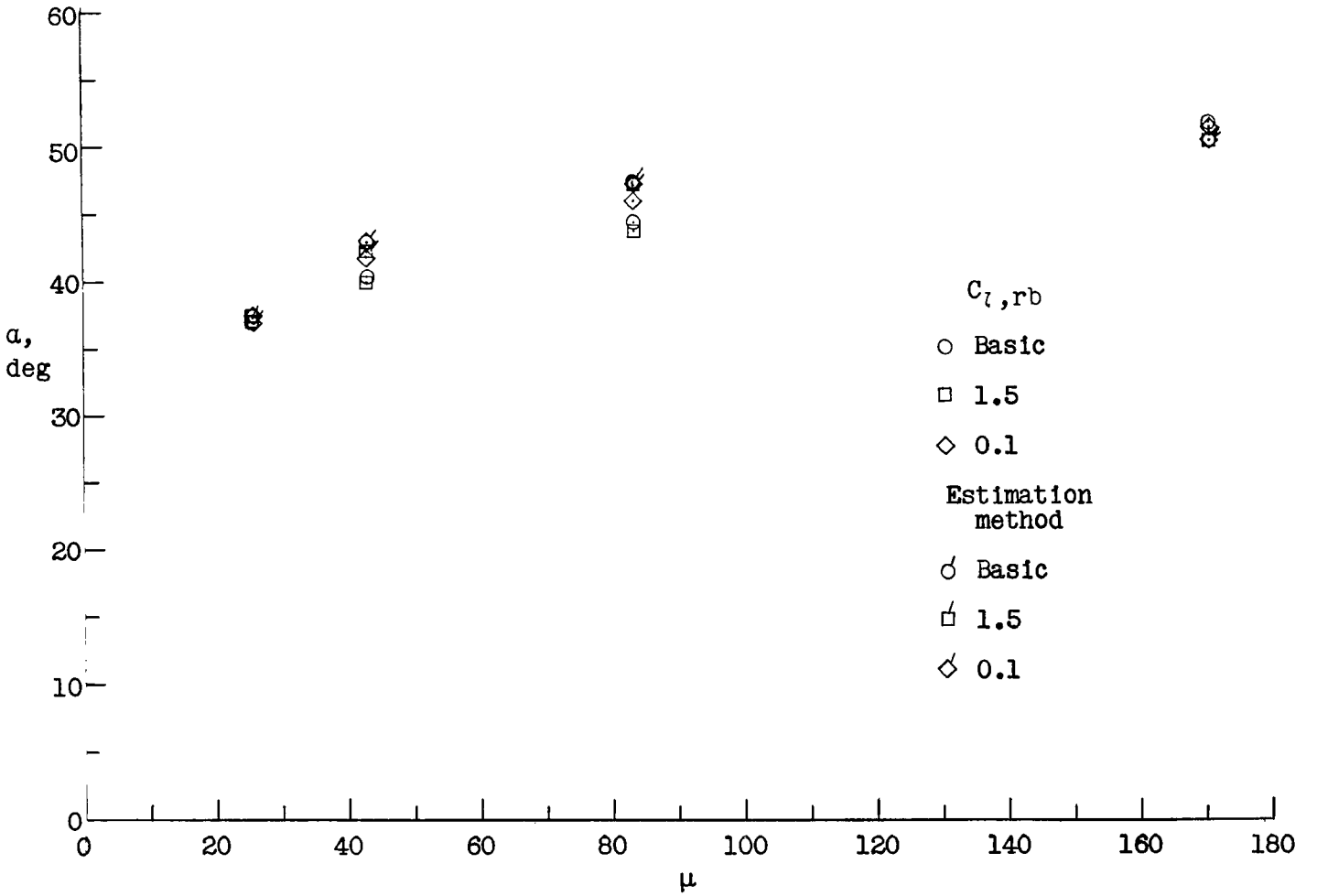

(a) α.

Figure 18.- Variation of α, Ω, and E_s with μ due to alterations from the basic measured aerodynamic rolling moment.

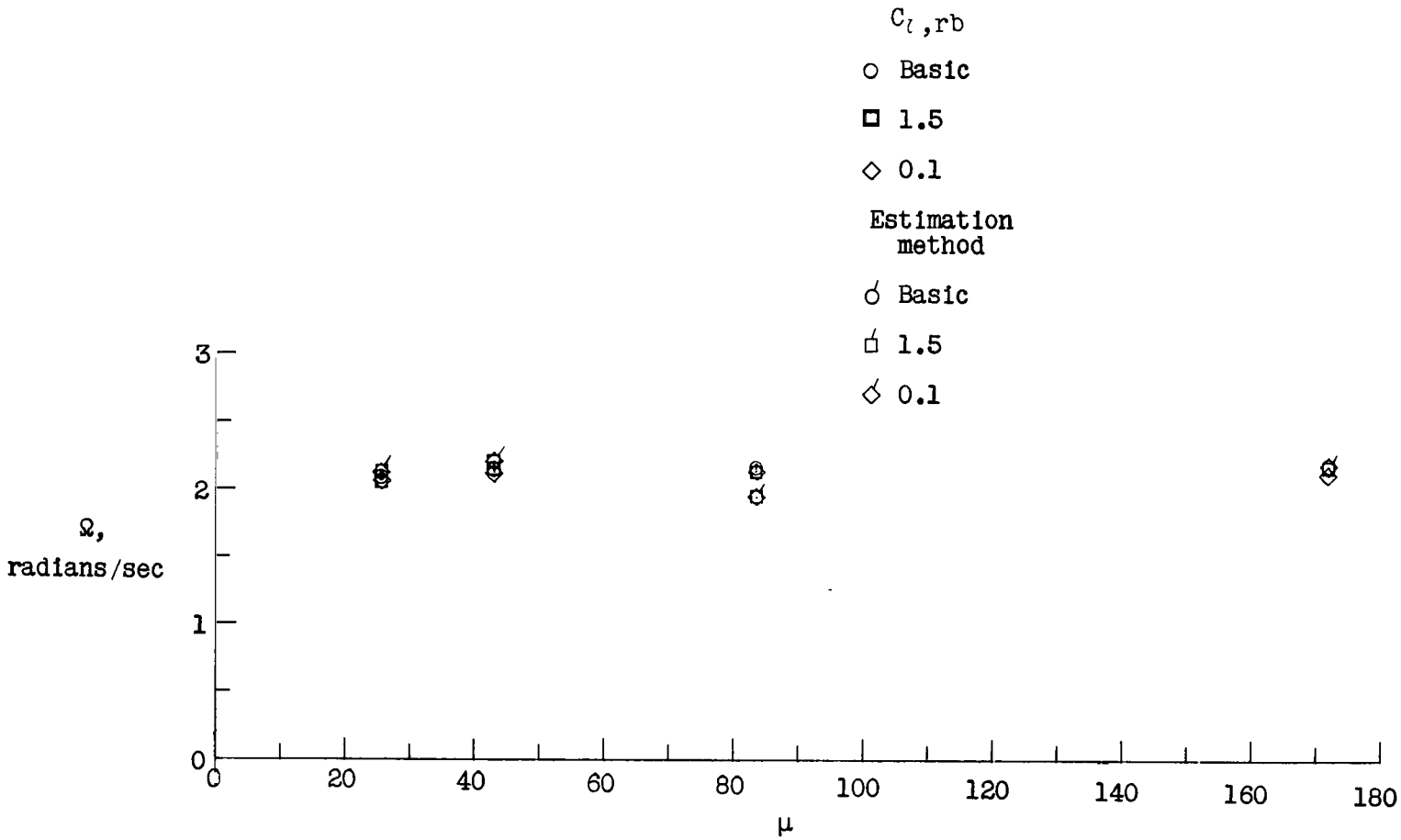

(b) Ω.

Figure 18.- Continued.

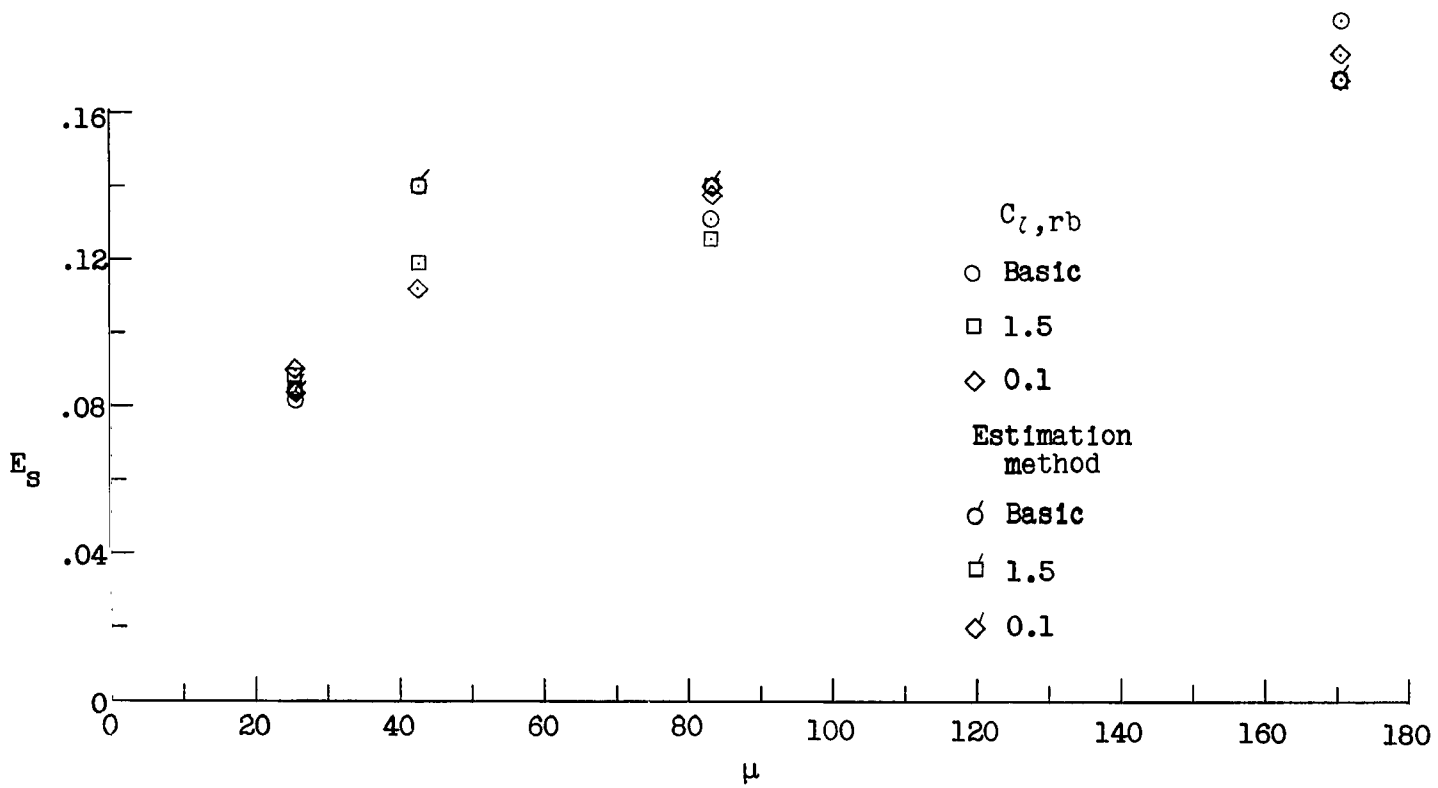

(c) E_s.

Figure 18.- Concluded.

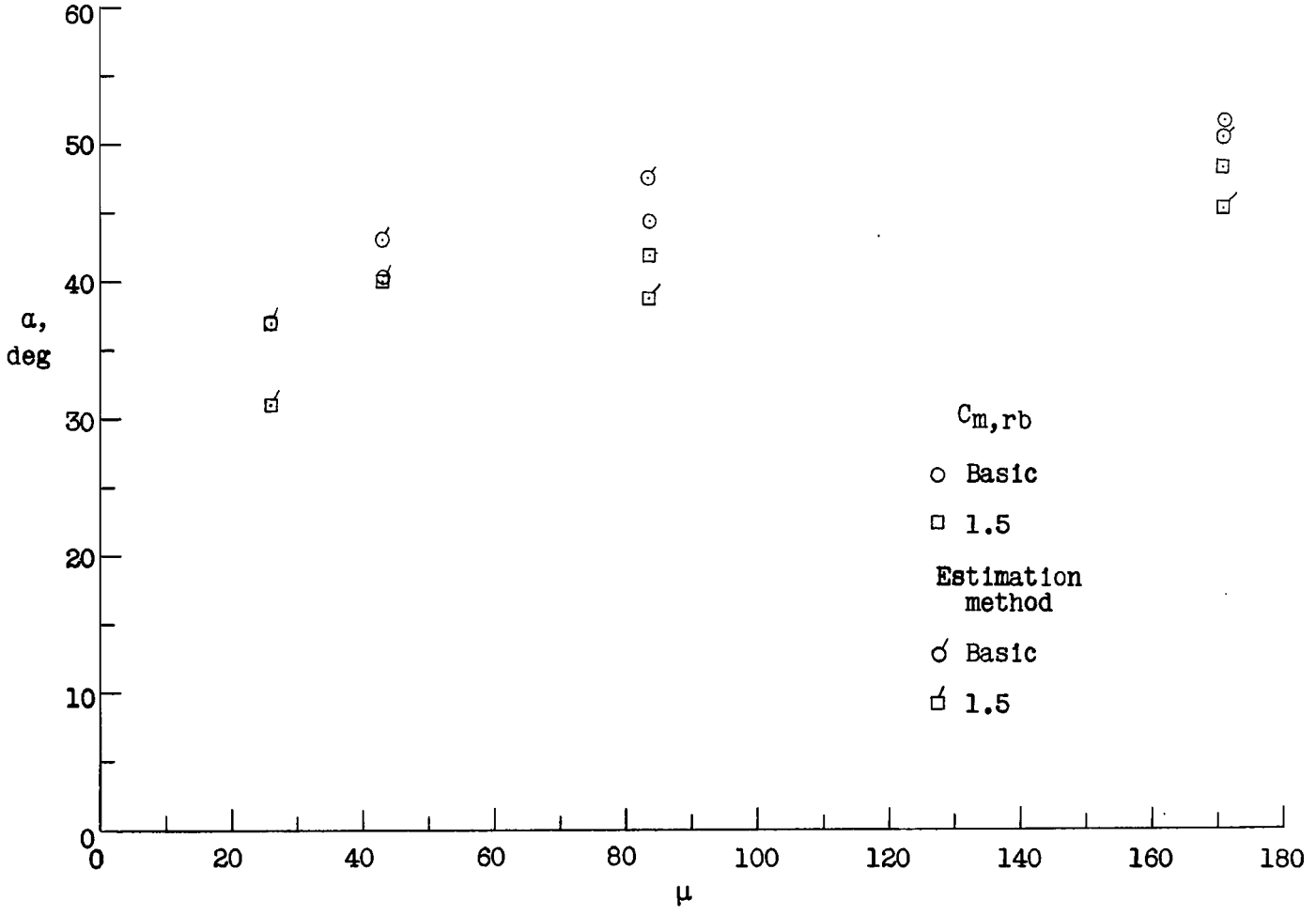

(a) α.

Figure 19.- Variation of α, Ω, and E_s with μ due to alterations from the basic measured aerodynamic pitching moment.

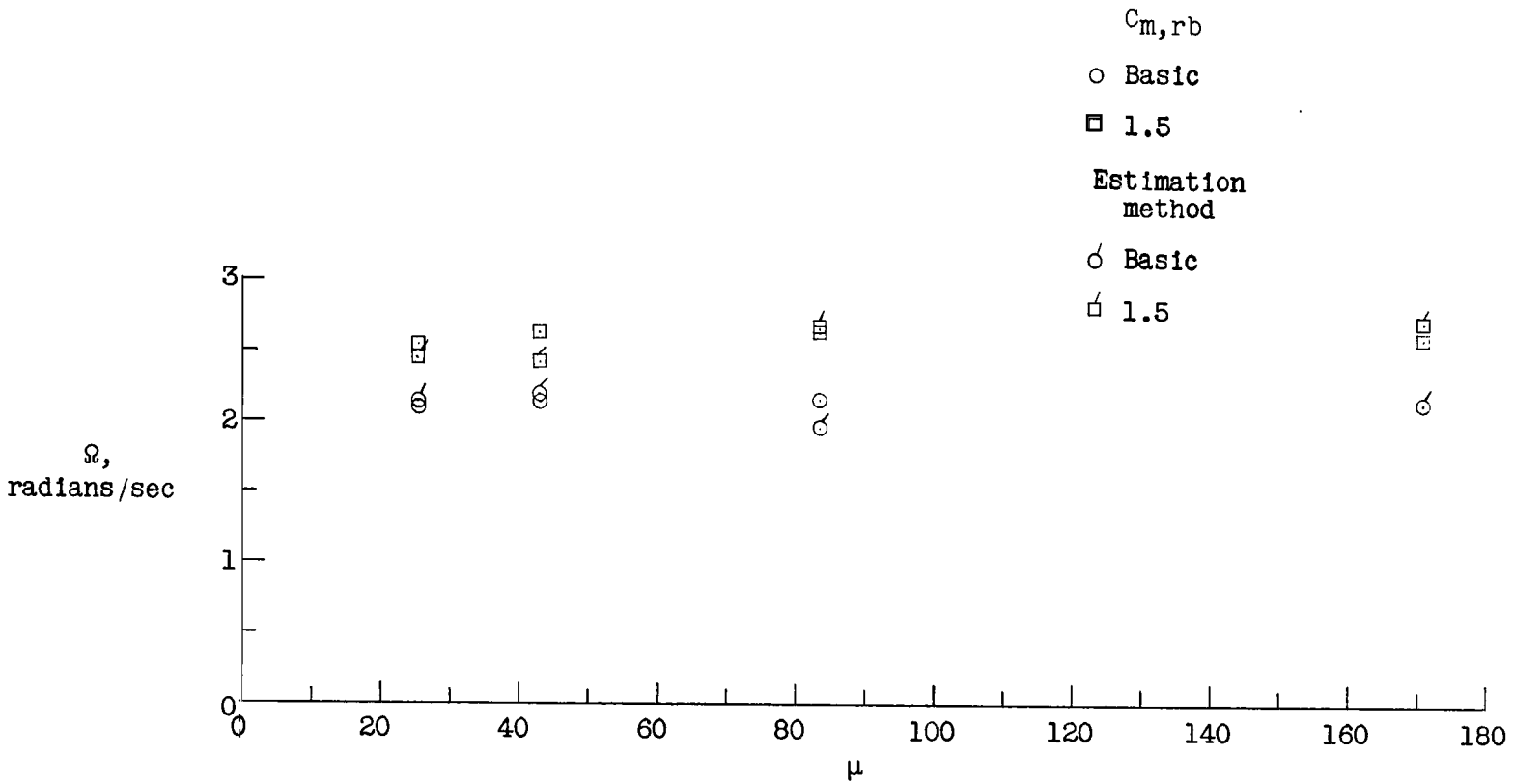

(b) Ω.

Figure 19.- Continued.

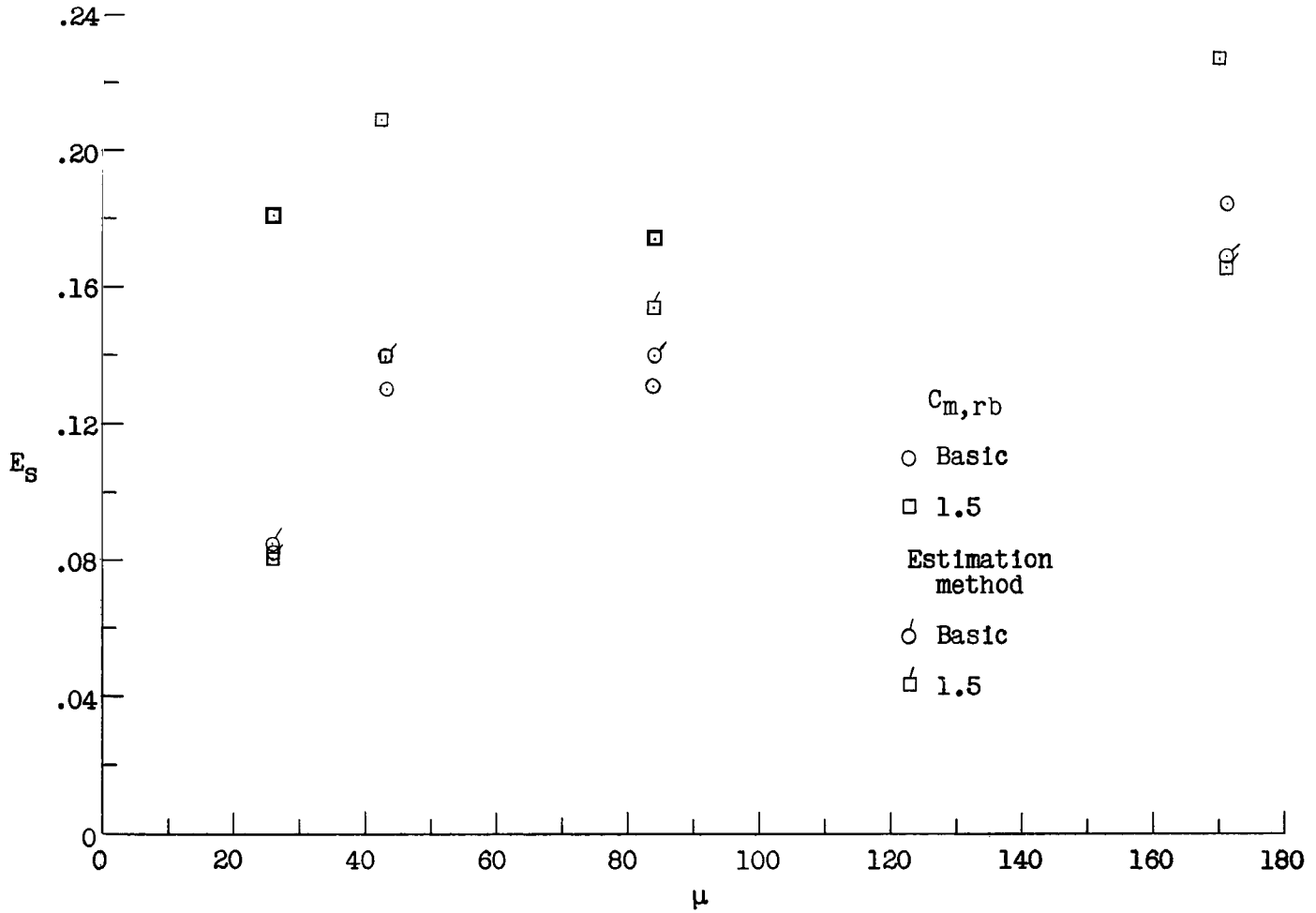

(c) E_s.

Figure 19.- Concluded.

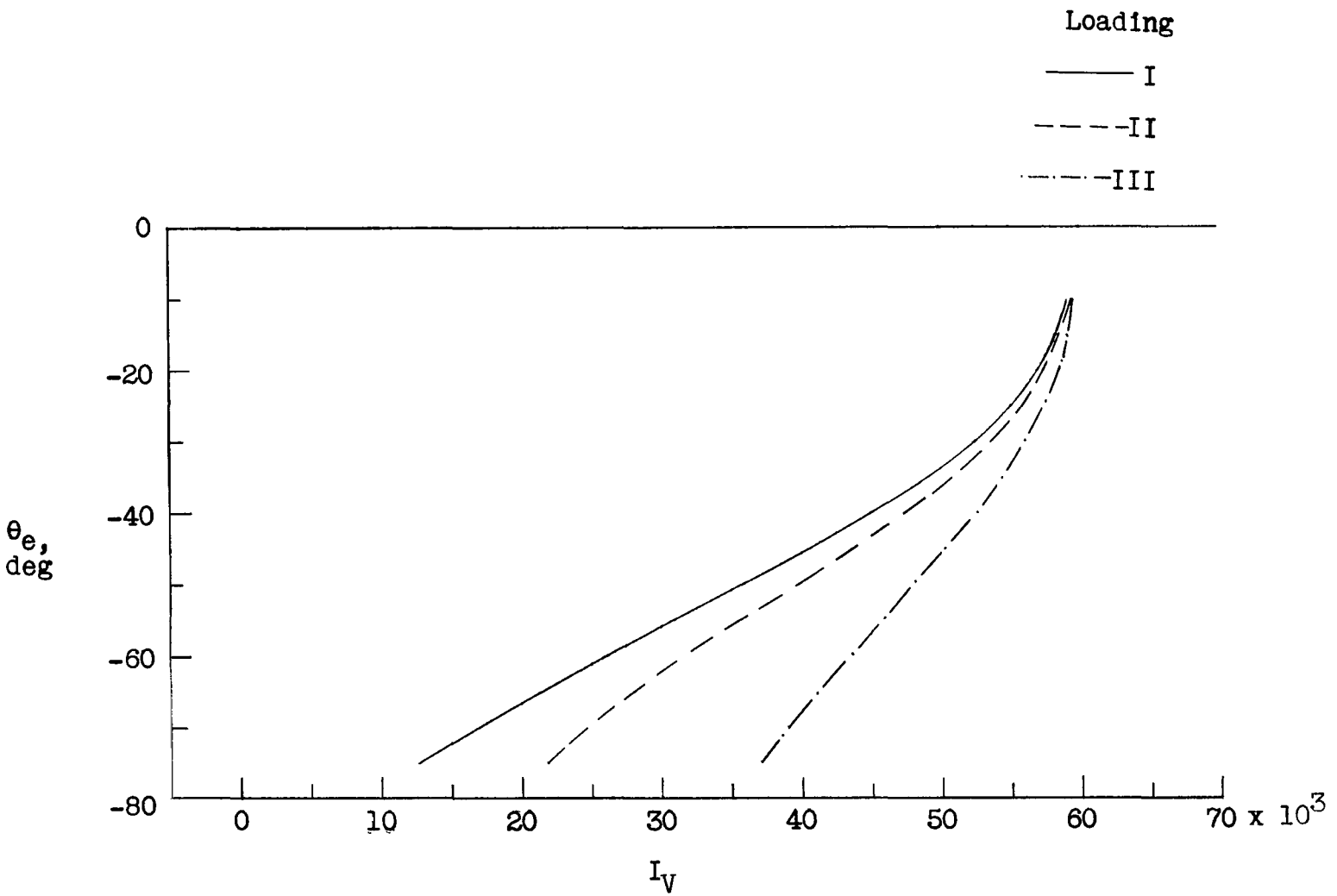

Figure 20.- Variation of I_V with θ_e for various loadings.

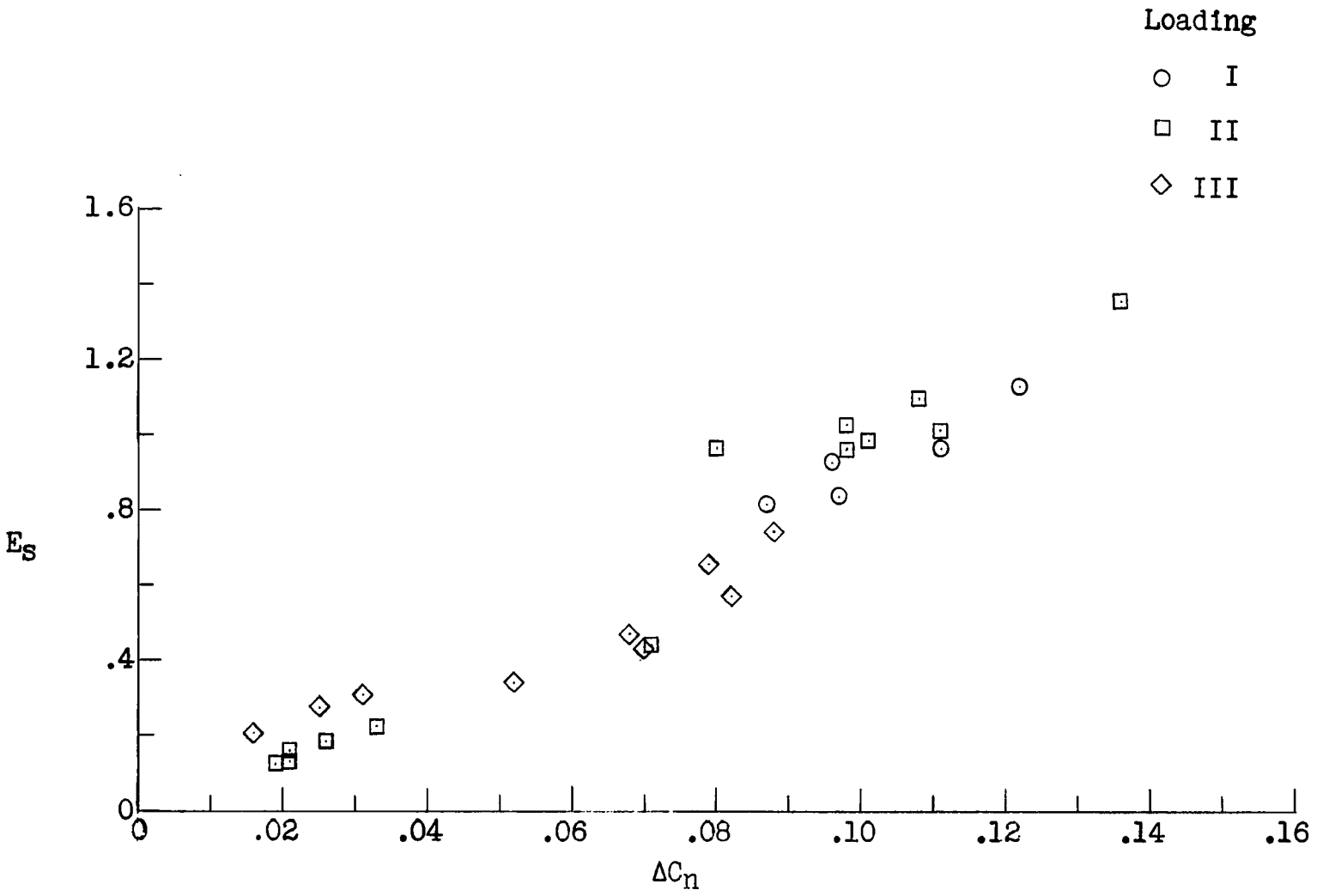

Figure 21.- Initial coefficient values of constant antispin yawing moments required for $2\frac{1}{4}$-turn recovery as a function of spin-energy factor.

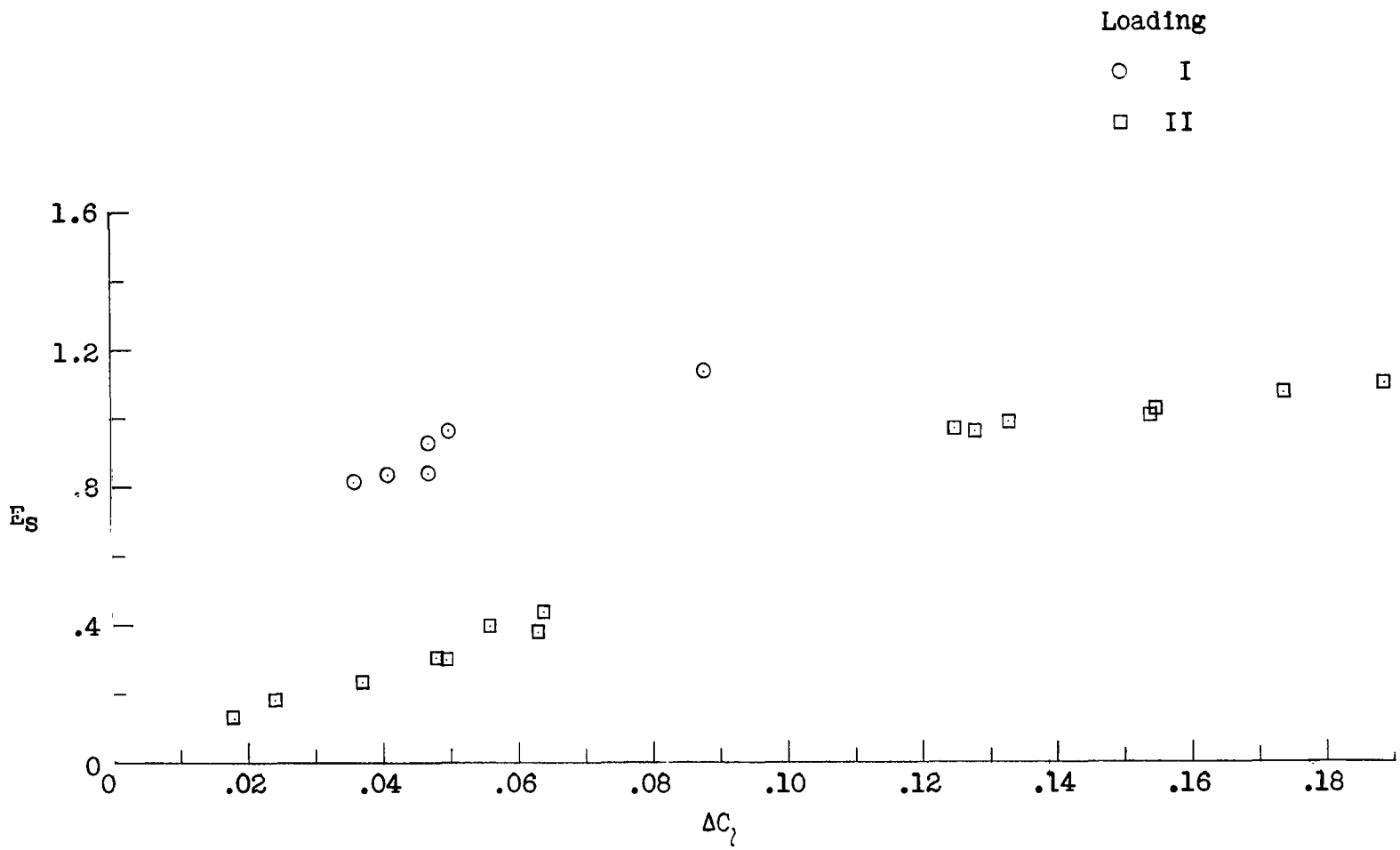

Figure 22.- Initial coefficient values of constant antispin rolling moments required for $2\frac{1}{4}$-turn recovery as a function of spin-energy factor.

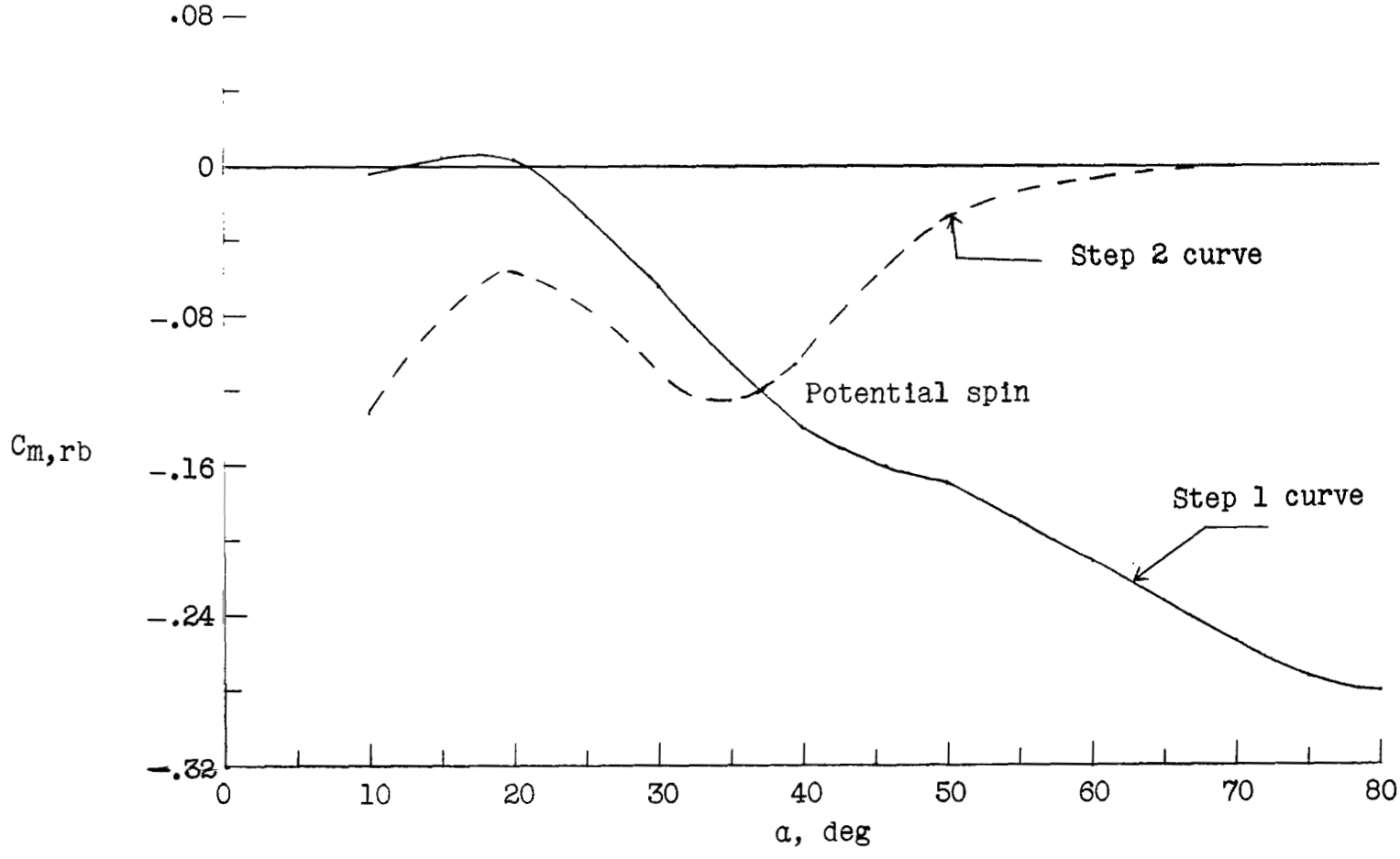

Figure 23.- Variation of $C_{m,rb}$ with angle of attack for step 3. Illustration of estimation method; see appendix C.